FE-2248-15
Distribution Categories UC-90g, UC-93

DEVELOPMENT, TESTING AND EVALUATION OF MHD MATERIALS AND COMPONENT DESIGNS

Quarterly Report for the Period
April 1 - June 30, 1977

John W. Sadler
William E. Young*
Larry H. Codoff*
James A. Dilmore*
Edward L. Kochka
John A. Kuszyk
Joseph Lempert*
Barry R. Rossing*
Stephen J. Schneider*
Abner B. Turner

Stewart Way, Consultant

*Westinghouse Research & Development Center

WESTINGHOUSE ELECTRIC CORPORATION
Advanced Energy Systems Division
P.O. Box 10864
Pittsburgh, PA 15236

Date Published - July 1977

PREPARED FOR THE UNITED STATES
ENERGY RESEARCH AND DEVELOPMENT ADMINISTRATION

Under Contract No. EX-76-C-01-2248

APPROVED:

J. W. Sadler, Project Manager
Advanced Energy Systems Division

TABLE OF CONTENTS

TABLE OF CONTENTS

TABLE OF CONTENTS

LIST OF FIGURES

LIST OF FIGURES

LIST OF TABLES

I. ABSTRACT

Efforts during the April-June 1977 quarter were directed toward the design, fabrication and evaluation of ceramic MHD electrodes for both clean fuel and coal fired environments. The Materials Test Facility (MTF) became operational this quarter following completion of several test runs using a "dummy" test section, as well as an initial run on a copper electrode (cold wall) test assembly. These tests verified design prediction of material temperatures and heat fluxes. Both the test facility and test section have demonstrated their suitability as test vehicles for long duration testing of generator materials and designs.

A number of designs reflecting various electrode to copper cooling block attachment techniques are being evaluated. These techniques involve the use of a compliant material (metal or organic) to reduce mechanical stresses in the ceramic electrode structures.

Laboratory screening tests indicate that both $MgCr_2O_4$ and Mo_2Si are resistant to slag corrosion and can be seriously considered as anode materials for semi-hot slagging wall operation (T_{wall}=900-1500°C). $MgCr_2O_4$ is the first oxide tested which has demonstrated promise as a cathode material.

Finally, work began on the U-02 Phase III Module effort. The electrode module has been designed, material property data is being gathered, orders for electrode materials have been placed with several vendors and several electrode designs are under evaluation. Proof tests of several materials and designs will be conducted in the next quarter, followed by a test in the U-02 facility in February 1978.

II. OBJECTIVE AND SCOPE OF WORK

In continuation of the program to develop MHD power generation to commercial feasibility, Westinghouse is conducting a 36-month program to test and evaluate materials and component designs in both laboratory scale apparatus and in an integrated MHD system facility. Primary emphasis has been given to "hot generator wall" concepts under slagging conditions. The program provides a link between the basic and supportive materials development and testing and the applied testing in a facility that offers an adverse MHD environment for extended periods of time. The program carries for the engineering development of selected MHD component(s), e.g., electrode and insulating wall systems through design, materials fabrication, initial screening tests, construction and finally to an MHD system test. The entire sequence is reiterative; i.e., each stage will involve an optimization of both design and materials.

These objectives are being pursued in accordance with a statement of work which is consistent with the National Plan for MHD development formulated by ERDA. The program consists of the following four tasks:

Task 1 - Long Duration MHD Facility System and Component Test and Evaluation

Task 2 - Materials Design/Development

Task 3 - Testing and Evaluation of Prototype Electrode Systems

Task 4 - Technical Support for the Cooperative US-USSR Program on MHD

1.0 TASK 1 - LONG DURATION MHD FACILITY SYSTEM AND COMPONENT TEST AND EVALUATION (WALTZ MILL TEST FACILITY)

The engineering purpose of this task is to establish the basic chemical, thermal and electrical properties of the MHD gas stream and materials of construction in an integrated system on a component-by-component basis as well as on a system basis. The facility is a test bed for sub-scale generators of advanced design. The general technical approach to be adhered to is embodied in the "hot generator wall" concept, slagging conditions representing greater than 85 percent ash rejection, and including 100 percent ash rejection and long duration operation.

1.1 Subtask 1.1 - Test and Evaluation with Existing Waltz Mill MHD Facility

These tests will investigate on a component-by-component basis and on a system basis and will include:

- Material balance, e.g., the disposition of seed and ash
- Slag deposition rates
- Corrosion/erosion rates (prediction of lifetimes) and assessment of degradative reactions.
- Heat transfer rates and efficiencies
- MHD generator electrical and overall performance characteristics
- Plasma properties, e.g., electrical conductivities and homogeneity
- Recommended guidelines to improve component and system performance

1.2 Subtask 1.2 - Conversion and Upgrading of Waltz Mill Facility to Materials/ Component Test Facility

Subsequent to, or simultaneously with, Subtask 1.1, the Waltz Mill Facility will be modified to reflect the following:

- Improved plasma properties exiting combustor/mixer (up to 2950°K through the use of preheated air with oxygen).
- Separate seed injection with capabilities for non-aqeous introduction of K_2CO_3, K_2SO_4, Cs_2CO_3, Cs_2SO_4, and combinations thereof.
- Capabilities to simulate ash carryover of between 0 and 15 percent (ash is meant to include other additives).
- Capability to test channel configurations of the diagonal or window frame construction and segmented Faraday-type contruction.
- Capability to test materials, electrode and insulator configuration designs at exit of channel proper. This channel extension will be constructed on a "modular" basis.
- Capability to impress current densities on electrodes in the channel proper and in the channel extension to a maximum of 4 A/cm^2, constant voltage or constant current modes.
- Capability to conduct materials screening testing in other major components such as the air preheater and mixer/combustor.

- Improved data sensing and acquisition instrumentation.
- Capability for round-the-clock operation.

1.3 Subtask 1.3 - Design of Coal Combustor and Coal Processing Equipment Compatible with Waltz Mill Facility

These subtask includes two design efforts. The equipment and facility design and supporting calculations will be deliverable to ERDA in the form of design reports for review and approval. ERDA will retain the option to proceed with fabrication or not.

Combustor Design - A multi-stage vortex type coal burning combustor will be designed to remove approximately 90 percent of the ash contained in the coal. The combustor will be designed to minimize heat loss and to be capable of burning either coal, char or a low-Btu gas derived from coal in the second stage. Combustor capacity will be 4 MW_t.

Coal Handling Equipment and Devolatilizer Design - Coal grinding, sizing and conveying equipment large enough to provide fuel continuously for the 4 MW_t combustors will be designed. A devolatilizer will be included as part of the coal handling equipment.

1.4 Subtask 1.4 - Component Testing and Evaluation (Long Duration)

Subtask 1.4 consists of two design/testing stages.

Advanced Generator Channel (Westinghouse Design) Design and Testing - Based on the information gained from Subtask 1.1 and from Tasks 2 to 4, improvements to the existing design or, if necessary, an advanced design will be developed to assure a durable long-life channel. The design will be evolved through a systematic sequence of materials screening, sub-element testing and modular testing with and without current as described in Tasks 2 to 4. Channel tests for this advanced generator will be designed along the lines described in Subtask 1.1.

Component Testing and Evaluation (Non-Westinghouse Design) - The Waltz Mill Facility (and other general laboratory screening equipment) will be made available to other ERDA contractors and foreign institutions such as the USSR - High Temperature Institute, as deemed necessary by ERDA. These tests will be conducted jointly with the participating institutions and Westinghouse. It is anticipated that Westinghouse will be involved in USSR materials testing in US facilities, Phase II of the U-02 materials test, and modular testing of U-25 channel segments.

2.0 TASK 2 - MATERIALS/DESIGN DEVELOPMENT (ELECTRODE SYSTEMS)

The objective of this task is to develop three reference electrode assembly designs for optimum MHD performance in coal-fired systems. These designs are expected to establish specific materials requirements and identify baseline criteria to guide materials selection and development. Each design will be a complete electrode system, including anode and cathode sections, insulating walls, inter-electrode insulators, electrode replenishment or slag materials, and all sub-structures through the exterior wall.

The three reference electrode designs will reflect the following:

- Electrode (or replenishment or slag material)/plasma interface temperature: 2200°K
- Electrode current density: 2.0 A/cm^2 with excursions to 4.0 A/cm^2
- Endurance greater than 100 hours even with accidental loss of an electrode system member
- Moderate rate of startup and shutdown (compatible with operational procedures)
- Negligible Joule heating otherwise due to high resistivity electrode material
- Electronically conducting electrodes
- Suitability for coal systems

The classes of electrode systems to be considered include:

- All ceramic electrode; graded or single phase structures; essentially electronic conductor
- Ceramic protected refractory metal electrode; ceramic to be electronic conductor
- Cermet electrode (intimate mixture of refractory metal and ceramic)

In consultation with available experts and working groups designated by ERDA, Westinghouse will assess the suitability of each electrode system provided under Task 2, rank them according to a priority system that includes judgement factors such as cost, ease of fabrication, technical performance, durability, and development time.

A recommendation as to which system should be incorporated in an advanced Waltz Mill channel will be made to ERDA. Additional recommendations will specify backup or alternate systems.

3.0 TASK 3 - TESTING AND EVALUATION OF PROTOTYPE ELECTRODE SYSTEMS

The objective of this task is to evaluate the selected candidate electrode system (prototype) designs and materials under dynamic thermal, chemical, and electrical conditions simulating generator service.

3.1 Subtask 3.1 - Laboratory Screening Tests

Testing equipment, Materials Test Facility, will be provided that is capable of measuring thermal and electrical conductivity under thermal gradient, replenishment (slag)/seed exposure, and general dynamic conditions typifying the electrode module design service.

If necessary, additional testing equipment (crucible test) will be designed and conducted to establish slag/seed compatibility or shock properties. These tests will be of the bench-scale type and are desinged to provide preliminary electrical, thermal corrosion, and erosion data as functions of microstructure.

All tests will include pre- and post-test characterization of materials. Materials selected as promising candidates will be fabricated and subjected successively or simultaneously for up to 100 hours to the thermal and electrical conductivity and compatibility tests. Characterization activities will be carried out to ascertain failure mechanisms. Improvements in the materials through compositional and microstructure control will be made. This series of tests will serve as the first materials screening activity.

3.2 Subtask 3.2 - Dynamic Screening Tests (Channel Extension - Waltz Mill Facility)

Selected candidate designs and materials will be fabricated and tested as a complete electrode system, including replenishment or slag deposition. Only the more promising materials/designs as evolved from previous tasks will be evaluated for up to 100 hours under projected service conditions. The electrode test elements will be subjected to the electrical (impressed current from an external source) and chemical and thermal conditions expected in service. Design related effects and materials effects will be distinguished. Characterization activites will be carried out. This series of tests will serve as the second screening activity.

3.3 Subtask 3.3 - Development of Analytical Model of Electrode System Materials

The objective of this subtask is to develop analytical models appropriate to the prototype electrode system so that the behavior and synergistic effects of the environment on the performance-limiting properties of component materials can be established.

Models that are applicable to each of the prototype desings described above will be developed. Such models will describe the following interrelationships:

- Materials properties having a critical bearing on component performance as functions of material composition and microstructure characteristics
- Materials properties requirements as functions of channel and combustor design variables

- Surface and interior chemical, mechanical and electrical transport reactions as functions of boundary layer and gas stream conditions corresponding to seeded combustion gases with the presence of coal slag materials.

The analytical models will be capable of being used for design optimization, sensitivity analysis, failure and life predictions, and interpretation of materials performance data from simulated or real channel testing programs.

4.0 TASK 4 - TECHNICAL SUPPORT FOR THE COOPERATIVE US-USSR PROGRAM ON MHD

This task provides technical support to the activities of the coopertive US-USSR program. Specifically, this will involve USSR testing in Westinghouse facilities, U-25 module testing in Westinghouse facilities, and materials testing in the U-02 facility.

Each of these activites is defined by an ERDA appointed committee. The work will include:

- Continuation and completion of Phase I of the U-02 materials test
- Completion of the U-02 Phase II activities in the same manner as performed under Phase I arrangements, namely: project coordination; design of electrode modules; construction and installation of working modules; diagnostic equipment; procurement, storage, cataloging and characterization of critical materials (major characterization activities also undertaken by other organizations); and test monitoring, including travel by selected personnel to the Soviet Union
- Participation in USSR materials testing program at US facilities (in cooperation with ERDA designated US organizations)
- Testing of U-25 modules at the Waltz Mill site under conditions designated by ERDA
- Completion of U-02 Phase III activities in the same manner as performed under Phase I arrangements with the addition of proof tests to be completed prior to electrode selection.

III. SUMMARY OF PROGRESS TO DATE

Figure 1 presents a summary program schedule and status.

1.0 TASK 1 - LONG DURATION DUCT DEVELOPMENT - WALTZ MILL

No significant activity this quarter.

2.0 TASK 2 - MATERIALS/DESIGN DEVELOPMENT (ELECTRODE SYSTEMS)

No activity this quarter.

3.0 TASK 3 - TESTING AND EVALUATION OF PROTOTYPE ELECTRODE SYSTEMS

Significant progress has been achieved in several areas in this task. The first test was conducted in the Materials Test Facility incorporating an electrode test section. Previous to this test, several tests were carried out using a "dummy" test section. In these tests, test procedures were confirmed and facility components were "de-bugged". With some 40+ hours of operation the MTF has demonstrated long duration operation. Plasma temperatures of 2450°K were achieved without the addition of oxygen. Installation of the oxygen system, to be completed in August, will permit operation at plasma temperatures of up to 2850°K. Measurements at the 2450°K temperature on the copper test assembly verified calculated material temperatures and heat fluxes. Longer duration operation, in this case with seed injection and with electrical evaluation of the test section is planned for early July.

Several electrode designs reflecting different bonds between ceramic electrodes and copper cooling blocks are being evaluated. These incorporate the concept of allowing the ceramic form its natural shape during operation, thus, minimizing mechanical stresses. Both conducting expoxies and silicones as well as metal structures that will easily deform are being tested. Electrode designs reflecting several of these attachments will be incorporated into the first hot wall ($T \approx 1700°C$) test assembly which will be tested in August.

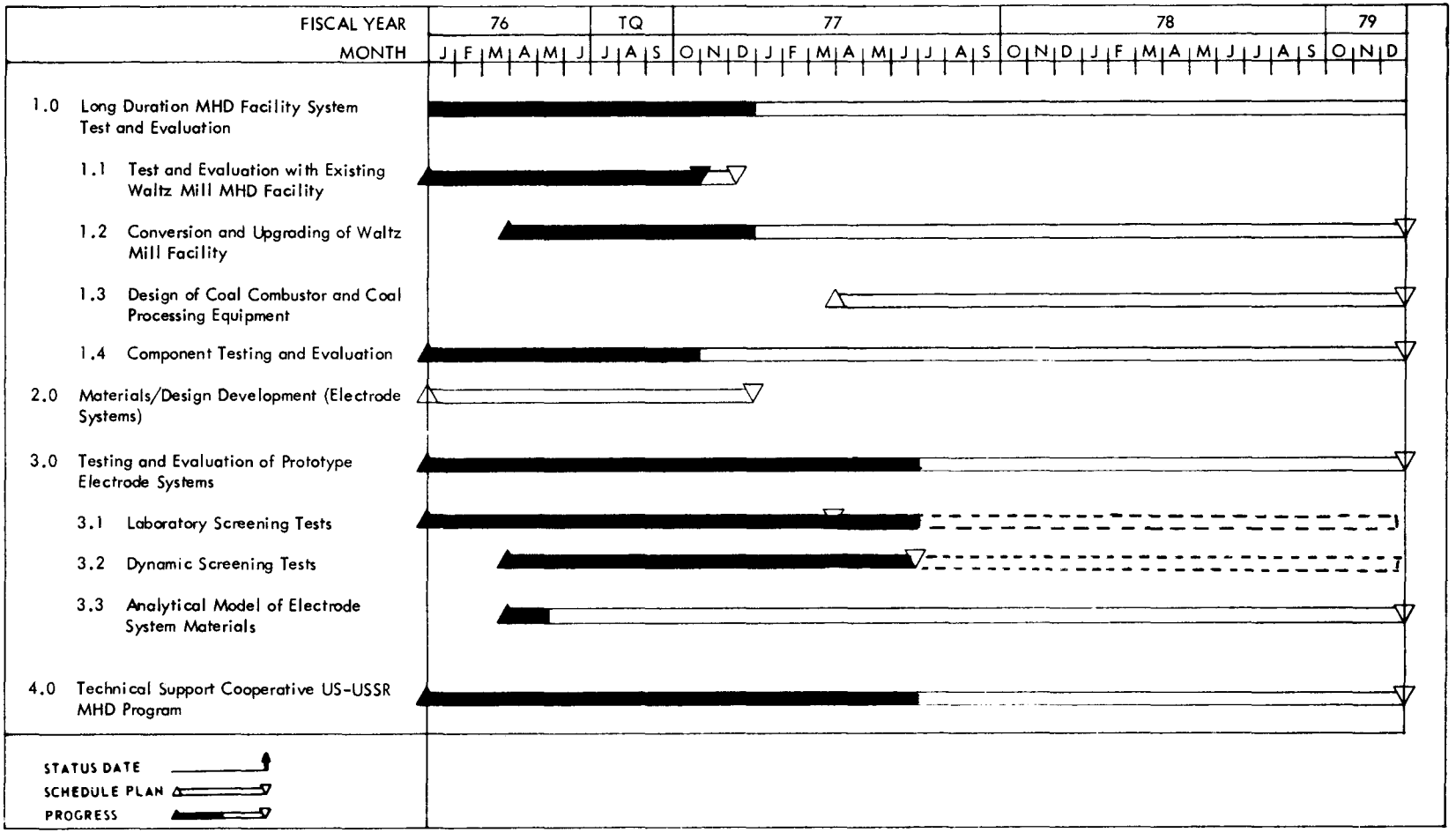

Figure 1. Program Schedule and Status

Two additional materials $MgCr_2O_4$ and Mo_2Si were tested in laboratory corrosion tests. The $MgCr_2O_4$ displayed the best corrosion resistance of any oxide tested to date and could be considered to both a cathode and anode for semi-hot wall operation. Mo_2Si displayed approximately the same resistance to slag corrosion and should be considered further as a semi-hot wall anode.

4.0 TASK 4 - TECHNICAL SUPPORT FOR THE COOPERATIVE US-USSR PROGRAM ON MHD

Work on the U-02 Phase III electrode tests has begun. This test will be conducted in February 1978, preceeded by proof tests of nine candidate electrode systems in the MTF in August-September. The design of the electrode modules has been completed. Thermal and stress analysis (elastic analyses) are underway to aid the design of electrode/insulator structures. Materials have been ordered from several vendors for proof test electrodes. Materials characterization studies and material property measurements are in progress. Electrodes based on MAFF ($MgAl_2O_4 \cdot xFe_3O_4$) and $LaCrO_3$ and insulators of $MgAl_2O_4$, MgO and $SrZrO_3$ will be tested. Electrodes and insulators will be fabricated using different processing techniques (sintering, hot pressing and plasma spraying). Attachment of these materials will be made with different attachment techniques, (graded layers, compliant layers, metal-oxide composites, etc.).

IV. DETAILED DESCRIPTION OF TECHNICAL PROGRESS

1.0 TASK 1 - LONG DURATION MHD DUCT DEVELOPMENT - WALTZ MILL

No significant activity was completed during this quarter.

2.0 TASK 2 - MATERIALS/DESIGN DEVELOPMENT (ELECTRODE SYSTEMS)

No activity was undertaken during this quarter.

3.0 TASK 3 - TESTING AND EVALUATION OF PROTOTYPE ELECTRODE SYSTEMS

The objective of this task is to evaluate candidate electrode and insulator materials and electrode systems under the thermal, chemical and electrical conditions realized in future base load, coal fired MHD generators. Candidate materials and designs will cover the full range of channel operating conditions, i.e., from cold wall-slagging to hot non-slagging.

Laboratory corrosion screening tests provide the basis for identifying promising electrode and insulator materials as well as electrode/insulator system designs suitable for testing under a second and more severe set of conditions. These latter tests would be conducted in the Materials Test Facility, a dynamic test rig, where most of the conditions found in an MHD generator are simulated. This is an interative process; i.e., at each stage, materials and designs are sequentially optimized through changes in composition, microstructure, processing or design, reflecting not only the results of the materials tests but also the results of subsystem design and test efforts. The test data generated at all levels of testing are analyzed and correlated to establish the use of screening test data and property measurements in predicting materials performance in dynamic and generator tests.

In this quarter effort was concentrated on 1) laboratory slag corrosion tests 2) hot channel structures development and evaluation ($T_{wall} \approx 1700°C$) and 3) fabrication of and testing of a cold wall test section (copper electrodes) in the Materials Test Facility (MTF).

TABLE 1

SUMMARY OF STATIC ELECTROCHEMICAL CORROSION TESTS*

Material	$MgCr_2O_4$	$MoSi_2$
Test ID No.	E-9	E-10
Temperature °C	1400°C	1400
Duration, min.	31	61
Electrode Separation, cm	0.64	0.64
Current Density A/cm^2	1.18	1.16
Voltage drop across slag, (Calculated) Start	9	28
End	14	19
Corrosion, ΔW, mm		
Cathode, ΔW_c	-0.019 (-0.118)**	-0.020
Anode, ΔW	-0.005	-0.006
$\Delta W_c/\Delta W_a$	3.8 (23.6)	3.3

*All runs were in a simulated eastern slag, E-03(A).
**Accounting for loss of partially spalled reaction layer.

3.1 Electrochemical Corrosion Screening Tests

Electrochemical corrosion tests have been shown to be a more severe but more realistic measure of the survivability of MHD electrode materials in hot slagging environments than simple immersion tests.[1] Static electrochemical corrosion experiments were run to evaluate the performance of $MgCr_2O_4$ and $MoSi_2$ electrodes in a simulated eastern slag. It was found that both these materials exhibited exceptionally good corrosion resistance, especially at the cathodes. The tests are summarized in Table 1 and the results are discussed below.

3.1.1 $MgCr_2O_4$ (E-9)

The $MgCr_2O_4$ material tested is an off-stoichiometric composition comprised of 60 m/o MgO and 40 m/o Cr_2O_3. It is predominantly $MgCr_2O_4$ with some MgO (saturated with Cr_2O_3) at the grain boundaries. Small amounts of Al_2O_3 and SiO_2 impurities were determined by SEM-EDAX to be concentrated in the $MgCr_2O_4$ phase. The average grain size is about 23 μm.

The mode of cathodic corrosion is illustrated in Figure 2(a). The major features are free Fe formation at the cathode due to electrolysis of the slag, grain boundary penetration by the slag and chemical transfer of Al and Fe from the slag into the reaction layer coupled with the removal of Cr from the scale into the slag.

An interesting feature shown in Figure 2(a) is the distribution of free Fe particles associated with the partially spalled off reaction scale. In all probability, Fe particles deposited first on the outer surface of the electrode but as the reactor scale grew and eventually split and spalled off, electrical conductivity was lost. This forced the slag electrolysis reaction ($Fe^{+2} + 2e \rightarrow Fe$) to occur at the inner reaction scale which was still intimately bonded to the electrode. Reactions such as these, illustrate the potentially complex nature of corrosion in an electric field, demonstrate why Faradic weight loss calculations are often inapplicable in predicting electrochemical corrosion of electrode materials, and point to the importance of running "static" tests as a means of monitoring the mechanism of the corrosion process.

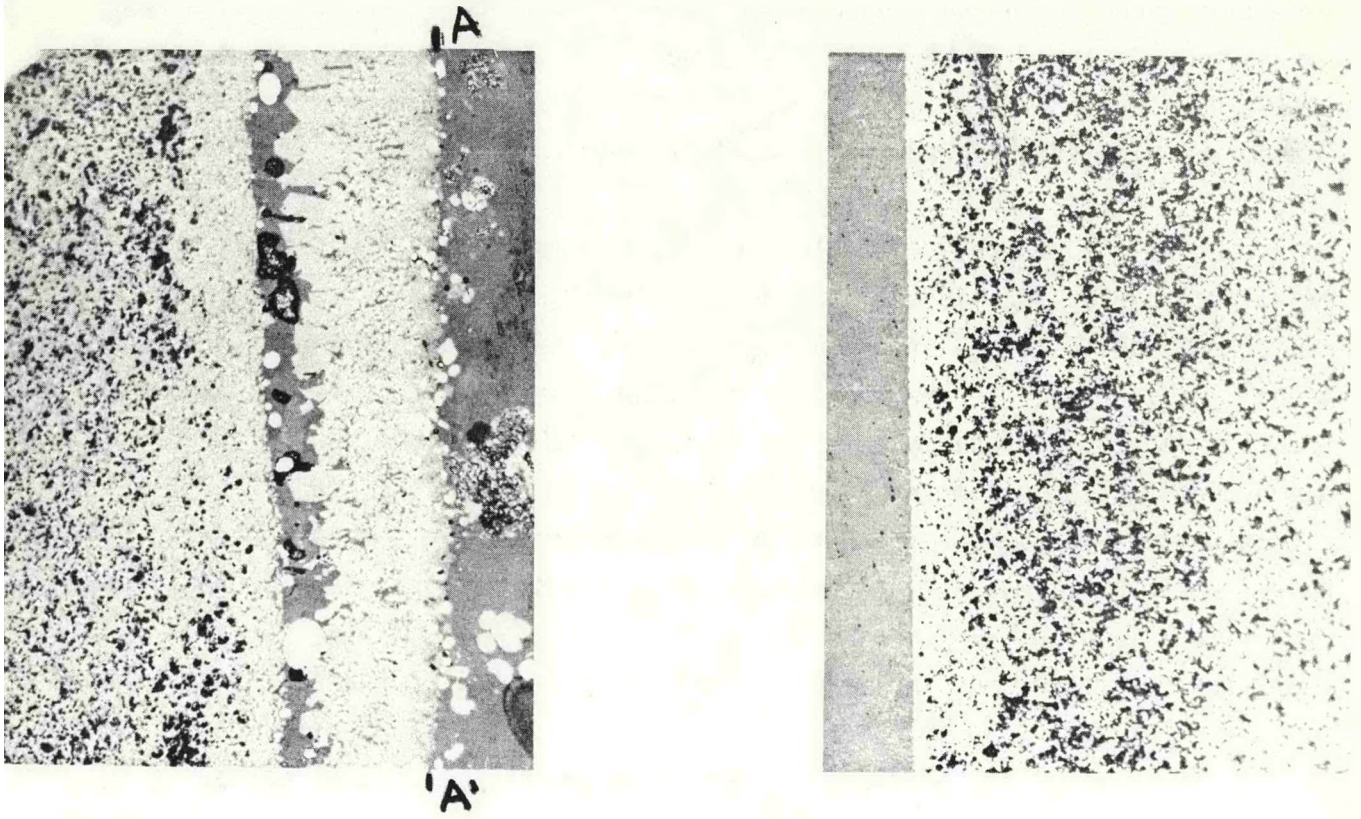

(a) (b)

Figure 2. Photomicrographs of $MgCr_2O_4$ Electrodes/Slag Interface after Electrochemical Corrosion Test E-9. 200X

a) A/A' White particles are free α-Fe.
Note: splitting of reaction scale

b) Anode/slag interface
Note: "porous" reaction tone

The major phase in the cathode reaction layer (still to be verified by X-ray diffraction) appears to be a complex spinel, Mg (Al, Fe, Cr)$_2O_4$, where both Al and Fe have replaced some of the Cr. At all locations adjacent to the reaction scale, the slag is enriched in Cr but depleted in Al and Fe.

At the anode (Figure 2b), the solutioning of chromium into the slag is much less extensive than at the cathode. Other than the existence of a very thin ($\approx$5 μm) rim of a MgCaAl silicate at the anode/slag interface, there are no major compositional gradients across the "porous" reaction zone. The porous nature of the "reaction zone" is probably due to the transformation of the MgO at the grain boundaries to a spinel material due to interactions with the slag. The resulting microstructure is similar to that found earlier in a slag immersion tested $MgAl_2O_4$ spinel material (S-2)[1] that contained $\approx$2.8 v/o MgO as the grain boundary phase.

Even when one factors in the loss of the partially spalled scale at the cathode, the extent of corrosion in $MgCr_2O_4$ is at least an order of magnitude less than that of other potential electrode materials previously tested in eastern slags.[1] Further improvements in corrosion resistance can be expected by reducing impurity levels and by utilizing a stoichiometric composition (i.e., eliminating the MgO phase at the grain boundaries).

3.1.2 $MoSi_2$ (E-10)

The "$MoSi_2$" tested is a composite material* containing $\approx$10 v/o SiO_2 in a matrix of molybdenum silicides. The matrix is in turn two phased containing $\approx$20 v/o Mo_2Si_3 and 80 v/o $MoSi_2$.

Figure 3 shows the cathode/slag interface after the electrochemical test. Again free iron has formed due to electrolysis of the slag at the cathode interface. There is a lightish colored band or reaction zone $\approx$70 μm thick at the slag interface (which unfortunately is not readily visible in Figure 3) that is predominantly Mo_5Si_3, formed by the preferential dissolution of Si from the matrix into the slag. Some Fe and to a lesser extent, Al, has diffused into this zone,

*Kanthal-Super heating element, Kanthal Corp., Bethel, Conn.

Figure 3. $MoSi_2$ Cathode/Slag Interface for Electrochemical Test E-10
Light particles in slag (right) are free α-Fe. 200X

although the quantities are small. There is no evidence for Mo dissolving into the slag. The original SiO_2 matrix particles in this sample are readily attacked at the slag interface and are converted into a potassium-alumino-silicate phase. The reactions at the anode are essentially the same as at the cathode although the quantities of K and Fe are somewhat less.

3.2 Electrode/Insulator Development

The first hot ($T_{wall} \approx 1700°C$) test section to be tested in MFT will consist of $LaCrO_3$ electrodes. Lanthanum chromite electrode systems can be prepared by plasma spraying powders directly onto a substrate or by attaching monolithic pieces machined from hot pressed or pressed and sintered blocks to a current leadout. Plasma sprayed electrodes generally have plasma sprayed insulators, but may have monolithic insulators. Monolithic electrodes almost always have monolithic insulators. Some of the advantages and disadvantages of plasma sprayed and monolithic electrode systems are listed in Table 2. Various aspects of the operations performed in preparing the two types of electrode systems are discussed below.

3.2.1 Plasma Sprayed Lanthanum Chromite Systems

Supplementing Westinghouse efforts in developing attachments for monolithic lanthanum chromite MHD electrode systems, a limited effort on plasma sprayed lanthanum chromite was undertaken for the primary purpose of supplying samples of plasma sprayed materials to Battelle Northwest Laboratories and the National Bureau of Standards for evaluation. In preparing samples from different powder sources, it was found that the density of the deposits ranged from below 80 to over 90 percent of the theoretical density of lanthanum chromite (6.64 gm/cm^3) with the finest sprayable powder yeilding the highest density deposit. Open porosity predominates, but decreases significantly with increasing density. These data, for powders of different particle size ranges, are given in Table 3.

A scanning electron micrograph of the coarsest powder is compared to a powder used for the preparation of hot pressed specimens in Figure 4. The coarse, high fired sprayable powder is found to consist of irregularly shaped particles with a fibrous

TABLE 2

COMPARISONS OF BASIC ELECTRODE SYSTEMS

	Plasma Sprayed	Hot Pressed/Pressed or Sintered
Advantages	• Direct Bond to Metal • Minimum Machining • Good Thermal Shock Resistance	• High Density - Closed Porosity • Machines Easily • Thermally Stable
Disadvantages	• Unproven in Thick Sections • Low Density - Open Porosity • Thermally Unstable - Sinters • Possible Chemical Change in Spray Arc	• Ceramic to Metal Attachment Required - Performance Depends on Attachment Method

TABLE 3

EFFECT OF STARTING POWDER ON SOME PROPERTIES OF PLASMA SPRAYED LANTHANUM CHROMITE(1)

Starting Powder			
Source	General Refractories	Cerac	Cerac
Size Range	-150+325	-200+10μ	-325
Plasma Sprayed Sample			
Density (% Theoretical)	77.6	85.3	90.4
Open Porosity (%)	22.5	10.4	4.0
Effect of Sintering(2)			
Shrinkage (%)			
Avg. length x width(2)	--	0.3	1.9
Thickness(4)	--	1.2	11.9
Density (% Theoretical)	--	88.9	92.4
Open Porosity (%)	--	6.5	3.0

(1) Data average of two determinations.

(2) Plasma sprayed samples held 2 hrs at 1650°C.

(3) In plane of substrate.

(4) In direction of plasma spray stream.

(a) Powder used for plasma spraying (1700X) Fired to 1800°C, 2 hrs.; Screened to -150 + 325 mesh.

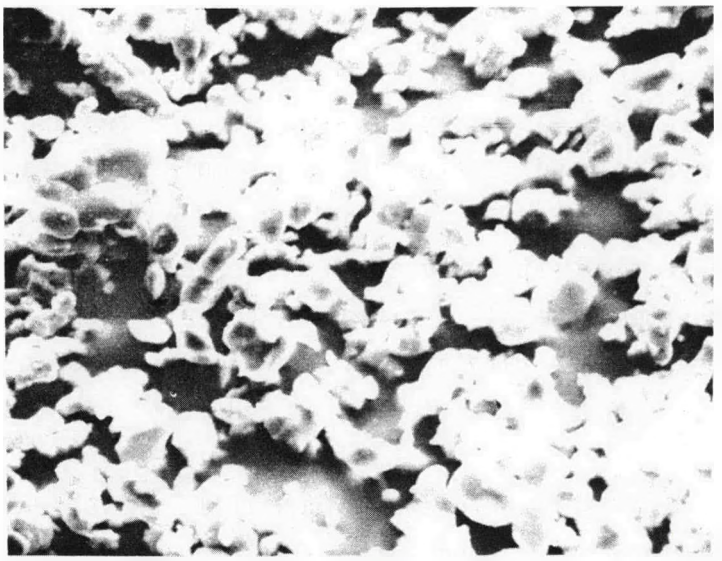

(b) Powder used for hot pressing (1700X) Fired to 1500°C, 6 hrs.; Screened to -325 mesh.

Figure 4. Scanning Electron Micrograph of Lanthanum Chromite Powders (Powder Soma - General Refractories).

texture and an apparently high degree of open porosity. These properties, i.e., the low density and high degree of open porosity are reflected in the characterization of the plasma sprayed deposit. Powders from other sources are yet to be characterized in this manner.

While high density and low open porosity are desirable features of MHD electrodes, an x-ray diffraction analysis of the most dense deposit showed that the material changed from a single phase powder with good crystallinity to a deposit of poor crystallinity with about 10% of an unknown phase and about 5% of lanthanum oxide. This data is presented in Table 4 and the change shown by the dense deposit (-325 mesh starting powder) may be a function of the amount of fine material in the powder and the volatilization of chromia from fine particles heated in the plasma arc. This problem should receive greater attention because of the potentially damaging effect that lanthanum oxide hydration can have on fabricated MHD electrodes.

It has been noted that the surfaces of plasma sprayed electrode systems tend to shrink during testing and sometimes pull away from the substrate. To explore this effect, samples of plasma sprayed lanthanum chromite were heated and held for 2 hours at 1650°C. The dimensions and density of each sample were measured before and after sintering. These data are given in Table 3 and related to the starting powder and plasma sprayed sample. It is noted that the sample sprayed from the finest powder shows the greatest overall shrinkage. For both samples the shrinkage is greatest in the thickness of the sample, i.e., in the direction of spraying. Both samples also show a slight densification and a reduction in open porosity.

One of the advantages of plasma sprayed systems identified in Table 2 is that the deposit is directly bonded to a metal substrate. The bond is basically mechanical. To get some relative numbers on the strength of the bond some pull strength specimens were prepared from a plasma sprayed Y_2O_3-ZrO_2 capped lanthanum chromite electrode sprayed onto a titanium substrate with an MIT-type pin structure. Three specimens were prepared by brazing the titanium to a silicon bronze bolt and attaching another bolt to the cap with silver spray adhesive. These samples were pulled on an Instron testing machine at a cross-head speed of 0.2"/min. Tensile failure occurred at the cap/electrode interface at an estimated 320 psi

TABLE 4

X-RAY DIFFRACTION ANALYSIS OF PLASMA SPRAYED SAMPLES OF LANTHANUM CHROMITE*

Starting Powder	Plasma Sprayed	Sintered 2 hrs 1650°C
Cerac, Inc. - 200 mesh + 10 microns. Medium crystallization, no parameter shifts, no other phases.	$LaCrO_3$ + 5% unknown phase. No La_2O_3.	$LaCrO_2$ + 5% Unknown phase, but with line shift from plasma sprayed unknown phase.
Cerac, Inc. - 325 mesh. Single phase, good crystallinity.	$LaCrO_3$ + 10% unknown phase + 5% La_2O_3; poor crystallinity.	$LaCrO_3$ + 5% $La(OH)_3$; good crystallinity.

*The x-ray diffraction analysis was performed by the National Bureau of Standards.

(based on the average breaking load divided by the average area of the broken surface). The tests were then repeated by attaching the bolts to the plasma sprayed lanthanum chromite. For this system, tensile failure occurred in the lanthanum chromite at the top of the pins at an estimated 1730 psi. This value represents the tensile strength of the plasma sprayed lanthanum chromite to titanium.

3.2.2 Plasma Sprayed Insulators

As stated earlier, plasma sprayed electrodes will generally have plasma sprayed insulation. For lanthanum chromite electrodes the insulation will be either magnesium aluminate or strontium zirconate. To evaluate these materials, plasma sprayed samples were prepared from different powders and tested along with the lanthanum chromite samples that were discussed above.

For the magnesium aluminate system, powder of the two particle size ranges tested produced plasma sprayed deposits having comparable densities (Table 5). Sintering these samples at 1650°C caused negligible shrinkage in the plane of the substrate upon which they were sprayed and an order of magnitude greater shrinkage in the spraying direction. Both samples showed a reduction in the amount of open porosity without appreciable changes in density. X-ray diffraction analyses (Table 6) of the starting powder and the plasma sprayed deposit showed that the deposit remained single phase with only a modest change in crystallinity due to plasma spraying.

For the strontium zirconate system, the finer starting powder was found to give a plasma sprayed deposit having a higher density and lower open porosity that the product obtained with the coarser starting powder. Upon sintering at 1650°C, both sprayed samples showed greater shrinkage in the plane of the substrate upon which they were sprayed and greater densification than magnesium aluminate. Shrinkage data in the other direction is questionable. X-ray diffraction analyses of the starting powder and the plasma sprayed deposit showed that a breakdown of strontium zirconate to yield free zirconia occurs upon plasma spraying. From the standpoint of fabrication, the data presented in Tables 5 and 6 indicate that

TABLE 5

EFFECT OF STARTING POWDER ON SOME PROPERTIES OF PLASMA SPRAYED INSULATORS(1)

Starting Powder	$MgAl_2O_4$		$SrZrO_3$	
Source	Cerac	Cerac	Cerac	Cerac
Size Range	-150+325	-325+10μ	-150+325	-325+10μ
Plasma Sprayed Sample				
Density (% Theoretical)	92.6	93.6	81.0	89.2
Open Porosity (%)	5.2	5.8	19.2	9.5
Effect of Sintering(2)				
Shrinkage (%)				
Avg. length x width(3)	0.1	0.4	1.0	3.3
Thickness (4)	2.8	6.7	-	+4.2
Density (% Theoretical)	91.5	92.0	85.6	95.3
Open Porosity (%)	0.8	0.8	11.7	4.2

(1) Data average of two determinations.

(2) Plasma sprayed samples held 2 hrs at 1650°C.

(3) In plane of substrate.

(4) In direction of plasma spray stream.

TABLE 6

X-RAY DIFFRACTION ANALYSIS OF PLASMA SPRAYED INSULATOR SAMPLES(1)

Starting Powder	
Cerac, Inc., $MgAl_2O_4$, -150+325, single phase, good crystallinity.	From Cerac, Inc., $MgAl_2O_4$, -325+10μ; plasma sprayed deposit single phase, medium to good crystallinity.
Cerac Inc., $SrZrO_3$, -150+325, single phase, good crystallinity.	Fr-m Cerac Inc., $SrZrO_3$, -325+10μ; plasma sprayed deposit $SrZrO_3$, good crystallinity +5-10% tetragonal ZrO_2, poor crystallinity.

(1) X-ray diffraction analyses performed by the National Bureau of Standards.

plasma sprayed magnesium aluminate is a better insulator choice than plasma sprayed strontium zirconate.

3.3 Electrode/Insulator Structures

Hot pressed lanthanum chromite electrodes have been joined to copper by direct brazing through low expansion metals, e.g., titanium, KOVAR, or molybdenum, through the use of a compliant layer, e.g., BRUNSBOND, a sintered metal felt product or, as in the UO2 Phase II module, through metallization with plasma sprayed copper and brazing to copper screens. Each of these methods have had problems that resulted in failure during test. These failures have been due to thermal-mechanical or electrical stresses generated during testing. Thus, alternate designs that minimize the effect of these stresses are being considered.

3.3.1 Direct Attachment Techniques

To insure good thermal and electrical conductivity, the ceramic electrode has to be well bonded to a metal or other conductive material. The bond can be formed by brazing, metallization, or using a conductive adhesive. These possibilities are discussed below.

Brazing - TiCuSil is the only braze alloy found to date that wets the lanthanum chromite surface. Other braze alloys can be used if the surface is first metallized by any one of a number of techniques. (Metallization will be discussed in one of the following sections). Due to the large expansion difference between the two materials, direct brazing of lanthanum chromite to copper has not met with much success. The use of a metal that more closely matches the thermal expansion of lanthanum chromite usually has to be present between the ceramic and copper. Titanium, KOVAR, and molybdenum have been successfully used in this attachment. Although these metals are compatible with lanthanum chromite on the basis of thermal expansion, they apparently do not overcome the problem of failure due to thermal stress.

What initially looks like a good strong bond apparently degrades with time. In preparing specimens for pull strength measurements, it was observed that a sample

of lanthanum chromite brazed to titanium with TiCuSil that had been around for a long time came apart with relative ease. The failure occurred slightly above the brazed joint and revealed an uncharacteristically smooth fracture surface. A reaction between the brazing alloy and the ceramic was postulated where the titanium reduces the Cr_2O_3 to metallic chromium and forming free La_2O_3, i.e., $4\ LaCrO_3 + 3T_i \longrightarrow 3\ TiO_2 + 2\ La_2O_3 + 4\ Cr$. To check on this, two samples of lanthanum chromite were prepared by drilling a small hole into the surface and filling it with TiCuSil foil. One sample was placed in a vacuum furnace and held at the brazing temperature (850°C) for one minute (normal brazing conditions) and the other sample was placed in the vacuum furnace and held at 850°C for one hour. These samples were sectioned and mounted for metallographic examination. During polishing it was noted that the zone between the brazing alloy and the lanthanum chromite was very reactive to water and polishing solutions and difficult to maintain. All of the evidence observed thus far points to the formation of lanthanum oxide at the interface between the brazing alloy and lanthanum chromite. Photomicrographs of these samples are shown in Figure 5.

Metallization - Because the brazing of lanthanum chromite with TiCuSil has been found to be unreliable, attention has been redirected to the metallization of the lanthanum chromite surface so that other brazing alloys can be used. Plasma spraying offers a convenient way of metallizing ceramics and lanthanum chromite has been coated with copper and mixed in this manner. The ease of metallization in this technique depends upon the density of the surface. The less dense it is, the easier it is to roughen the surface to achieve the mechanical hold needed for adherence of the plasma sprayed layer, and hot pressed lanthanum chromite presents a very hard, dense surface that is difficult to roughen by abrasive blasting. Differences in thermal expansion and thermal conductivity between the metal and the substrate create stresses that limit the thickness of these layers to a few mils. The application is quite sensitive to thickness and higher thicknesses may spall off of the lanthanum chromite. Although the process in the laboratory is operator controlled and, consequently, subject to variable results, it is also one of the more positive methods at this time.

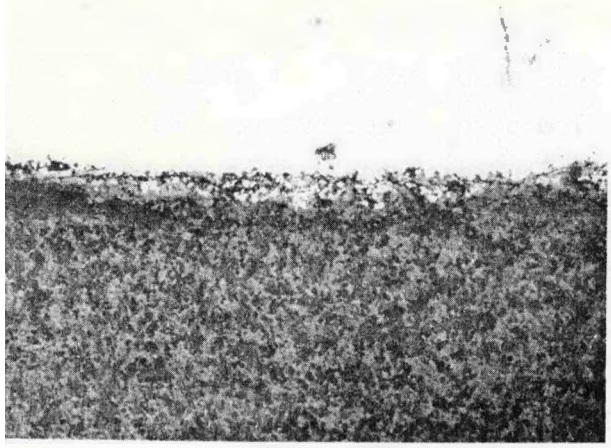

a) Edge, 1 min. hold (400X)

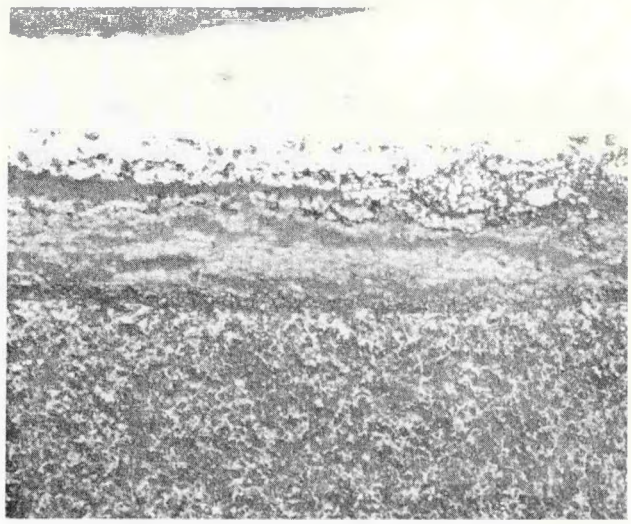

b) Edge, 60 min. hold (400X)

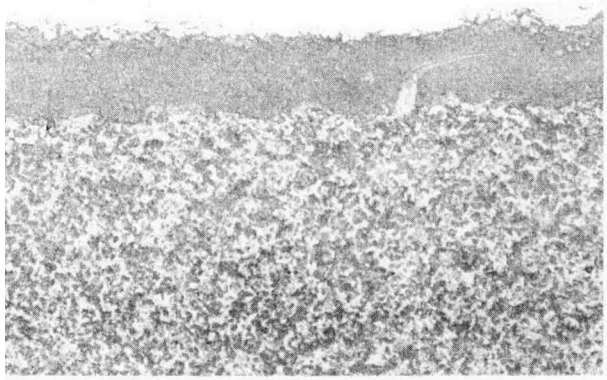

c) Base, 1 min. hold (400X)

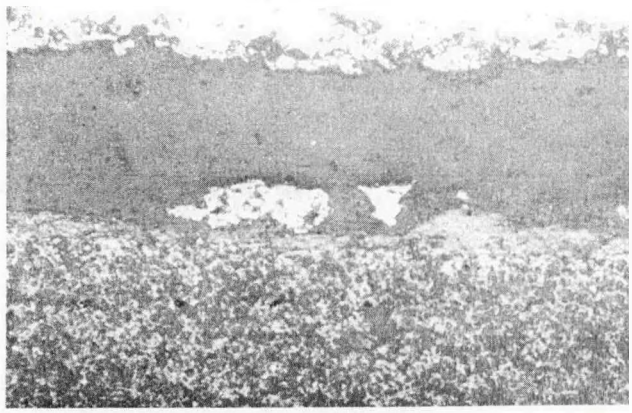

d) Base, 60 min. hold (400X)

Figure 5. Extent of Interfacial Reaction Zone at Interface of TiCuSil Brazing Alloy and Lanthanum Chromite

Dense surfaces can be coated by spattering, but the metallized layers obtained by this technique are only a few microns thick and can be taken into solution during the brazing operation. Ion plating has also been tried, but requires additional study to evaluate the relationship between thickness, adherence, and brazing performance. A four mil nickel plating was applied to lanthanum chromite, and separated from it during brazing. Although the ion plating process is reproducible, unless thinner coatings are more adherent, the bond strength of ion plated nickel to lanthanum chromite may not be adequate in this application.

The feasibility of another reproducible process, electroplating is also being investigated. It appears that at a very high current density a very adherent copper strike can be deposited that can be overplated with copper, nickel, or other metals. The similar application of a nickel strike will be explored, and a test program involving brazing, thermal cycling, etc. will be pursued.

Some fired on coatings have been looked at, but only noble metal coatings may be satisfactory. Nickel and copper coatings turn out to be mainly oxides even when fired under reducing conditions. Since these pastes, ink, and solution were developed for thin film applications, repetitive operations are needed for a deposit of adequate thickness for brazing.

Adhesives - Adhesives provide another method of directly attaching a ceramic electrode to metal. Conductive epoxies and silicones are available and useful to 200 to 250°C. Because lanthanum chromite has adequate conductivity to room temperature, it is possible to use these adhesive attachments. A silver filled epoxy and a silver-filled silicone are being evaluated. They both bond well to lanthanum chromite. The epoxy gives an especially strong bond while the silicone is attractive because it remains flexible. Simi-quantitative evaluations have been made on the strength of their bond to lanthanum chromite and, also, their performance as a primary adhesive in a torch test. Both strength and performance are satisfactory.

3.3.2 Compliant Layers

Compliance is provided for these electrode systems by a layer of material that will permit the ceramic electrode to deform to relieve thermal stress and at the same time maintain electrical and thermal conductivity. The compliant layer is between the ceramic electrode and the copper leadout and has to be cemented or brazed to both or be mechanically held in place.

One compliant layer already tested was a 40% dense, 0.040 inch thick sintered metal felt brazed between the ceramic and copper by Technetics Division of Brunswick Corporation. This material may not have provided sufficient compliance because, upon testing in the M.I.T. facility, the cermaic failed above the braze line. Greater compliance would have been provided by less dense material, but the already poor thermal conductivity of the mesh would have been worse. Conductive low modulus fillers could be used with compliant layers that have open structures to overcome this problem.

Brunswick Corporation is providing lanthanum chromite electrode systems brazed to a 35 to 40 percent dense nickel mesh for the UO2 Phase III proof testing program. The nickel is a softer and more compliant than the Hoskins 875 alloy mesh that they used in previous assemblies.

Westinghouse will be using several different compliant materials in electrode designs that will be prepared for hot channel tests. Materials on hand include woven nickel mesh, stainless steel felt, monel wire braid, and nickel-filled silicone rubber pad. These materials are representative of commercially available materials. A design based on a compliant corrugated metal sheet is also being manufactured and simple torch tests are being run on small samples to evaluate attachments and compliant layers.

3.3.3 Mechanical Attachments

Any number of mechanical attachment designs for holding a ceramic in contact with a metal leadout are possible with or without compliant layers. The important

thing is that they permit the natural deformation of the ceramic and maintain structural, thermal, and electrical integrity.

The larger the ceramic piece that has to be held, the greater the possibility of mechanical attachment. For a U-02 type channel with low heat flux and thick electrodes, the design of mechanical attachments is easier than it is for a U-25 type channel with high heat fluxes and thin electrodes. Several mechanical attachments for a U-02 type cannel are being considered as redundant attachments in evaluating other attachment materials in a hot channel test.

3.3.4 Electrode Modification

Attachment techniques can benefit from changes in the electrode properties at the surface to be joined to the leadout. These changes should increase the thermal expansion of the ceramic electrode and/or reduce its modulus, especially in the area of attachment. Composite structures graded from an electrode cap to a leadout are under development and are prepared by mixing powders of different compositions in different ratios. Another method is to alter the properties of the ceramic electrode by forming solid solutions of varying composition, e.g., the addition of alumina to make lanthanum chromite more refractory. In order to improve attachment possibilities, the effect of $LaCoO_3$ with its low modulus and high coefficient of thermal expansion (28×10^{-6} at 1000°C [2]) on lanthanum chromite was examined.

A series of powders having the following compositions

$$LaCoO_3$$
$$La_{.95}Mg_{.05}Cr_{.25}Co_{.75}O_3$$
$$La_{.95}Mg_{.05}Cr_{.50}Co_{.50}O_3$$
$$La_{.95}Mg_{.05}Cr_{.75}Co_{.25}O_3$$

were prepared from the individual oxides or oxide formers by slurry milling, drying, and calcination techniques. Samples were pressed from these powders and sintered (1300°C for $LaCoO_3$; 1500°C for the others) to provide samples for properties

measurements. The variation of some properties with composition is shown in Figure 6. Figure 7 shows the thermal expansion curves for the above composition and for lanthanum chromite. The effect of cobalt on the thermal expansion of lanthanum chromite is large enough to tailor compositions to match the expansion of copper or other leadout materials on one side of the electrode and to tailor it to match the expansion of zirconia based cap materials on the plasma side of the electrode. Although the melting point of pur $LaCoO_3$ is around 1450°C, all of the mixed powder compositions that were prepared were heated above 1700°C without any signs of melting. Further development of this system should continue.

3.3.5 Testing of Electrode Structures

Given the number and variety of possible attachments obtained above, the problem becomes one of a narrowing them down via intuitive judgements or discriminating tests. Various mechanical, electrical and chemical (oxidation with and without seed) tests can be developed in the laboratory. Thus far, only a limited number of crude bond strength measurements and simple torch tests have been made. This effort must be expanded to establish the confidence level necessary prior to placing an electrode system in a full generator.

Bend Strength Measurements

A sketch of the assembly used to obtain strength measurements in shown in Figure 8. This simple system provides the engineering data given in Table 7. The plasma sprayed systems shown in the table were discussed earlier in this report. It was in preparing samples for strength measurements that the problem of using TiCuSil brazing alloy with lanthanum chromite (also discussed in a previous section of this report) was discovered. This problem accounts for the low strength and smooth fracture surfaces on most of the TiCuSil brazed samples tested. It is estimated that the samples were tested about 5 months after they were prepared, and was more than enough time for hydrolysis of free lanthanum oxide to occur. Samples of lanthanum chromite, metallized with plasma sprayed copper or nickel, and brazed with silver-copper eutectic alloy turned out to be surprisingly strong with one exception in each case. The exceptions indicate the variability inherent in the operator-controlled plasma spray process.

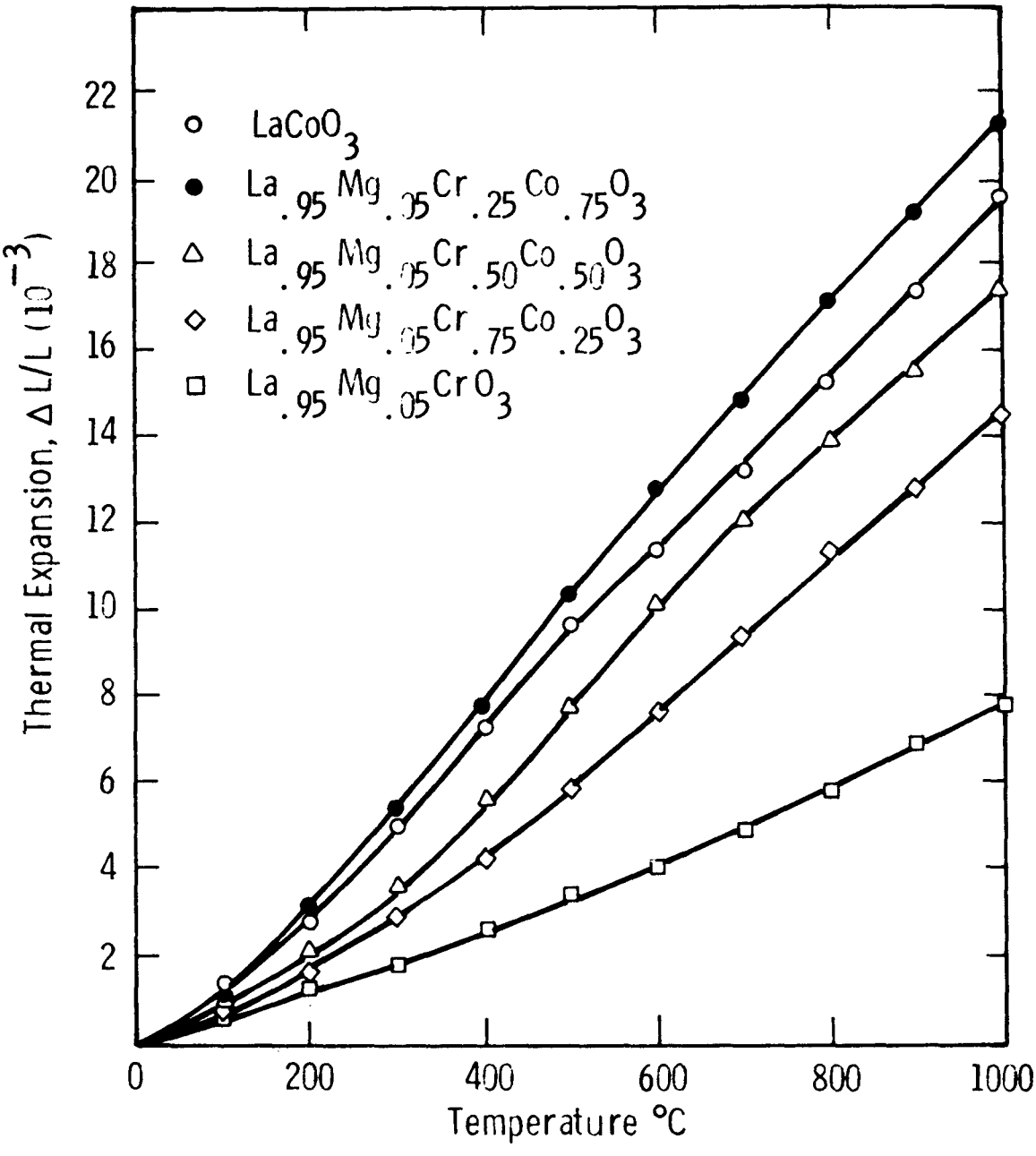

Figure 6. Thermal Expansion of Cobalt Doped Lanthanum Chromite

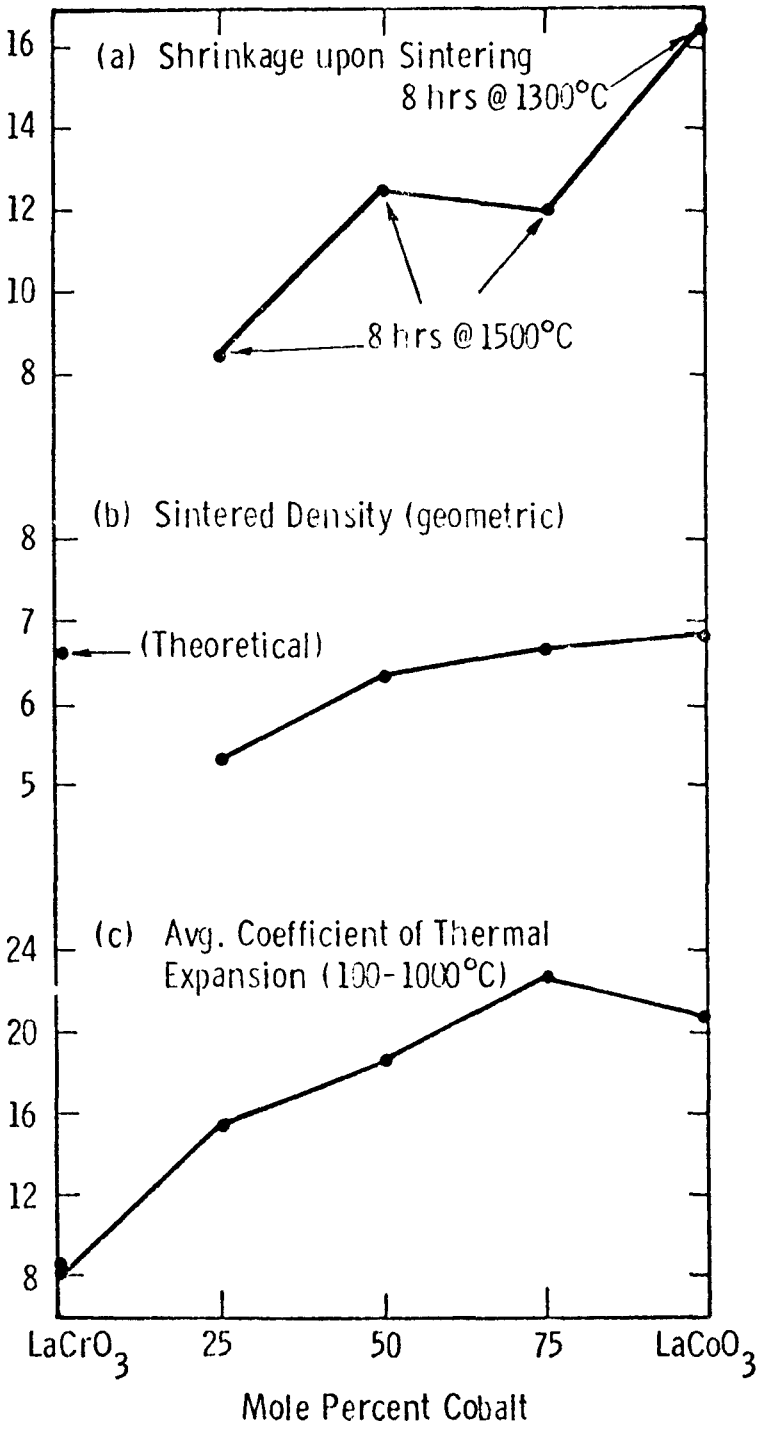

Figure 7. Variation of Properties of Cobalt Doped Lanthanum Chromite

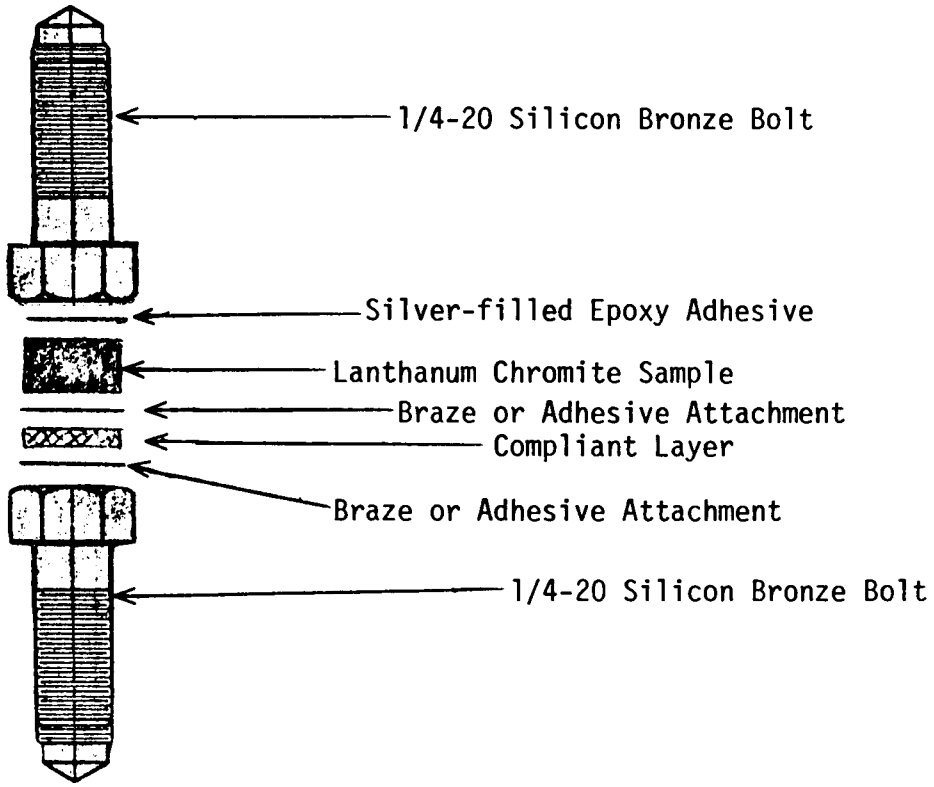

Figure 8. Sketch of Assembly Used for Bond Strength Measurements

TABLE 7

STRENGTH MEASUREMENTS ON SIMULATED ELECTRODE SYSTEMS[1]

System Tested	Breaking Strength	Failure Description
Plasma Sprayed		
Y_2O_3 cap on $LaCrO_3$	22.5, 71.3, 60.1	At cap to electrode interface
$LaCrO_3$ on Ti pin structure	295.0, 380.0, 224.0	In $LaCrO_3$ at top of pins
Monolithic Systems		
$LaCrO_3$ + TiCuSil braze to Ti	176.4	Cup fracture within $LaCrO_3$
	79.5	Partial failure within $LaCrO_3$
	22.7, 20.0, 32.7	Smooth fracture slightly above braze line
$LaCrO_3$ (plasma sprayed with copper) BT braze to bolt	82.2, 84.2	Partial failure within $LaCrO_3$
	28.0	Failure mostly at plasma sprayed copper
$LaCrO_3$ (plasma sprayed with nickel) BT braze to bolt	72.7, 136.0	Partial failure within $LaCrO_3$
	28.0	Failure mostly at plasma spray nickel

(1) Crosshead speed = 0.2"/min.

Some tests were run on adhesive attachment but were not included in the table because the data was misleading. The silver-filled silicone was thought to give a weak bond, but the specimen tested may not have been fully cured and the tests will be repeated. The silver-filled epoxy was found to give a very strong bond to lanthanum chromite and although it is used in preparing the samples for tensile testing, no quantitative data on the silver filled epoxy system has been obtained. However, from some of the tests on other systems, the silver-filled epoxy bond is apparently stronger in these tests than the lanthanum chromite itself.

Torch Tests

A number of torch (oxygen-propane) tests were conducted to primarily evaluate two important MHD material areas: 1) Determine the thermal shock resistance of a number of interelectrode insulators, and 2) Check the performance of different electrode attachment methods.

The electrode/insulator assemblies used for the torch test were fabricated to one third the size of the assemblies to be used for the U-02 Phase III proof tests. Two assemblies are shown in Figure 9. The copper cooling blocks were designed as two separate copper units, screwed together to facilitate easy replacement of the insulator/electrode unit. Harklase* brick was placed around each electrode/ insulator assembly during the test. Each of the copper blocks was water-cooled individually. The results of the six completed tests are shown in Table 8.

12 m/o Y_2O_3-88 m/o ZrO_2 was used as the electrode material in all but one case due to the unavailability of $La_{.95}Mg_{.05}CrO_3$ at the time of testing. All of the tests were run up to the selected maximum surface temperature within 1 1/2 hours of startup. The maximum surface temperature was maintained for 1 hour prior to the 1 1/2 hour cool down. Thermocouple readings within the electrode and copper were taken to calculate the backface temperature of the electrode, along with the surface heat flux. Surprisingly, the silver epoxy and silastic used in a majority of the tests did not show signs of bond failure even though the electrode backface temperatures surpassed the recommended maximum temperature use of 250°C.

*MgO, Harbison-Walker, West Mifflin, Pa.

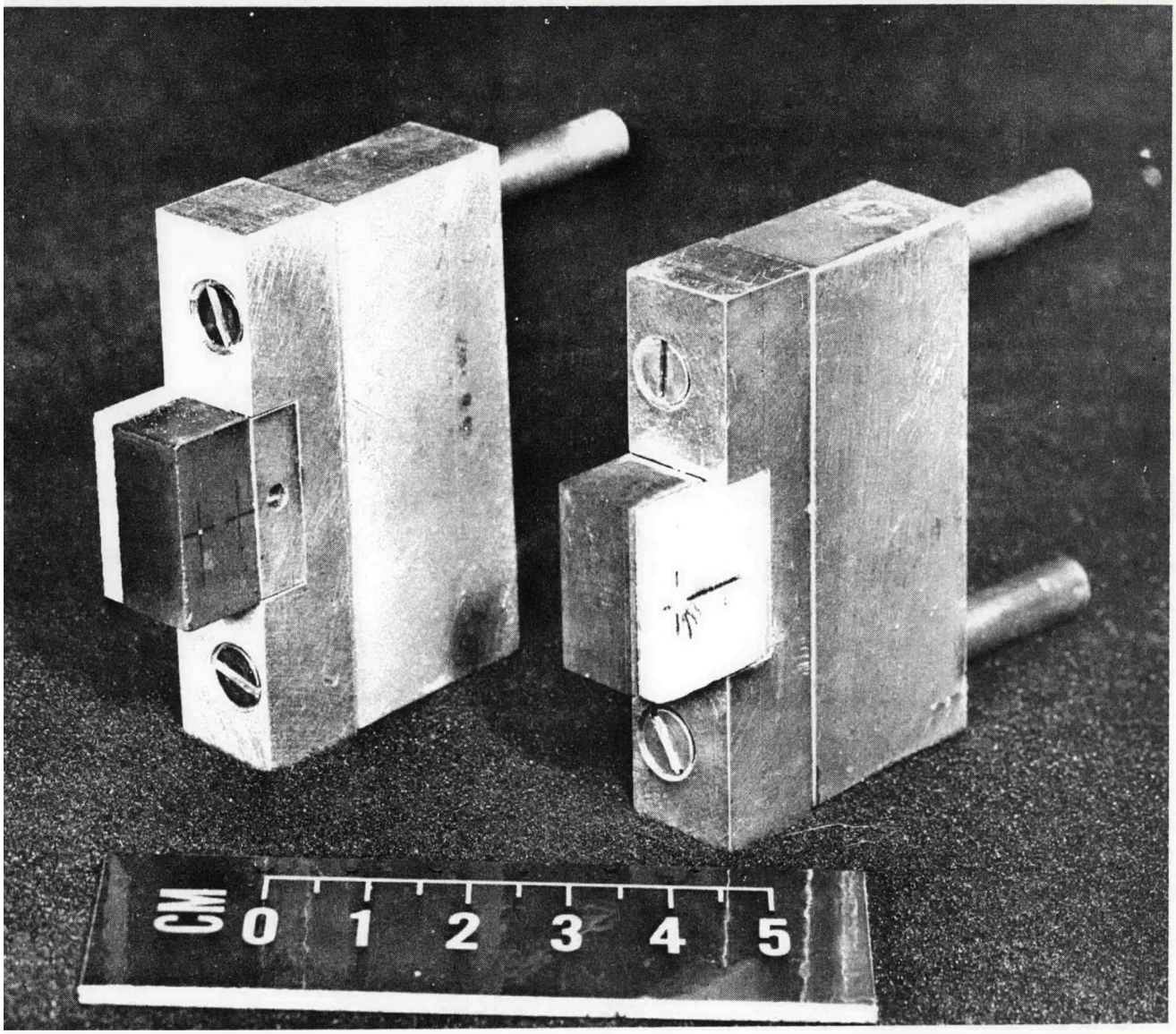

(White - MgO insulator; Dark - Lanthanum chromite electrode)

Figure 9. U-02 Phase III Electrode/Insulator Assembly Used for Preliminary Torch Tests

TABLE 8

U-02 PHASE III MATERIALS/ATTACHMENT TORCH TEST (Oxygen/Propane)

Test	Electrode	Insulator	Attachment	Thermal (electrode) Conductivity w = cm°C	Maximum Surface Temp.	Electrode Δx	Heat Flux w/cm^2	Observations
1	$La_{.95}Mg_{.05}CrO_3$ (General Refractories)	$MgAl_2O_4$ HP- W	Silver Epoxy	$K_{av} \cong 0.0225$	1700°C	1 cm	24.5	Back face temp reached ∿611°C, expoxy bond broken, spinel cracked at copper insert interface, epoxy still bonded to copper on spinel.
2	12 w/o Y_2O_3-88 w/o ZrO_2	$SrZrO_3$ (Ceraç)	Silver	$K_{av} \cong 0.0123$	1700°C	1 cm	14.8	No cracks in either electrode or insulator, epoxy still bonded to both; back face temp. reached 506°C.
3	12 Y_2O_3-88 ZrO_2	MgO (Norton)	Silver Silastic	$K_{av} \cong 0.0123$	1725°C	1 cm	14.4	No cracks in insulator or electrode, silastic still bonding to electrode, insulator loose at interface between ceramic and copper. Backface temp. reached 555°C.
4	12 Y_2O_3-88 ZrO_2	MgO (Norton)	Silver epoxy between Copper and Techfelt,* Techfelt brazed to electrode with Nicosil	$K_{ave} \sim 0.0123$	1715°C	1 cm	13.8	No observable cracks in either electrode or insulator; all attachments held. Backface temp. reacted 591°C. Slight bowing of electrode was observed.
5	12 Y_2O_3-88 ZrO_2	MgO (Norton)	Silver epoxy between Copper and Brunsbond; Brunsbond△ brazed to electrode with Nicosil	$K_{ave} \approx 0.0123$	1705°C	1 cm	13.7	Corner cracked on electrode before test. Insulator cracked upon rapid cooldown. Backface temperature reached 592°C.
6	12 Y_2O_3-88 ZrO_2	MgO (Norton)	Silver epoxy	$K_{av} \cong 0.0123$	1700°C	1 cm	16.1	Epoxy bond was unbroken; insulator had cracked into 2 pieces during the test. Backface temp. of electrode reached 392°C. Conducting grease was applied between the mating copper interfaces, may account for decrease in backface temperature.

*Stainless steel mesh, Technical Wire Products, Inc. Crawford, N.J. 07016
△Hoskins 875, Technetics Div., Brunswick Corp., Milford, Conn. 06460

3.4 Test Section Fabrication

3.4.1 Cold Wall Test Assembly-(Copper Electrodes)

Assembly of the first cold wall, copper electrode, test assembly with alumina interelectrode insulators and insulating walls was completed and is currently under test in the MTF (Materials Test Facility) Figures 10 through 18 illustrate the construction of the test assembly.

Figure 10 shows a view of an electrode wall. There are twelve electrodes in each of the identical anode and cathode walls. The electrodes are one centimeter wide in the direction of plasma flow and about six centimeters long with an area of about five square centimeters exposed to the plasma flow. The pitch between electrodes is about 1.4 centimeters. Each electrode is machined from OFHC copper. Cooling water passages are located at different distances from the electrode surface to give an electrode surface temperature profile of from 100 to 400°C for this first test. Passage plugs and coolant tubes are brazed to the copper electrode with silver-copper eutectic alloy. Interelectrode insulators were machined from 87 percent dense alumina and cemented to the step in the copper electrode with silver-filled epoxy cement applied to the base of the insulator. Other insulation on the electrodes consists of an insulating varnish painted on the sidewalls and bases of electrodes designed to operate below 200°C and plasma sprayed alumina on the sidewalls and bases of electrodes designed to operate above 200°C. "O" rings are placed over the coolant tubes at the base of the electrode and the electrodes are attached with machine screws to a NEMA G-11 laminated phenolic mounting block that is the main channel support structure for both holding the electrodes and supporting the top and bottom insulating walls.

Another view of an electrode wall appears in Figure 11. One of the two machine screws used to fasten the electrode to the mounting block also serves as an electrical connection and this view shows the electrical wiring from the machine screws holding a crimped ring terminal to a rectangular quick-connect terminal used for final hook-up in MTF. Cooling water flow is supplied through flexible tubing clamped to the copper tubes brazed to the electrode coolant passages.

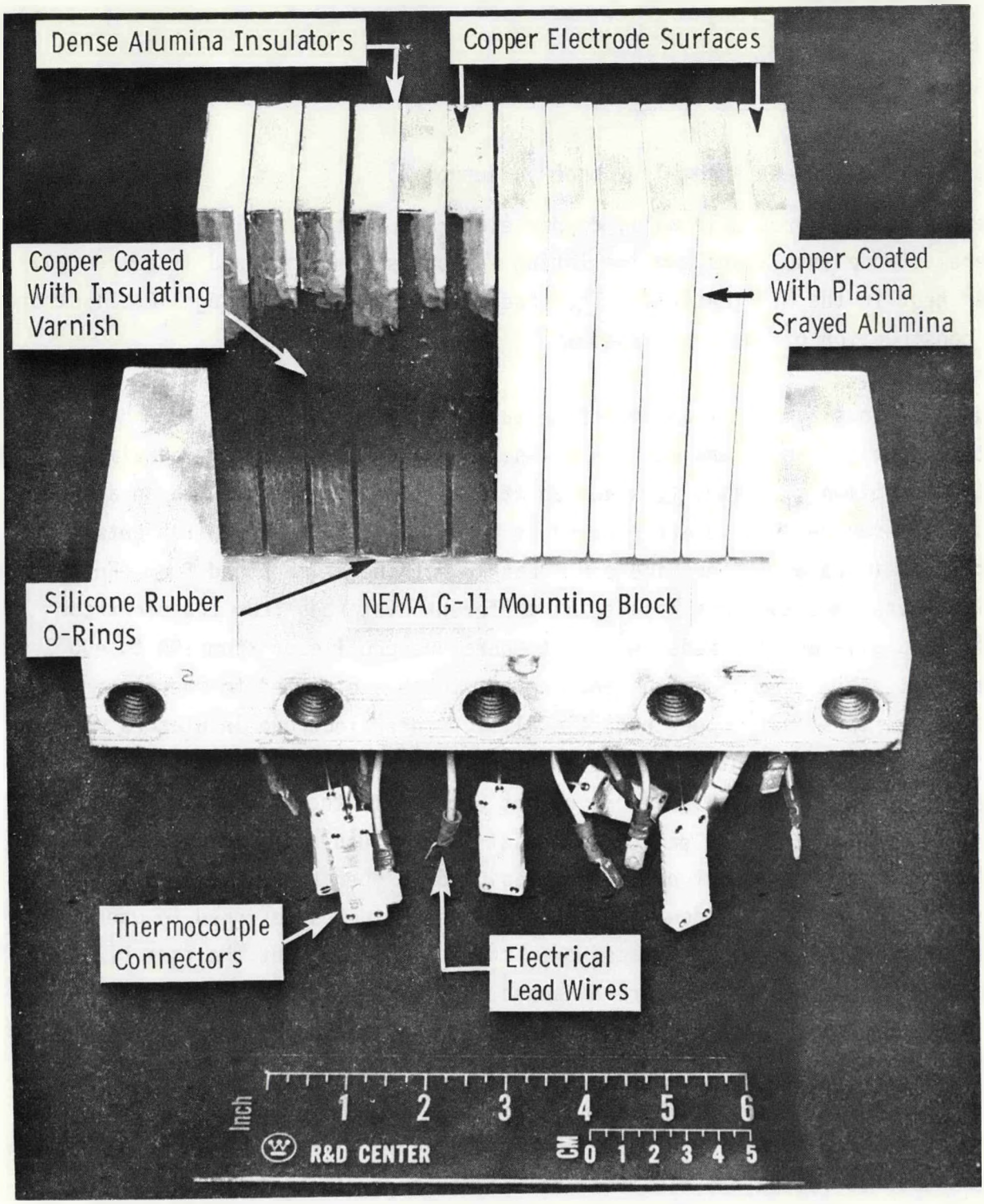

Figure 10. Side View of Electrode Wall

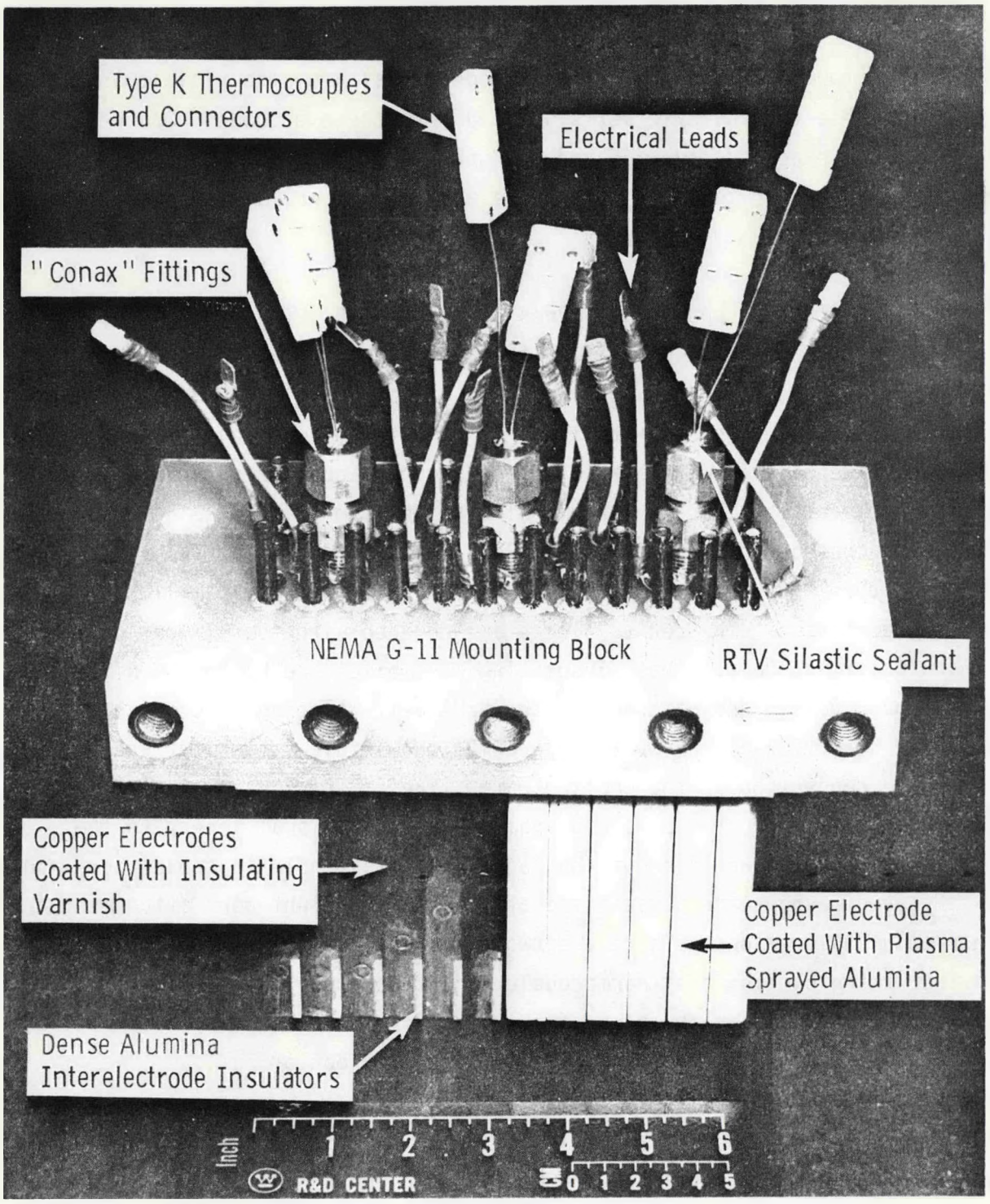

Figure 11. View of Outer Surface of Electrode Wall

Thermocouples (two per each of three electrode pairs) are also visible in the photograph. These terminate in wells drilled into the electrode. One well is located near the electrode surface and the other well is located near the coolant passage. As stated earlier, both the anode and cathode walls are of identical construction.

The insulating walls are shown in Figures 12 through 15. The bottom insulating wall is the simpler of the two walls in that it does not have a view port or other instrumentation. As seen in Figure 12, it consists solely of alumina brick insulation attached to copper heat sinks. The center blocks, over which the plasma will flow, are metallized with plasma sprayed copper and brazed to the copper heat sink with a silver-copper eutectic alloy. The remaining alumina insulators are bonded to the copper heat sinks with RTV silastic adhesive. The sidewalls and bases of the long, outer copper blocks are painted with a 10 mil thickness of insulating varnish. The center blocks are covered with four layers of 0.025 inch thick polyimide tape. These insulating assemblies are backed up with a flat silicone rubber gasket and attached to the NEMA G-11 mounting block with machine screws. The rear view of the wall (Figure 13) shows this attachment and the copper tubes for the connection of the cooling water lines. The top insulating wall contains a hole drilled at a compound angle to provide visual access to the channel interior. Figure 14 shows the location of this hole in the center insulating block. Figure 15 shows the positioning of the optical sight port attachment and the thermocouple locations. There are two thermocouples each in the second and fourth insulating blocks; one thermocouple is located near the surface of the ceramic and the other near the base of the ceramic. The remaining construction of the top insulating wall is the same as that of the bottom wall.

The raised portion of the center insulators cover a portion of each edge of the electrode to give a channel with a one by two inch cross section. The fit of adjacent electrode and insulator walls is shown in Figure 16.

There are inlet and outlet transition sections that are mainly water cooled copper sections lined with alumina brick. The ceramic blocks are metallized with plasma sprayed copper and brazed to copper blocks. The copper blocks are then joined

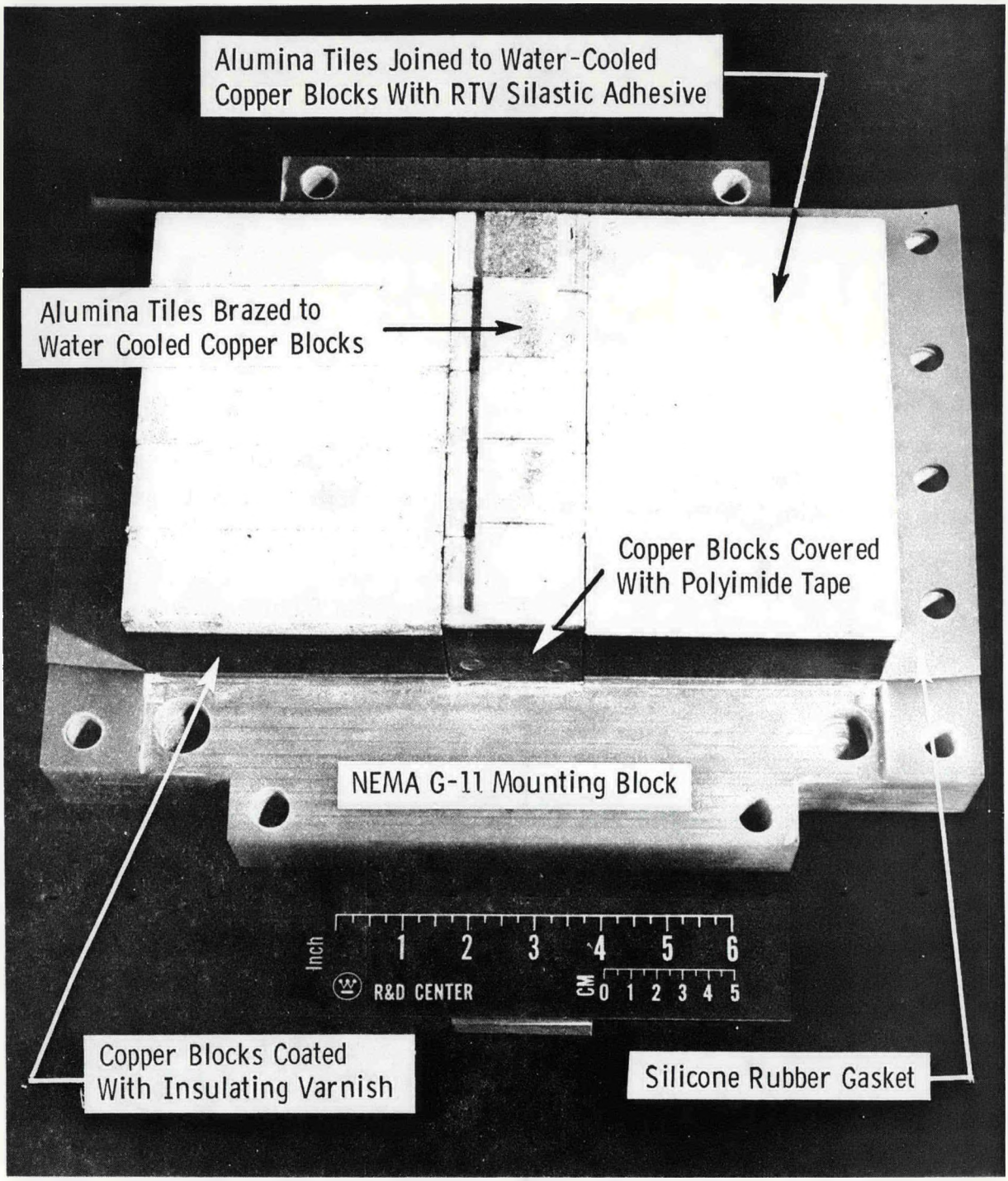

Figure 12. View of Bottom Insulating Wall

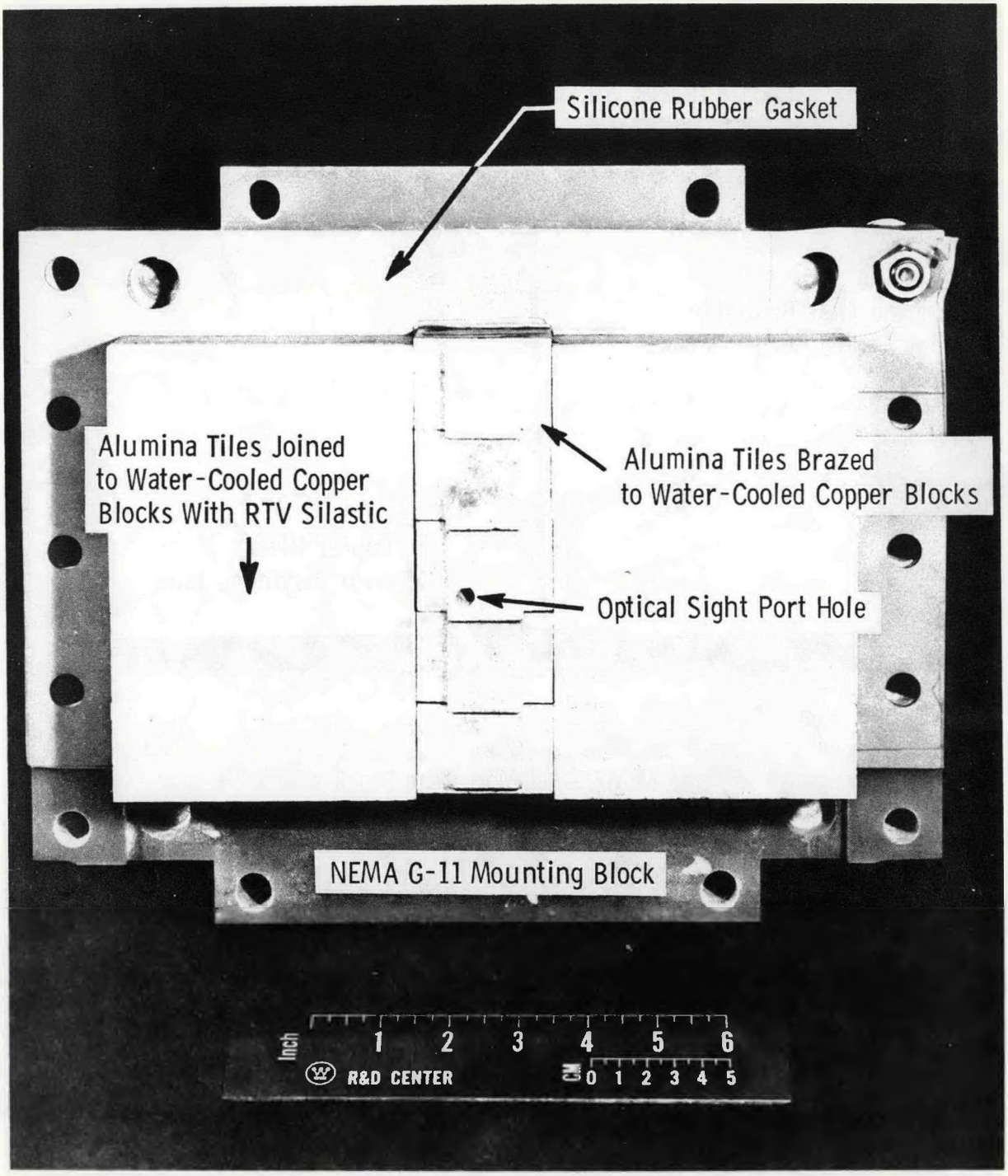

Figure 13. View of Top Insulating Wall

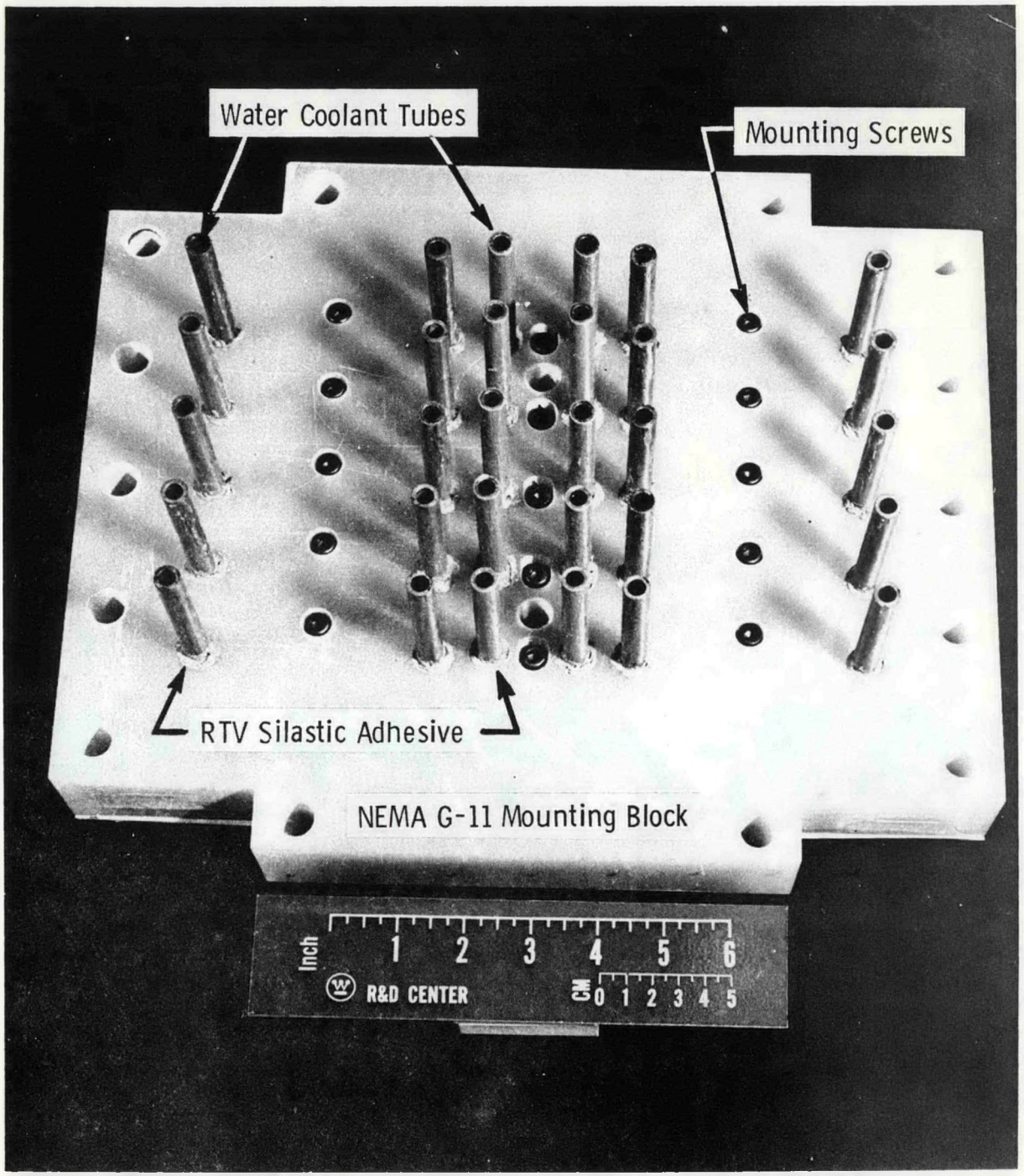

Figure 14. View of Outer Surface of Bottom Insulating Wall

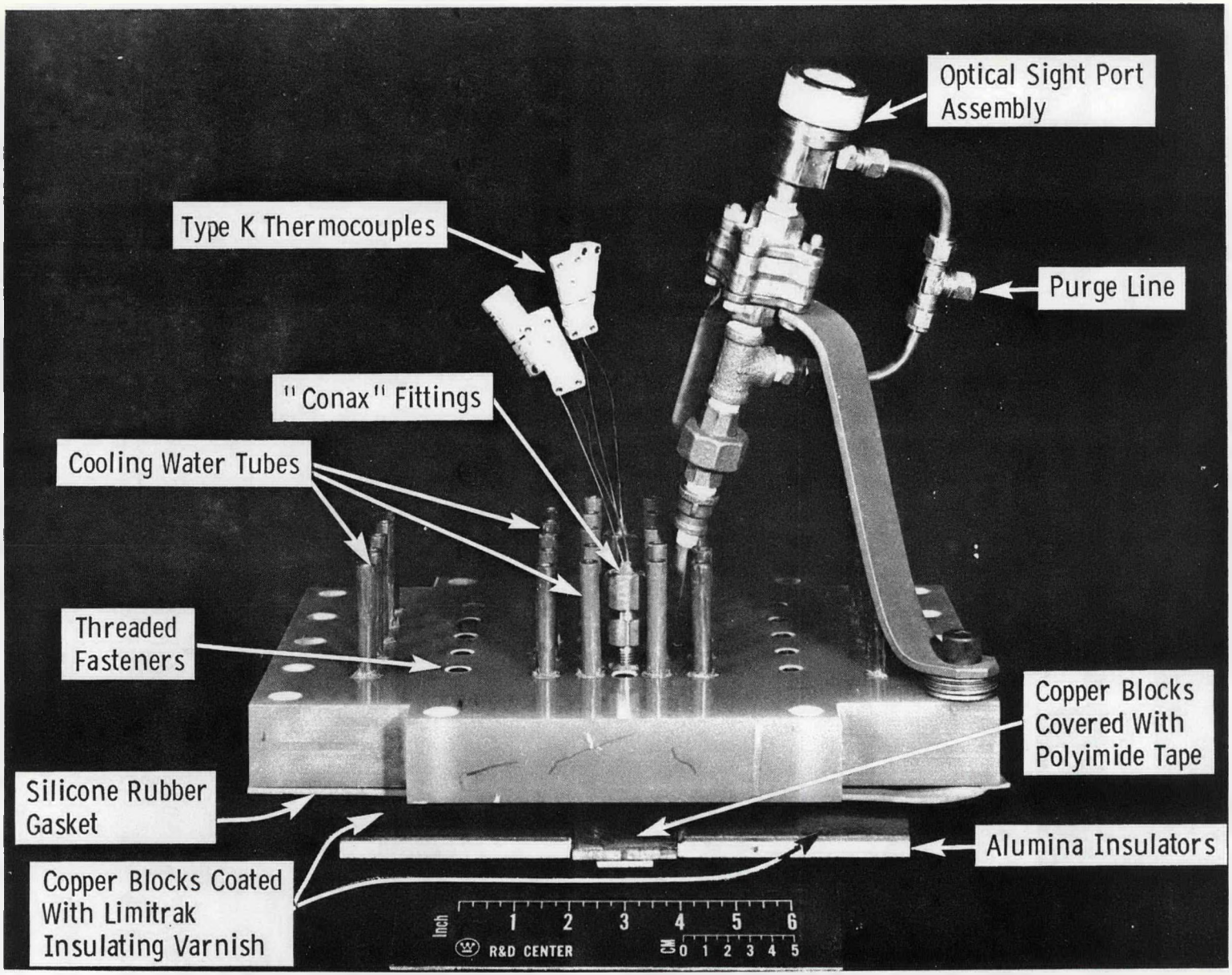

Figure 15. Side View of Top Insulating Wall with Optical Sight Port

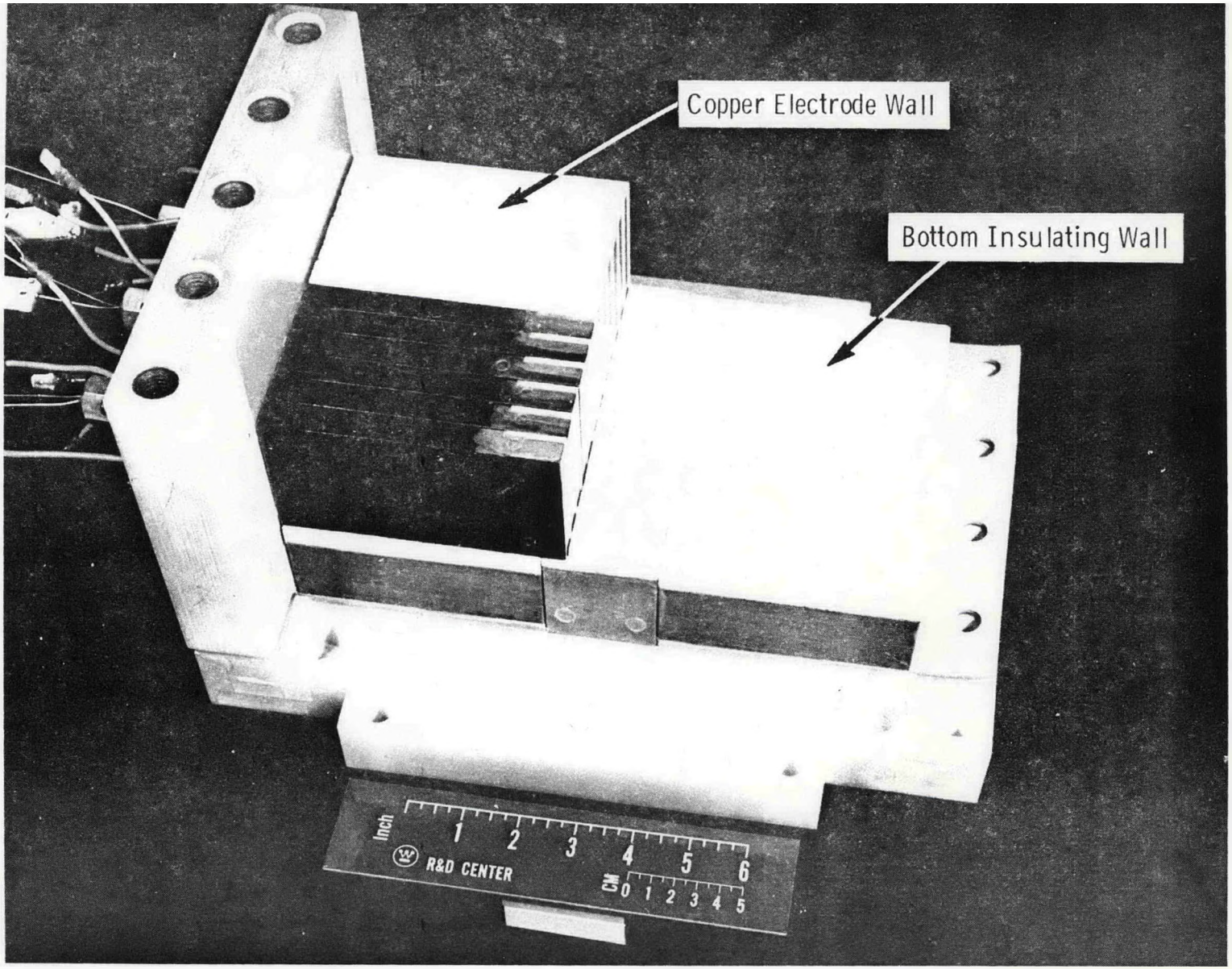

Figure 16. View Showing Assembly of Electrode and Insulating Walls

to the housing with RTV silastic adhesive. A pair of thermocouples are inserted in the center block of one of the walls. A pressure tap is available on the opposite wall. The surface of one of the transition sections that faces in toward the electrode/insulator walls is shown in Figure 17. The surface that mates with the mixer or exhaust flange is shown in Figure 18.

The electrode and insulating walls are bolted to each other and to the transition sections. Some minor alignment problems were encountered in assembling the component parts due to the gasketing and also due to interference between ceramic-to-ceramic and ceramic-to-metal surfaces. Appropriate adjustments were made during final assembly. All penetrations through the NEMA G-11 laminate and gasketed joints were sealed with RTV silastic sealant. After the initial sealing, the test assembly was tested to a dynamic pressure of 150 psig to insure that the walls were structurally sound. After this test, bolts were retightened and penetrations and gasketed joints resealed with RTV silastic sealant to retain a pressure of 40 spig. Electrical checks of the interelectrode insulations were made both during assembly and prior to delivery to the MTF facility.

Figure 19 shows the copper test assembly bolted between the large diameter mixer and the exhaust pipe. In the figure can be seen the water flow rators for the individual electrodes and insulators, the thermocouples for the material temperatures and cooling water temperatures, and the optical sight ports located on the mixer and test assembly.

3.4.2 Hot ($LaCrO_3$ Electrodes) Test Assembly

Component parts are available for the fabrication of the first hot wall test assembly. The electrodes for this test assembly will be lanthanum chromite and yttria stabilized zirconia and will be attached to the copper electrode bases by a number of different materials and attachment designs. Interelectrode insulators will include magnesia, magnesium aluminate and strontium zirconate and will be attached to the copper electrode bases by a number of different techniques. The insulating walls and transition sections will be of water cooled copper protected by dense magnesia brick insulators. The fabrication of these walls is in progress.

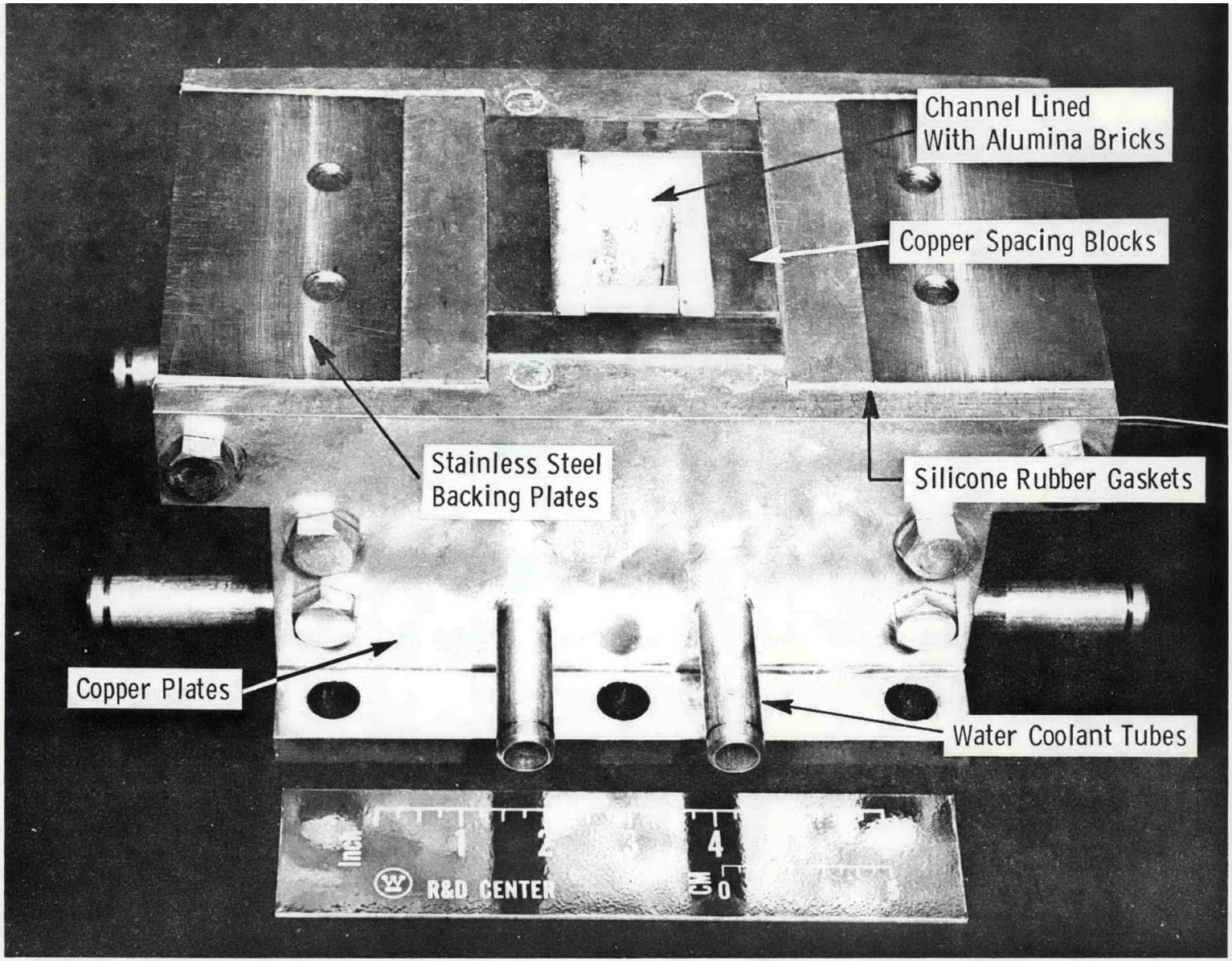

Figure 17. View of Transition Section Adjunct to Test Assembly

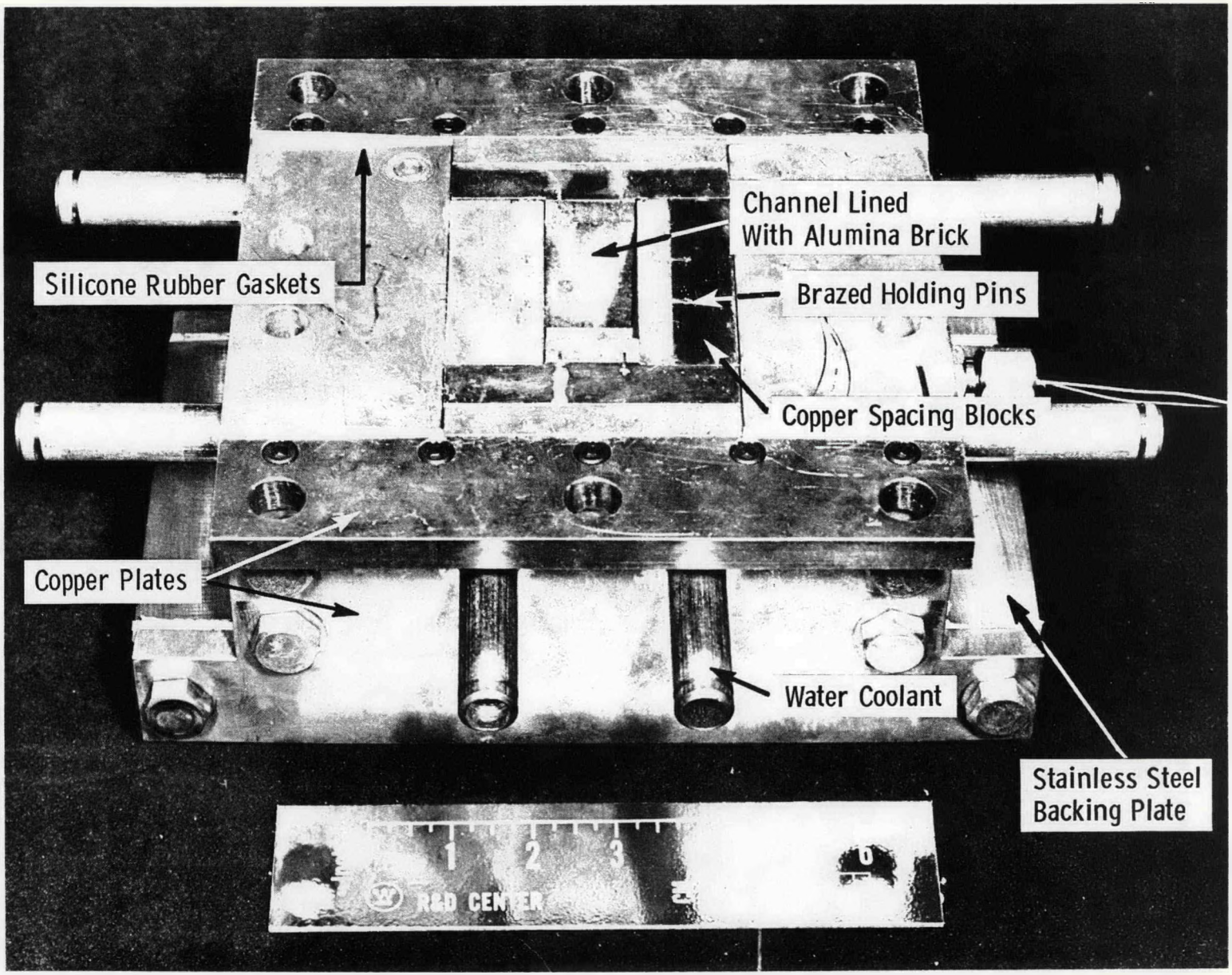

Figure 18. View of Transition Section with Mating Flange

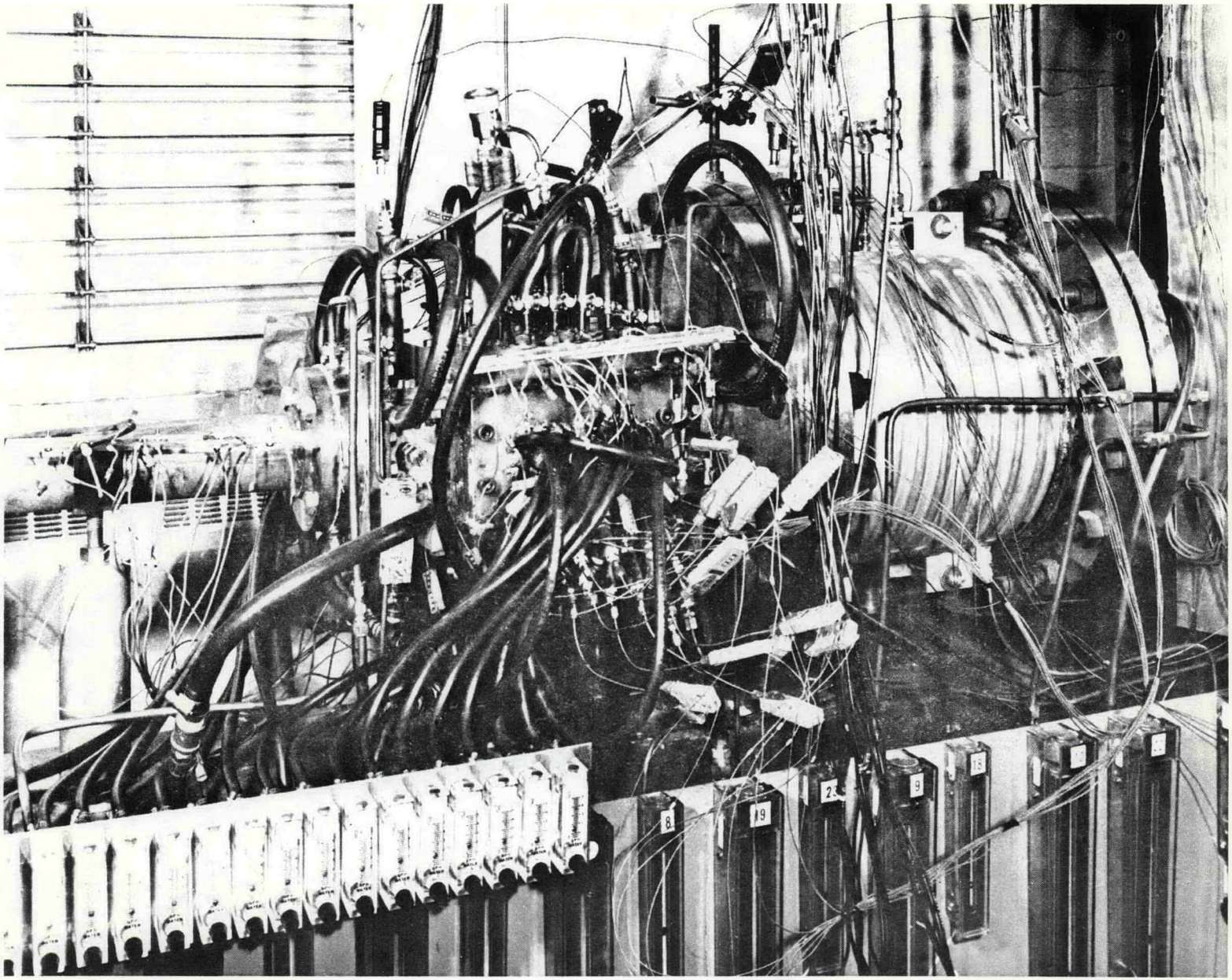

Figure 19. Cold Wall Test Assembly Assembled in MTF

3.5 Materials Test Facility

Test Summary

A total of eight tests were run in the MTF in the second quarter of 1977. These tests represent the initial tests in the facility and were run to confirm the operation of the controls and provide operational data on the equipment. The initial tests were run with a "dummy" test section equipped with optical pyrometers, iridium thermocouples in the plasma (for pyrometer calibration purposes), and platinum thermocouples imbedded in the walls and were designated DI-D7 (diagnostic test 1 through 7). The last test of the quarter was run on the copper cold wall test assembly and was designated 35-1 (test channel 35 fast temperature cycle). The duct design program was verified as well as the operation of the test assembly.

A photo of the test hardware is shown in Figure 20. Fuel is pressure atomized in the upstream end of the swirl combustor and the combustion products are exhausted into a large diameter mixer. Seed is injected into the mixer where combustion is completed and the homogeniety is attained. The plasma then passes through a nozzle to accelerate the flow before passing into the test section. Water is sprayed into the plasma at the test channel outlet to cool it to 600°C which is the maximum operating temperature of the back pressure valve. Subsequent water sprays reduce the temperature to 80°C for scrubbing.

3.5.1 Diagnostic Tests

The first eight tests were run on a test section constructed of a four inch diameter pipe, fifteen inches long that had internal cross section of one inch by two inches which was cast using a KR gunning mix. The test section had two optical ports for optical determination of wall temperature as well as an iridium/iridium-rhodium thermocouple located in the plasma. An optical sight port is also located in the mixer directly upstream of the nozzle. A plasma temperature drop of approximately 50°C was measured as the plasma accelerated from the mixer into the test section.

Since the maximum temperature at which thermocouples can be used in the MHD environment is of the order of 2150°C, it is necessary to use optical techniques

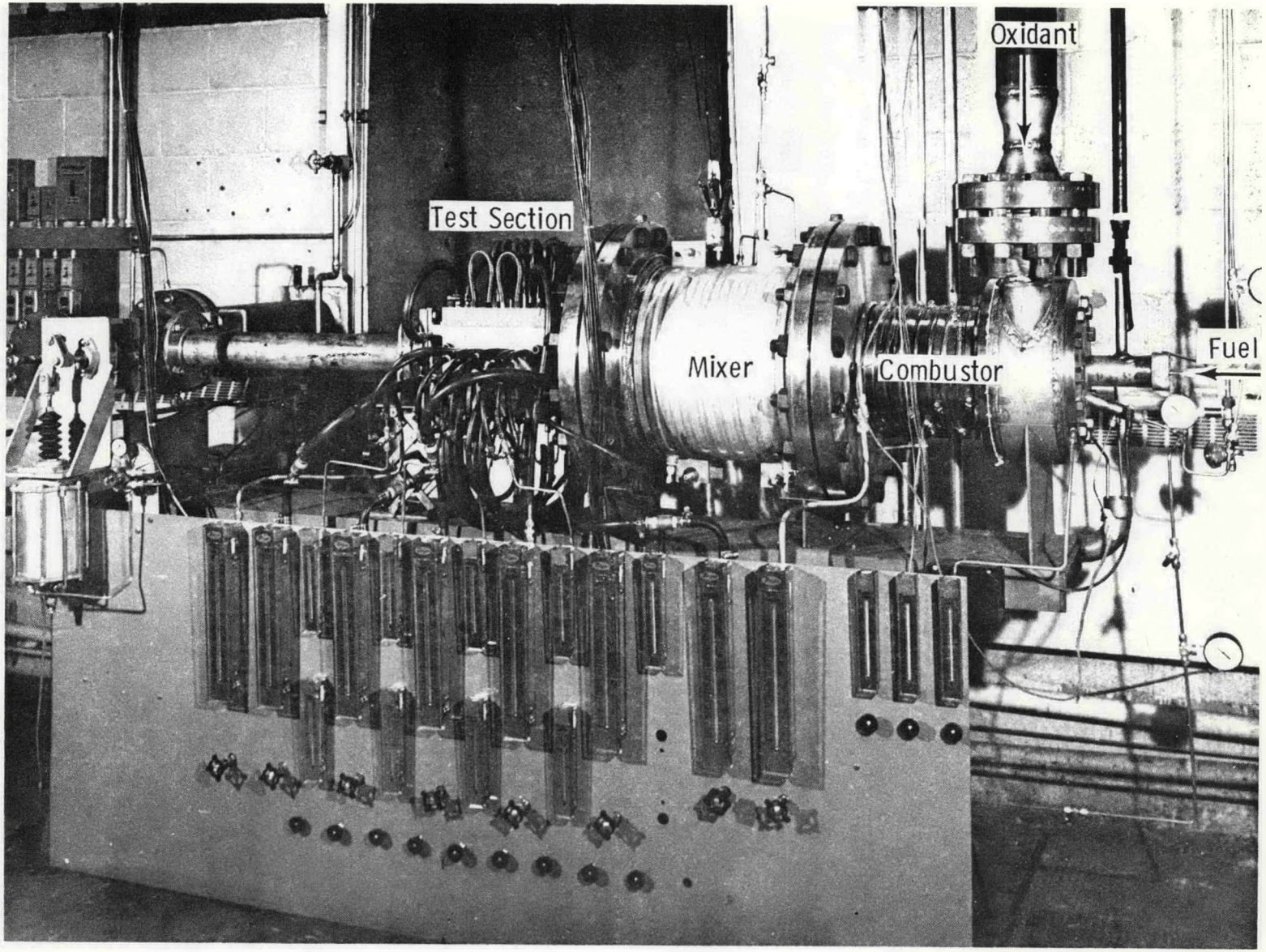

Figure 20. Westinghouse Materials Test Facility

for measurements in the 2200° to 2600°C range. Test runs of the MTF combustor using a dummy channel on 6/13 and 6/17/77 were taken as an opportunity for comparing different types of optical temperature instrumentation by holding temperatures at the beginning of the test low enough so that thermocouples mounted in the plasma could be used to calibrate the optical instrumentation.

In these test runs on Ir/Rh thermocouple was mounted in the center of the dummy channel, and a platinum-rhodium thermocouple mounted about 5" upstream in the same channel. A two color pyrometer was used for the measurement of mixer temperatures on the downstream side of the mixer using a gas protected quartz port. An additional port with a quartz window was inserted in the side of the central region of the dummy channel which could be used interchangeably for making temperature observations using a 2.2 μ Ircon pyrometer, a 0.7 to 0.97 μ Ircon pyrometer, and a vanishing filament pyrometer (0.65 μ).

The Ir/Rh thermocouple consistently read roughly 200°C low. After the tests it was found that it was mounted somewhat behind the inner ceramic wall of the channel instead of about 1/4" into the plasma.

As the test section was brought up in temperature, it quickly became evident that the optical pyrometer readings (vanishing filament type) were lagging substantially behind the temperatures read on the Pt/Rh thermocouple. The data supported the conclusion that the pyrometer (0.65 μ) was "looking" through the plasma and reading the temperature of the ceramic lining on the back of the dummy test section.

On the other hand the 2-color pyrometer, confirming our Waltz Mills experience, apparently reads plasma temperatures. Just why plasma temperatures are observed requires further investigation. A similar observation has been made by experimenters at Stanford University.

Comparisons were made of temperatures read on the Pt/Rh thermocouple with those read on the 2 Ircon pyrometers. In the test of 6/17 agreement between the temperatures read on the 0.7 to 0.97 μ pyrometer and the Pt/Rh thermocouple was obtained

in the 1600°C range by setting the emissivity connection on the pyrometer at 0.65. The emissivity connection had to be set at 0.7 in the 1700°C temperature range, and at 0.75 for the 1800°C temperature range. The Pt/Rh thermocouple failed as the temperature went over 1700°C, and the comparison at 1800°C was made using the 2-color pyrometer.

The 2 μ pyrometer had satisfactory agreement with the Ir/Rh thermocouple of 1625°C when the emissivity correction was set at 0.65 in the test of 6/13/77. At this time the 2 color pyrometer in the combustor was reading 1690°C.

3.5.2 Cold (Copper Electrodes) Test Assembly (Test #35-1)

The first test on the cold wall channel was run on June 30, 1977 and was run only in preparation for the ten hour test scheduled in July. The history of the air and fuel flowrates as controlled automatically can be seen in Figure 21. Air preheated to 800°C was passed through the system until thermal equilibrium was achieved. Then, in sequential order, the air flow was reduced, fuel was introduced, ignition was confirmed, and the air flow was increased to 100% mass flowrate. This method results in an increase of plasma temperature of 100 to 300 centigrade degrees. Some typical materials temperatures during this test can be seen in the following figures:

Figure 22: Insulating Wall
Figure 23: Electrode Wall

The purpose of the test was only to achieve peak plasma temperature and ramp down. The time accumulation at temperature was obtained and no seed was introduced. There are two temperature plots in each figure. The two temperatures are from two thermocouples located at different depths in the same electrode or insulator.

Thermal Measurements

The heat fluxes measured on the individually water cooled electrodes in this test were in the range of 100-115 watt/cm^2 and are 15% higher than the 90-100 watt/cm^2 predicted by the one-dimensional duct design computer program. The copper electrode wall ran in the temperature range of 400°C at the inlet to 125°C at the

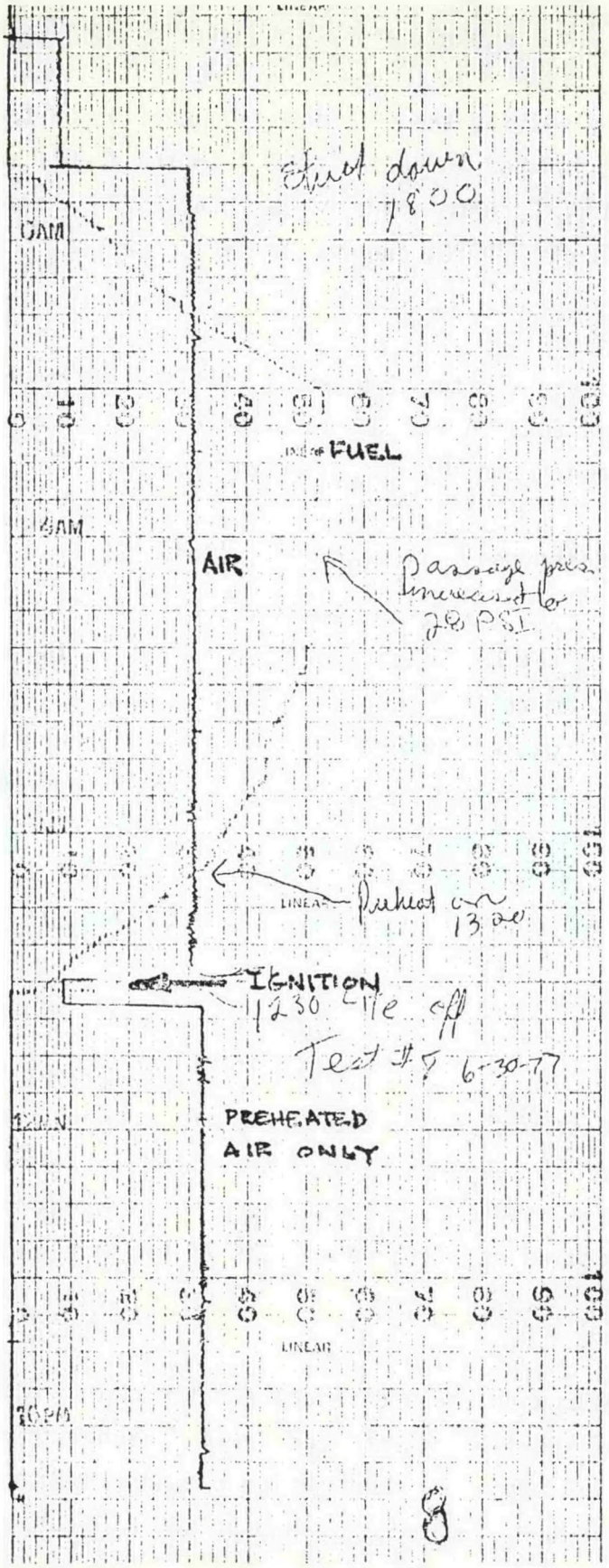

Figure 21. Air and Fuel Mass Flowrate History of Test 8

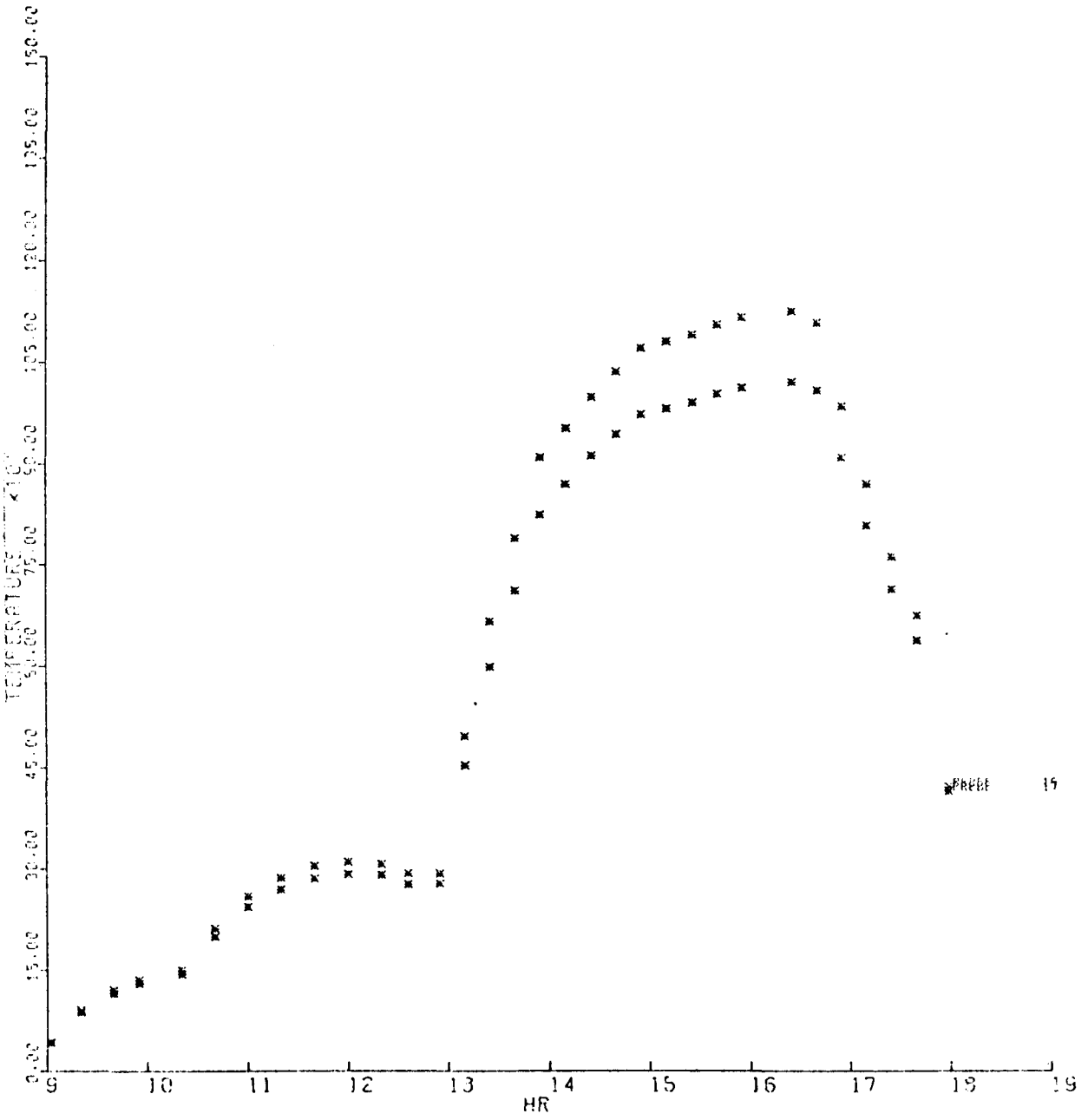

Figure 22. Alumina Insulating Wall Temperature of Test #35-1

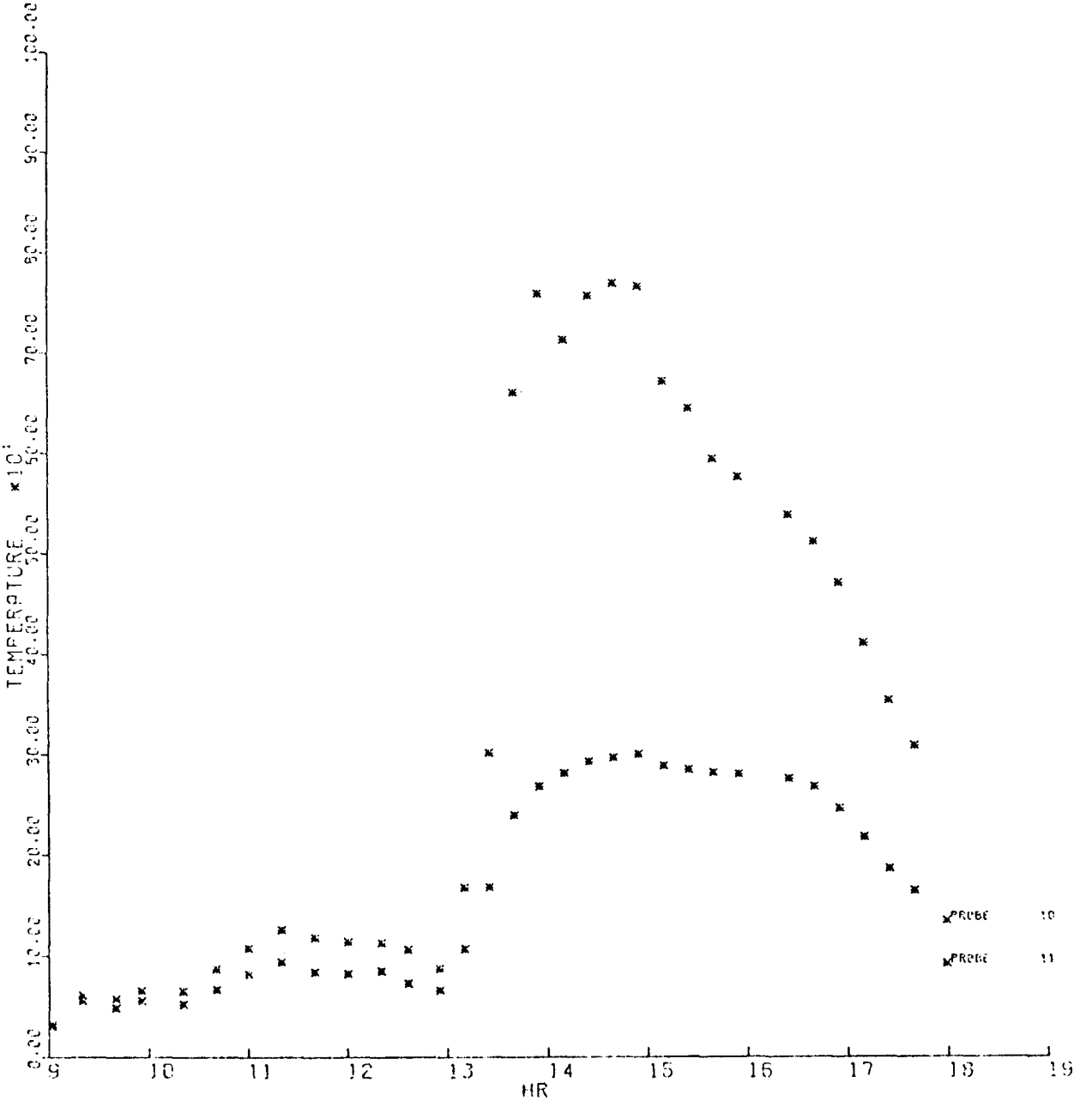

Figure 23. Copper Electrode Wall Temperature of Test #35-1

exit. Back pressure was varied from 1.0 to 2.0 atm during the test while maintaining constant mass flow. The effect on the heat transfer was negligible as expected. Velocities ranged from 300 m/sec at 1.0 atm pressure to 150 m/sec at 2.0 atm pressure.

Electrical Measurements

Prior to installation in the MTF test facility the interelectrode leakage resistances between electrodes of the copper test assembly, and their leakage resistance to ground, were in the high megohm range, i.e., greater than 1000 megohms. The leakage resistance dropped to the order 10 megohms when the water cooling hoses were connected without the water being turned on. With water running in the test assembly the leakage resistance of the electrodes to ground decreased to the 10^5 ohm range. The leakage resistances gradually decreased as the plasma temperature increased. Leakage resistance values of the order of 5000 to 10,000 ohms were observed at the maximum loading of the channel without seed having been introduced. Leakage resistances to ground, between adjacent electrodes, and between opposing electrodes all had comparable magnitudes at any given time. Once the cool-down cycle was initiated and plasma temperature were brought down to the order of 1600°C, the interelectrode leakage increased by roughly a factor of 100 to the 10^5 ohm range. An investigation as to the specific paths taken by the electrical leakage observed is being conducted.

A 10 hour test is scheduled to be run of the cold wall test assembly in the first week of July. The test will be run 10 hours at peak temperature (approximately 2450°K without oxygen) with one percent potassium seeding. A large number of electrical tests will be run during this test to determine seed penetration, plasma conductivity, interelectrode leakage, and leakage to ground.

3.5.3 Facility Modification

The Materials Test Facility has been set up with 8 power supplies on the basis that the major emphasis in the electrical testing would be concentrated on the central 8 electrode pairs of the 12 electrode pair channel. However, a procedure has been devised which permits investigating the change in characteristics of all

12-electrode pair with a minimum of electrical lead changing using the 8 available power supplies.

The electrical test circuitry has been set up with 2 ammeters to help distinguish between plasma currents and leakage currents.

All of the power supplies have been fitted with protective diodes capable of passing the maximum desired currents in the forward direction. Should a breakdown occur between adjacent electrodes, the diode is capable of withstanding the maximum anticipated voltage in the reverse direction. In the absence of the protective diode, an electrical breakdown between electrodes in instances where different potentials are applied to neighboring electrodes, could result in breakdown of the lower voltage operating power supply.

Tests on MHD materials in the Materials Test Facility could be made considerably more meaningful if this facility was modified to allow test of electrode materials and configurations under actual operating conditions. The use of a superconducting magnet would not only permit testing of MHD electrodes and insulating materials under operating conditions, but would also permit magnet fabricators to evaluate proposed design improvements in the construction of superconducting magnet.

A preliminary design of a MTF test assembly suitable for use with a superconducting magnet has been submitted to the National Magnet Lab at MIT through ERDA, and interface problems between the channel and the proposed magnet discussed with Dr. P. Marston of the Magnet Laboratory. A further coordinating meeting is scheduled after the MIT personnel have had an opportunity to draw up a proposed outline drawing for the magnet.

4.0 TASK 4 - TECHNICAL SUPPORT FOR THE COOPERATIVE US/USSR PROGRAM ON MHD

4.1 U-02 Phase III Program

The objective of the Phase III test in the U-02 MHD plant is to test two U.S. electrode walls consisting of materials and designs that could be used in larger MHD generators such as the U-25 or future CDIF. The electrodes are based on either $LaCrO_3$ or MAFF ($3\ MgAl_2O_4 \cdot 1\ Fe_3O_4$) and will be fastened to copper cooling blocks by several different designs. Selection of materials and fastening techniques will be made on the basis of proof tests conducted in the MTF in August-September. The U-02 electrode walls will be assembled, inspected and delivered to the Soviet Union by January 20, 1978. The overall schedule is shown in Figure 24.

4.1.1 Electrode Wall Design

The drawings for the glass laminate mounting blocks have been completed and the blocks have been fabricated except for the electrode mounting holes. Details of the electrode wall are now being considered such as the modification of one of the cooling blocks to provide a sight port and the location and routing of the instrumentation. The electrode pitch has been changed from 1.36 cm to 1.35 cm to allow for the 0.35 cm offset required to mate the electrode wall to the Russian entrance transition section. The revised layout is shown in Figure 25. Each group of six electrodes will be tied together with two tie rods to form a module of identical electrode/insulator material and attachment as shown in Figure 26. The tie rods will be of laminated glass epoxy thread on either end for a 1/4-20 nut. A layout of the electrode assembly is shown in Figure 27 which shows the expansion clearance required in the electrode material. The ceramic insulation between electrodes is mechanically held in position by the tie rods. The 0.010 inch polyimide insulation taped on each cooling block is indicated. Figure 28 is the basic cooling block drawing showing the water cooling passages and the instrumentation passage. This basic cooling block will be modified to provide a sight port into the channel. This requires a rerouting of the water cooling passages.

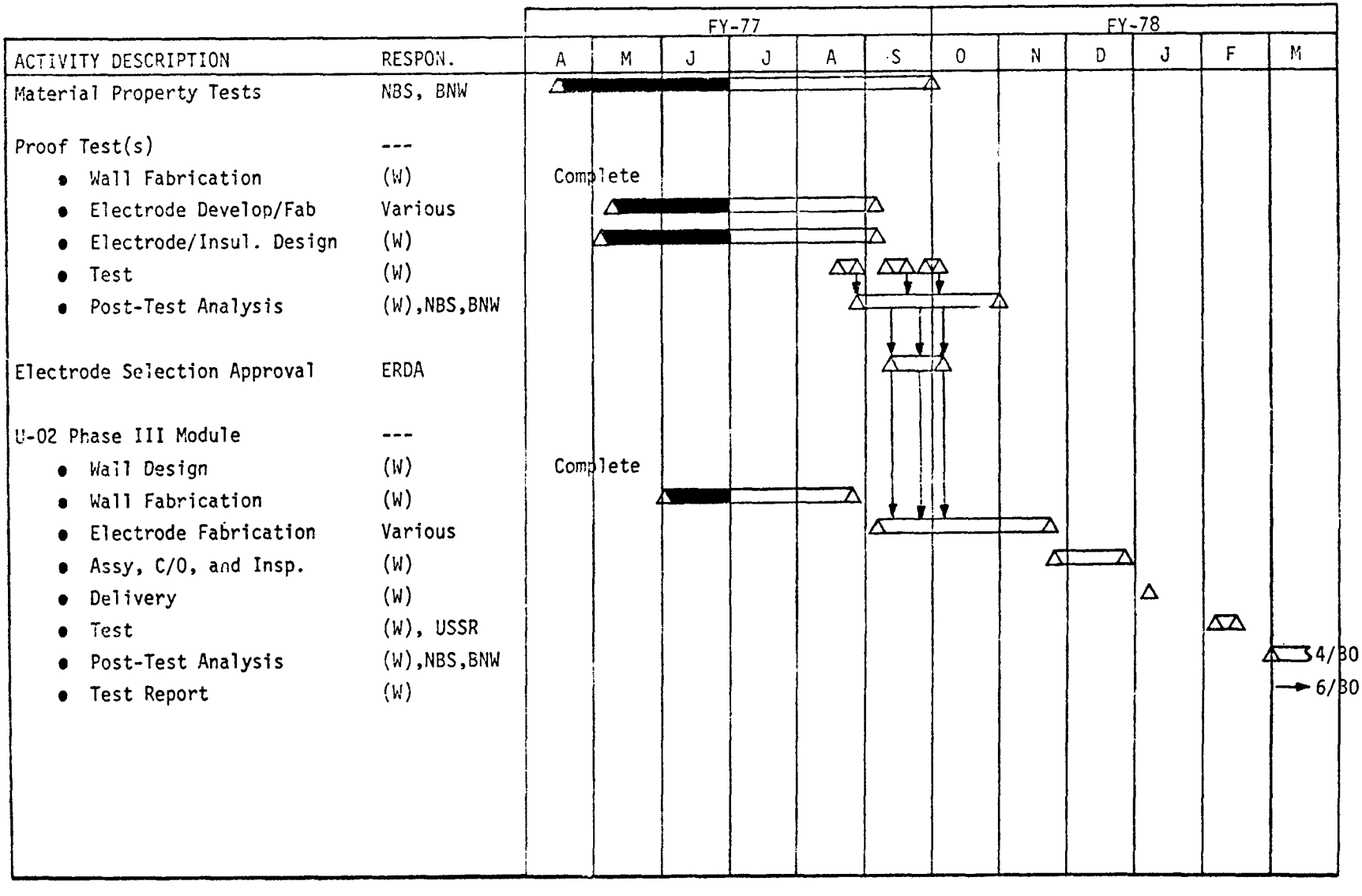

Figure 24. U-02 Phase III Program Schedule

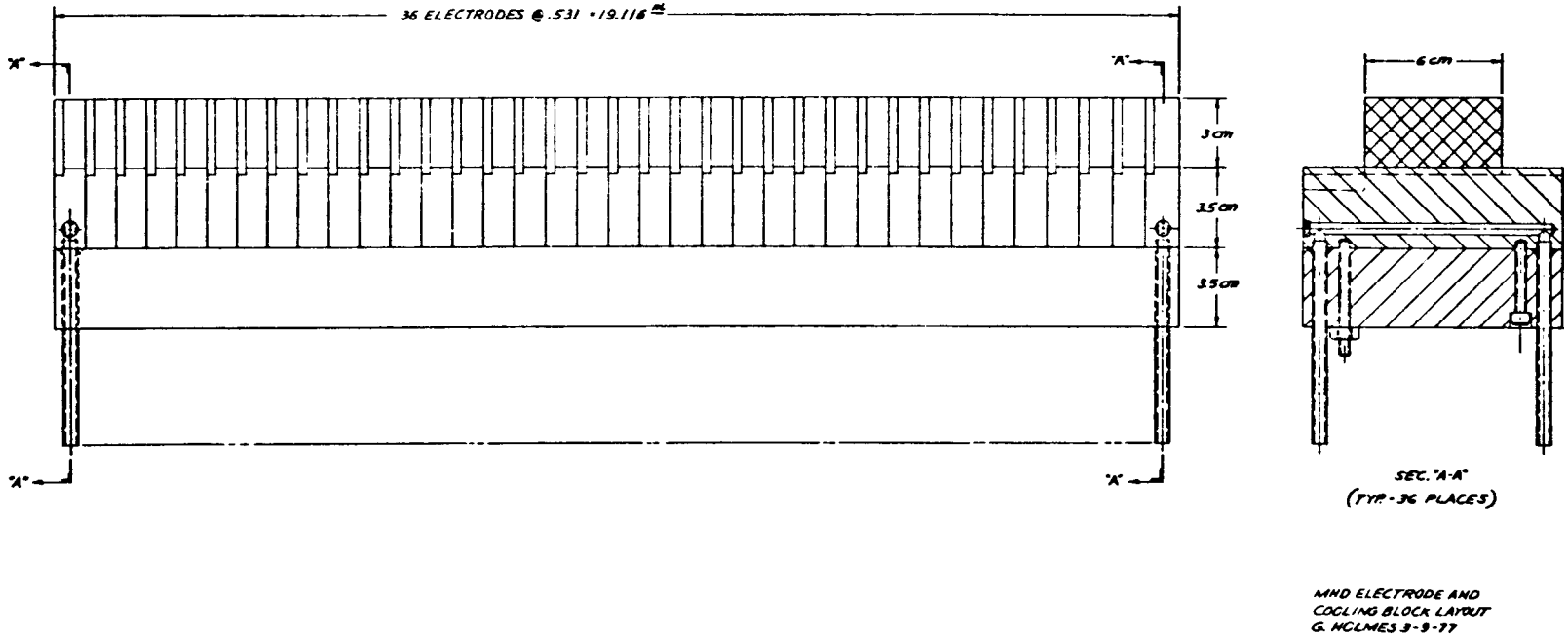

Figure 25. Revised Electrode and Cooling Block Layout

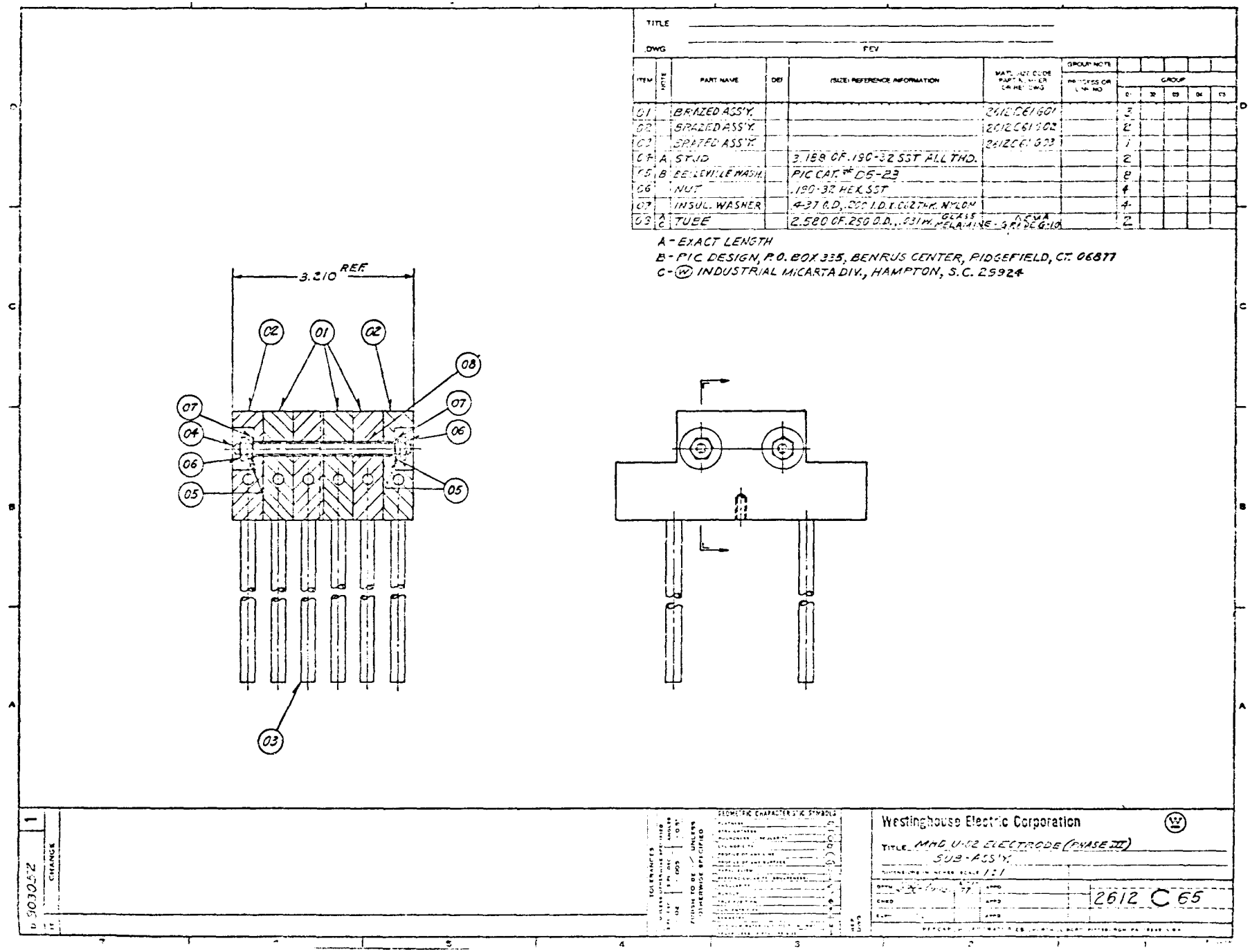

Figure 26. Electrode Cooling Block Subassembly

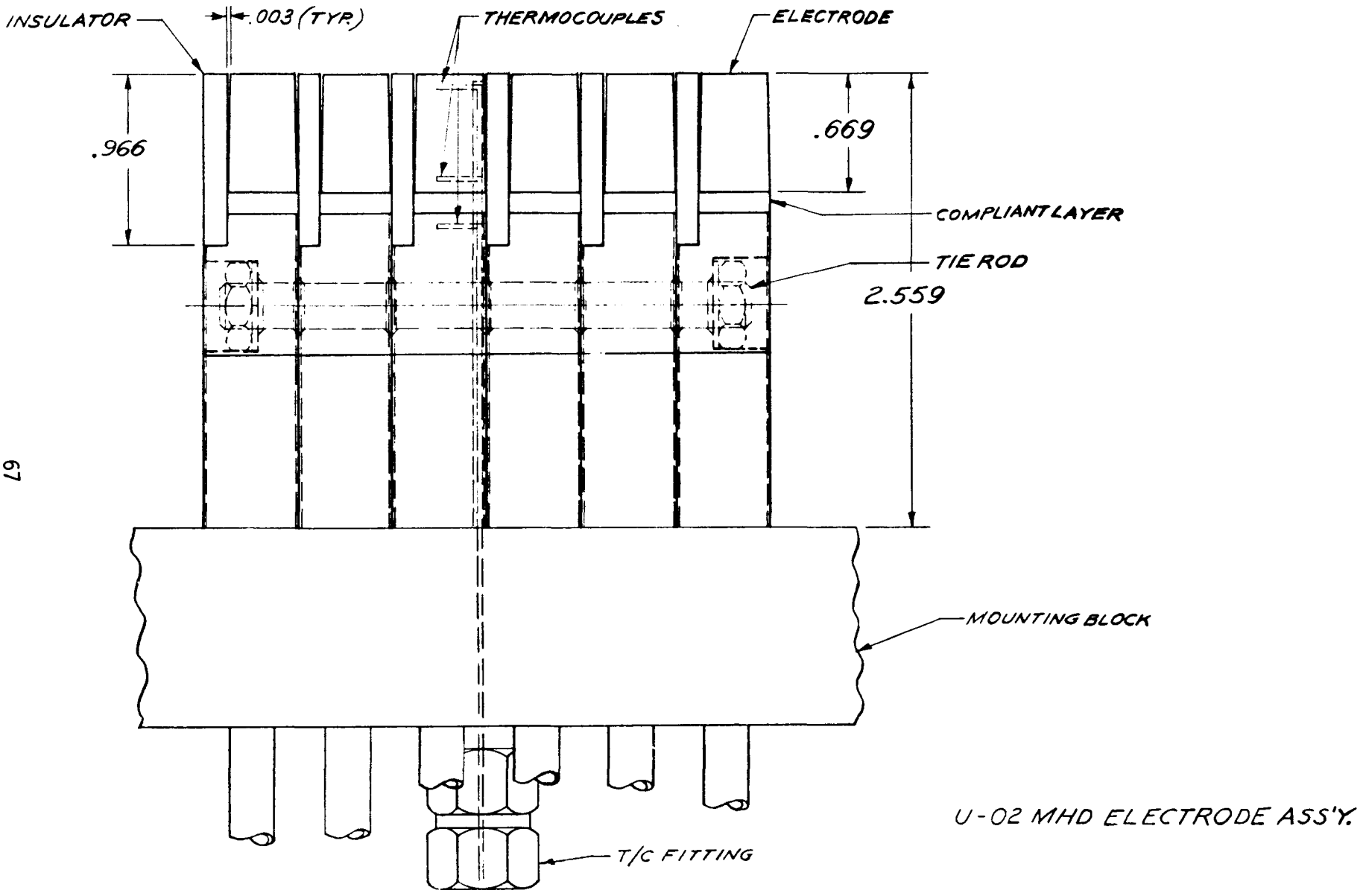

Figure 27. Electrode Module Layout

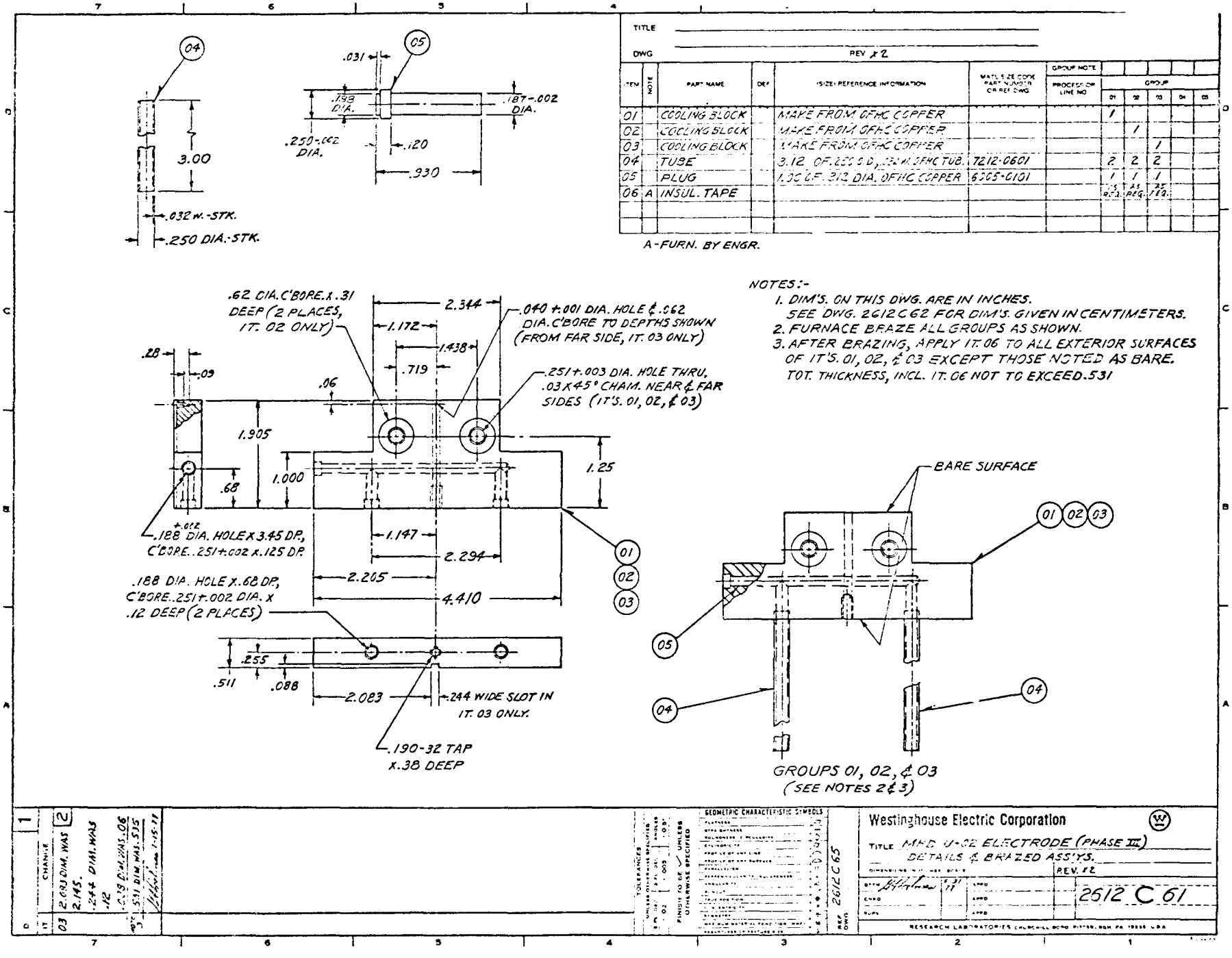

Figure 28. Basic Cooling Block

Figure 29 is the proof test electrode which will be used to test the different electrode/insulator material and attachment methods. Three electrodes will be assembled together as shown in Figure 30 with tie rods for a basic assembly of identical electrode/insulator materials and attachments. The middle electrode will be instrumented with thermocouples with two in the electrode material and one in the cooling block.

4.1.2 Electrode Stress Calculations

Finite element analysis of electrodes and inter-electrode insulators using the "Westinghouse Electric Computer Analysis" program has continued. The 20 watt/cm^2 heat flux at 1700°C wall temperature of the Russian U-02 facility was the assumed loading for this steady state analysis. The transient analysis was not considered at this time since the steady state analysis was yielding stresses severe enough to cause mechanical failure of the materials.

The lower bound analysis, which assumes a perfectly flexible support structure with good thermal contact, was chosen as a parametric analysis tool to yield some design criteria for electrodes and insulators. The upper bound, perfectly rigid, support structure analysis yielded excessive stresses in every case and was not a useful design tool.

The steady state analysis requires three material parameters as a function of temperature - k(T) thermal conductivity, E(T) elastic modulus, and α(T) coefficient of thermal expansion. Poisson's ratio is also needed but is assumed constant. The properties used in the analysis of $La_{.95}Mg_{.05}CrO_3$ electrode material are given in Figure 31 and those of MgO (85% theoretical density) insulator material are given in Figure 32. Thermal conductivities and coefficients of thermal expansion were determined by Battelle Northwest Laboratory and the elastic modulus of $La_{.95}Mg_{.05}CrO_3$ was determined by Westinghouse. American Ceramic Society data was used for the elastic modulus of MgO.

The simple support analysis of $La_{.95}Mg_{.05}CrO_3$ loaded with a heat flux of 20 watt/cm^2 at a surface temperature of 1700°C yielded the maximum tensile stress vs. length

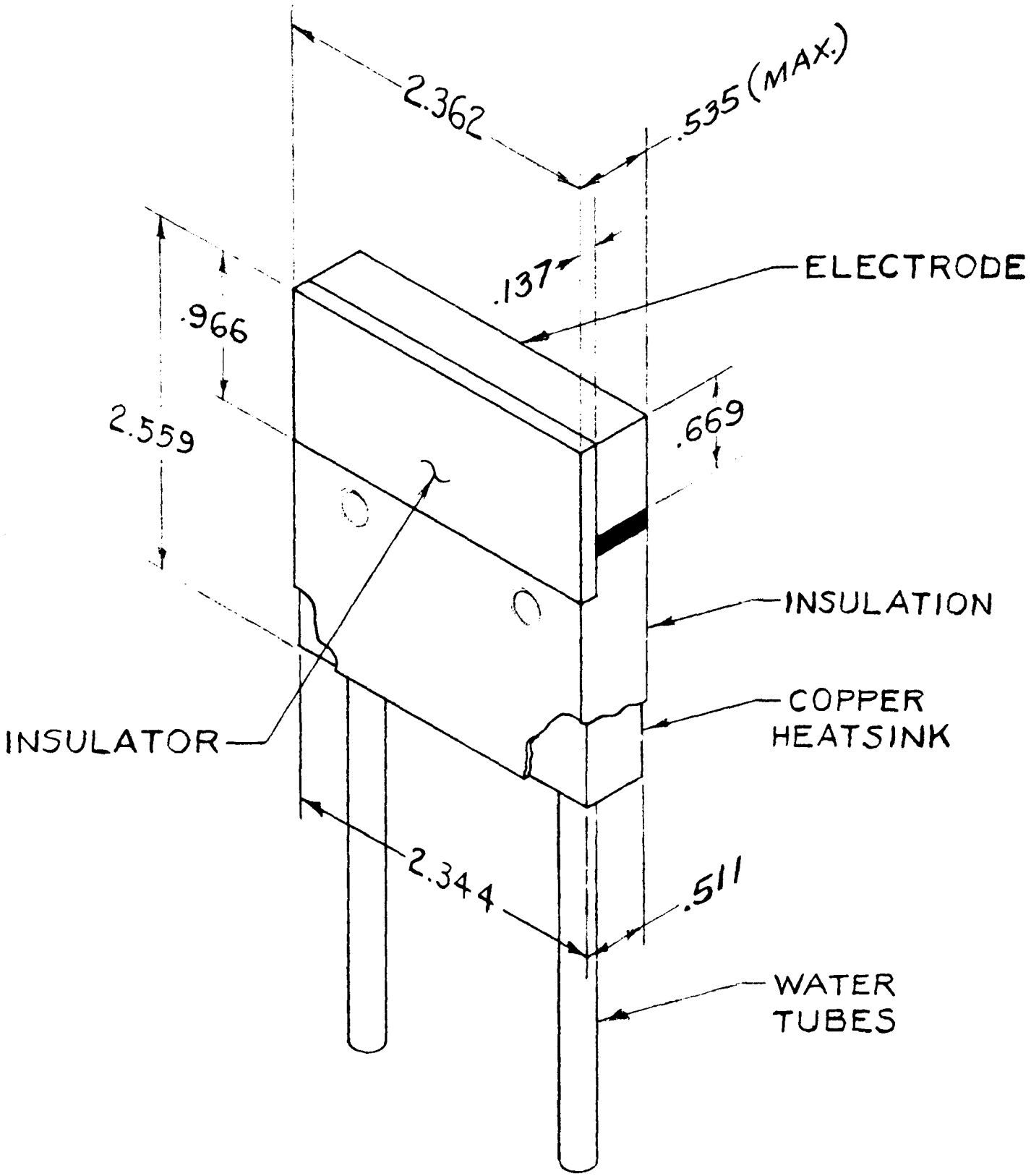

Figure 29. Proof Test Electrode

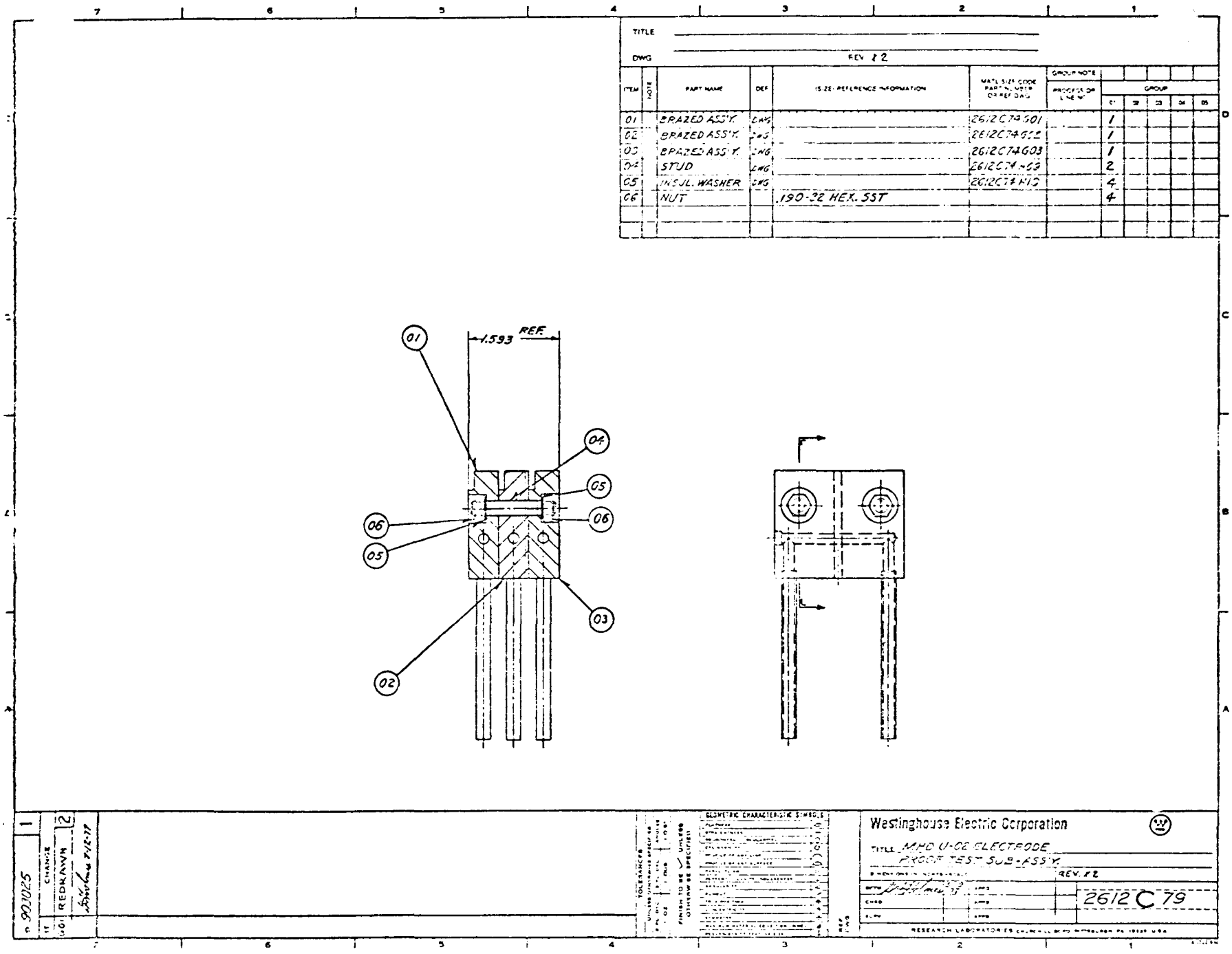

Figure 30. Proof Test Electrode Cooling Block Sub-assembly

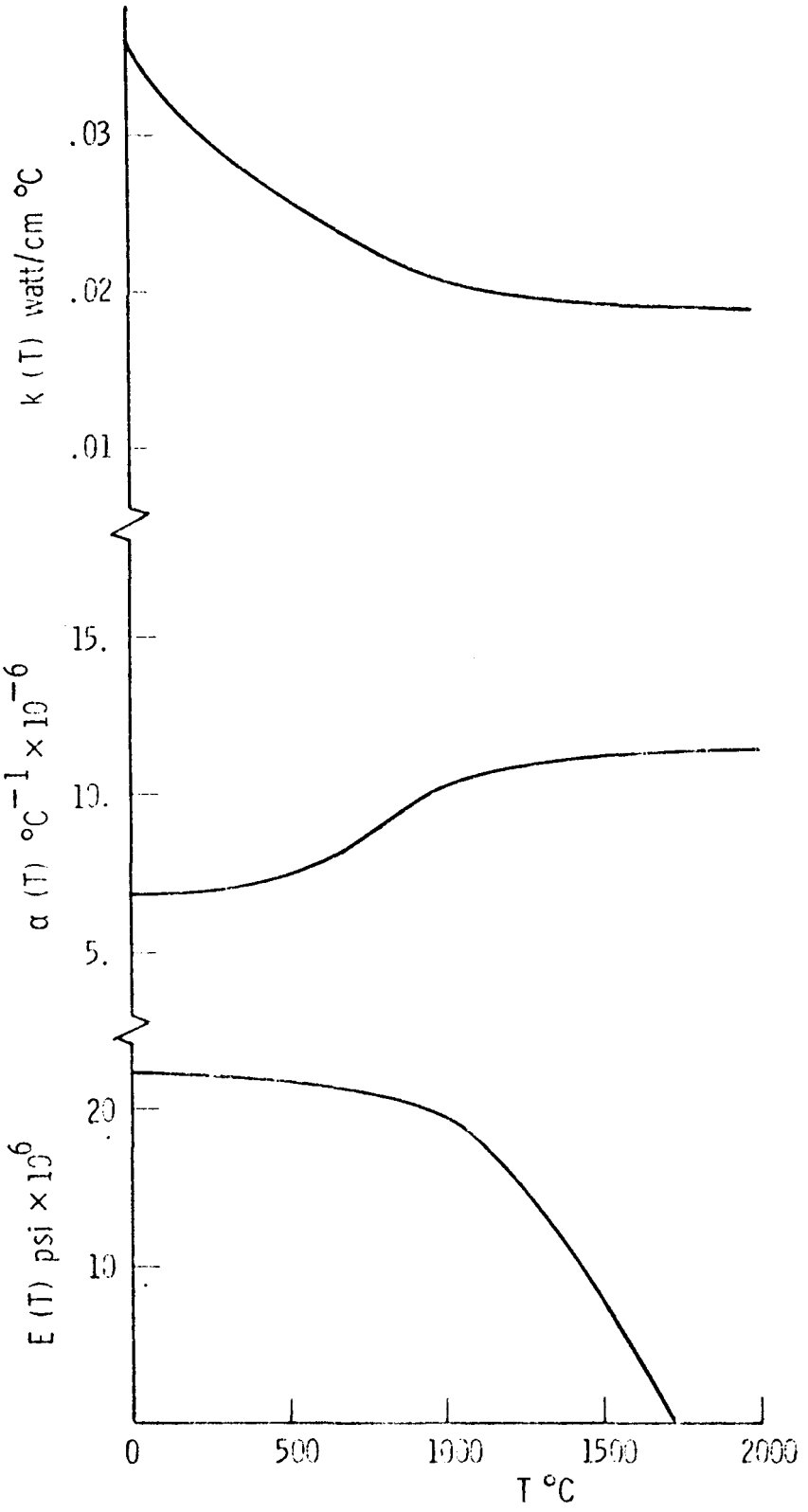

Figure 31. Material properties of $La_{.95}Mg_{.05}CrO_3$ used in electrode Stress Calculations

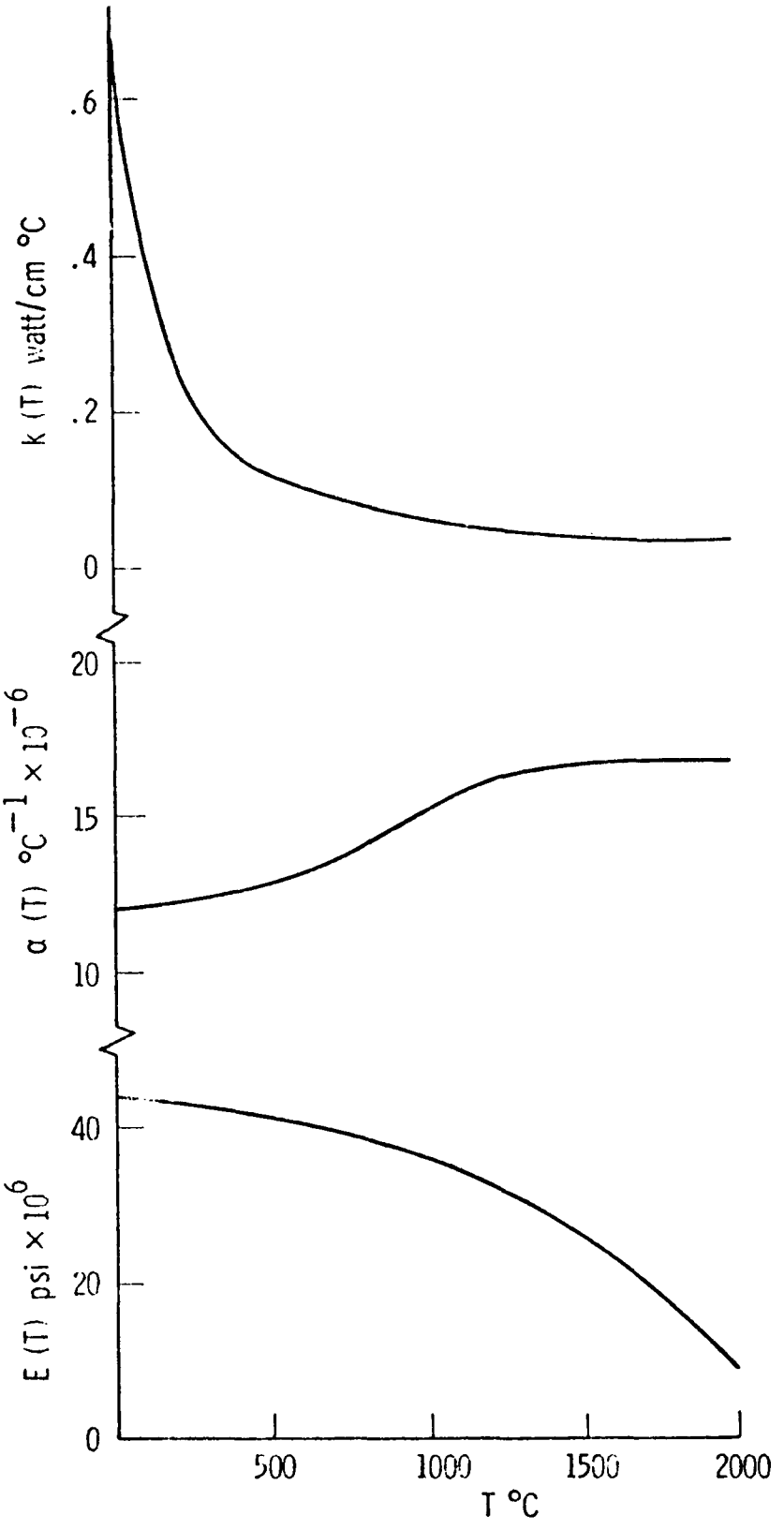

Figure 32. Material Properties of MgO (85% Theoretical Density) Used in Inter Electrode Insulator Stress Analysis

of specimen curve shown in Figure 33 when operated 1.7 cm thick at a back face temperature of 200°C. The ultimate strength of the material was 24,150 psi. The two dimensional, plane stress analysis would indicate that the electrodes must be segmented into at least 3.0 cm lengths. A three dimensional analysis was then applied to the 2 cm long, 1 cm wide, by 1.7 cm thick electrode since the two dimensional plane stress analysis is not a good model of this case. The resulting maximum tensile stress point is also shown in Figure 33 and indicates that the electrodes must be segmented into at least 2.0 cm lengths to survive a steady state test on a perfectly flexible support. This maximum tensile stress is generated at a point on the interior of the structure and not on the surface as was the case of the flexure test which determined the ultimate strength of 24,150 psi. A margin of safety exists when the maximum stresses are not generated on a surface.

A monolithic inter-electrode insulator of 6.0 cm length, loaded with a heat flux of 20 watt/cm^2 at a surface temperature of 1700°C was modeled next using the material properties of MgO (85% theoretical density) given in Figure 33. The parameter that was varied in this case was the thickness of the insulator and therefore the back face temperature. The simple support analysis yielded the maximum tensile stress vs. back face temperature T_B or thickness t of the insulator as shown in Figure 34. The ultimate strength in flexure of MgO is given as 25000 psi by the American Ceramic Society. Therefore the back face of the MgO insulator should run around 850°C to keep the simple support maximum stress at about 20,000 psi. This corresponds to a thickness of 2.3 cm. Stresses will be more severe if heat is lost from the insulator to the electrode and effort should be made to thermally insulate the insulator with a gap or mesh material.

4.1.3 Electrode Development

The nine electrode/insulator structures that have been selected for proof tests are shown in Table 9. Five of these electrodes are based on $LaCrO_3$, three on MAFF and one is a HfO_2-metal composite. Interelectrode insulators of $MgAl_2O_4$, MgO and $SrZrO_3$ will be tested. Materials processed by plasma spraying, sintering and hot pressing will be tested. Several attachment approaches will be evaluated.

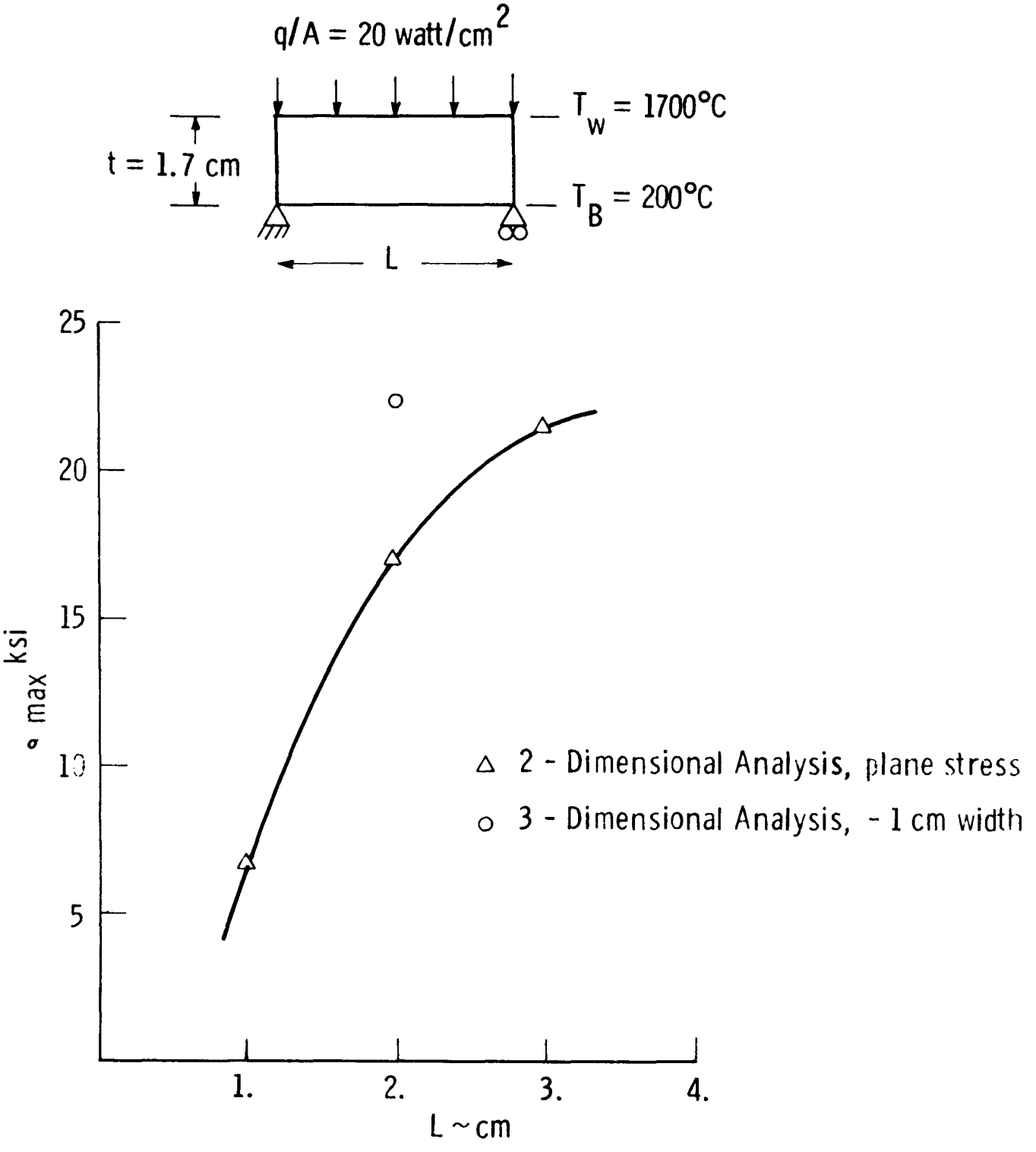

Figure 33. Maximum Tensile Stress in $La_{.95}Mg_{.05}CrO_3$ vs. Length of Electrode

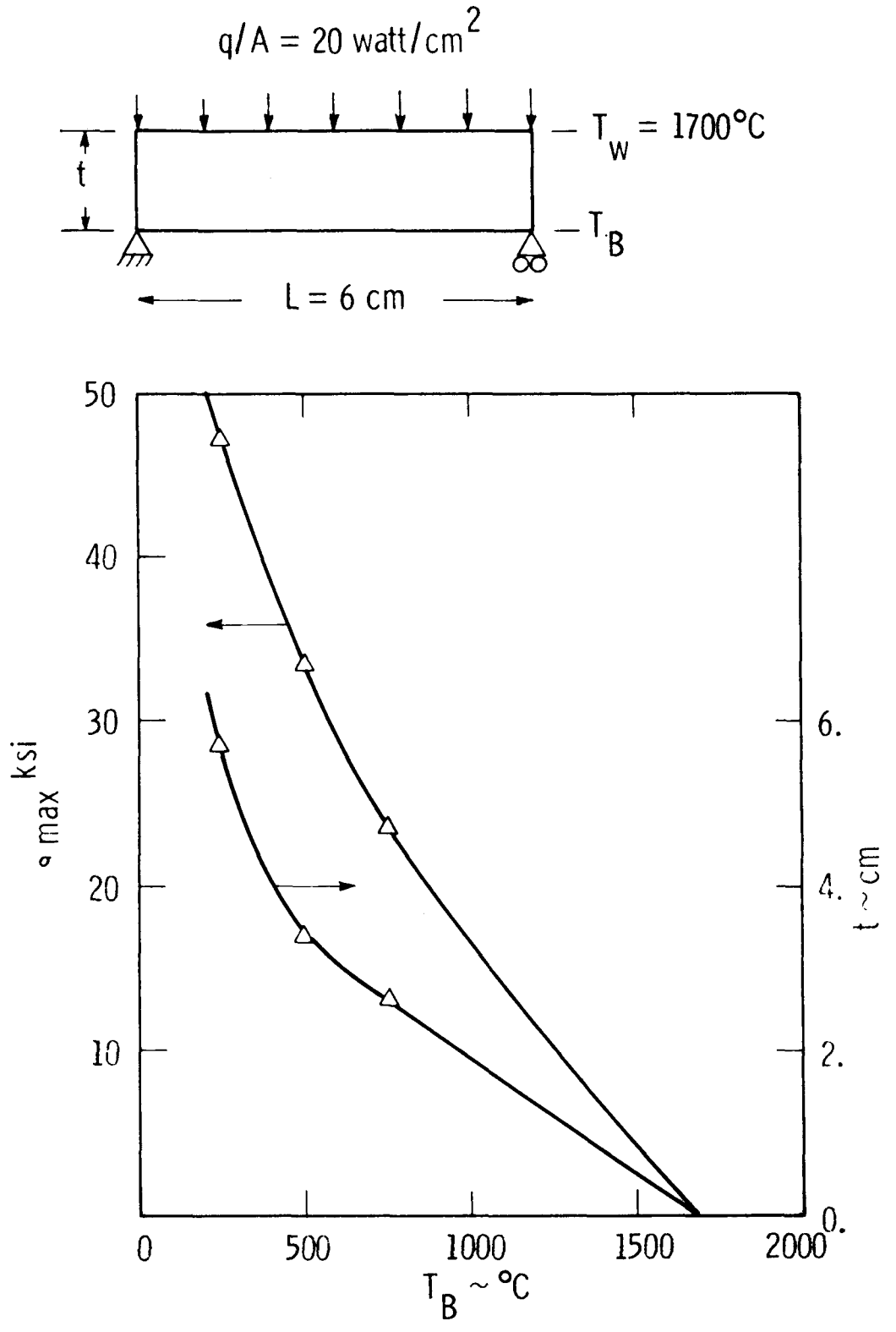

Figure 34. Maximum Tensile Stress in MgO (85% Theoretical Density) vs. Back Face Temperature T_B or Thickness t of the Insulator

TABLE 9

PHASE III U-O2 CANDIDATE ELECTRODES

No.	Supplier	Fab. Tech	Attachment	Electrode	Insulator	Delivery Date	Proof Test #
1	APS	PS	Cermet or $FeAl_2O_4$	$MgAl_2O_4(Fe_3O_4)/ZrO_2$ cap	$MgAl_2O_4$ (PS)		2
2	Tech	PS	Mesh	$MgAl_2O_4(Fe_3O_4)$	$MgAl_2O_4$		1
3	GE	M	Flexbed	$MgAl_2O_4(Fe_3O_4)$	$MgAl_2O_4$		1
4	ANL	M		HfO_2-metal composite	$MgAl_2O_4$		1
5	APS	PS	Cermet	$LaCrO_3/ZrO_2$ cap	$MgAl_2O_4$ (PS)		3
6	Tech	M	Mesh	$LaCrO_3$	$MgAl_2O_4$		2
7	W	M	Complaint	$LaCrO_2$-$LaAlO_3$	$MgAl_2O_4$		2
8	W/EP	M	Complaint	$LaCrO_3/ZrO_2$ cap	MgO		3
9	W	M	Complaint	$LaCrO_3$-$SrZrO_3$ or $LaCrO_3$-ZrO_2 composite	$SrZrO_3$		3

PS - plasma spray
M - monlithic (sintered or hot pressed)

Several purchase orders have been placed with subcontractors to produce powders, ceramic blocks and electrode structures; these supporting activities are summarized in Table 10.

In addition, General Electric Company and Argonne National Laboratories will each submit one set of electrodes for proof tests.

A more detailed summary of the seven electrode system that Westinghouse is responsible for are shown in Table 11. T_H and T_c refer to the hot and cold face temperatures of each material. Electrode system 1 and 2 are based on plasma sprayed 3 $MgAl_2O_4$ · 1 Fe_3O_4 (MAFF). The APS electrode incorporate a graded metal (or ceramic) structure for attachment to copper while the Technetics use attachment via their complaint BRUNSBOND^{TM} layers. In addition, the APS electrodes may be 'capped' with ZrO_2 layer to increase refractoriness. The performance of these electrodes can be compared to GE's sintered MAFF electrodes. Electrode system 6 is the basic $LaCrO_3$ composition tested in Phase II. It will be brazed to a nickel BRUNSBOND^{TM} layer. Electrode systems 7, 8 and 8 are more refractory versions of $LaCrO_3$ utilizing either ZrO_2 'caps', grading or addition of second phase. These three electrode systems will be attached at Westinghouse using one of the techniques described in Section 3.3. Also electrode systems 7, 8 and 9 allow for a comparison between $MgAl_2O_4$, MgO and $SrZrO_3$ insulators. Finally, APS will provide a plasma sprayed electrode system based on $LaCrO_3$ for comparison with the four monolithic sets.

4.1.4 Characterization of Electrode/Insulator Materials

To fully evaluate and design the insulator/electrode assemblies to be used in the U-02 Phase III MHD test, a number of different properties of the selected channel materials need to be determined. These properties include the electrical and thermal conductivity, the elastic modulus and fracture strength, the thermal expansion, and the x-ray analysis and emission spectroscopy of both the starting powders and sintered/hot-pressed components. In addition, the electrode assemblies will be evaluated as to their resistance to seed penetration, thermal shock resistance, and reliability of current/power leadout attachment. The material

TABLE 10

VENDORS FOR ELECTRODE MATERIALS

Vendor	Product
APS Materials Inc. (Dayton, Ohio)	Plasma sprayed electrode/insulator structures
Technectics Div., Brunswick Corp. (Milford, Conn.; LeGrande, Fla.)	Plasma sprayed and sintered ceramic attached BRUNSBOND™ complaint metal mesh layer (electrode structures) - W supplies monolithic insulator
Eagle-Picher Co. (Miami, Okla.)	Hot pressed graded ceramic electrode block
General Refractories (Philadelphia, Pa.)	$LaCrO_3$ ceramic blocks and powders
A-T Research (Vichy, Mo.)	Sintered graded $LaCrO_3$ blocks, Special $LaCrO_3$ powders
Trans-Tech Co. (Gaithersburgh, Md.)	$MgAl_2O_4$ and MgO insulators, MAFF and $LaCrO_3$ powders
Norton Co. (Worchester, Mass.)	MgO insulators
Cerac Co. (Milwaukee, Wis)	Various ceramic powders

TABLE 11

SUMMARY OF MATERIALS USED IN PHASE III U-02 PROOF TEST ELECTRODES

Electrode System	Material	(°C) T_H	T_c	Powder or Ceramic Source
1 (APS)	85 ZrO_2-12 CeO_2-3 Y_2O_3 (PS)	1700	A	Cerac
	MAFF-31 (PS)	A	?	Transtech
	Attachment not defined	?	?	?
	$MgAl_2O_4$ (PS)	1600	<100	
2 Technetics	MAFF-31 (PS)	1700	600-900	Transtech
	Hoskins 875 mesh	600-900	<100	Technetics
	$MgAl_2O_4$ (M)	1600	<100	Transtech
5 (APS)	85 ZrO_2-12 CeO_2-3 Y_2O_3 (PS)	1700	A	Cerac
	$La_{.95}Mg_{.05}CrO_3$ (PS)	A	?	Transtech
	Attachment not defined	?	?	?
	$MgAl_2O_4$ (PS) or	1600	<100	Transtech
	$SrZrO_3$ (PS)	1600	<100	Cerac
6 Technetics	$La_{.95}Mg_{.05}CrO_3$	1700	~200	1) Sintered - A-T Research 2) W hot pressed from gen. ref. powder
	Nickel (alloy 205 (mesh)	~200	>100	Technetics
7 (A-T/W)	$La_{.95}Mg_{.05}Cr_{.5}Al_{.5}O_3$	1700	1300	1) Sintered - A-T Research
	$La_{.95}Mg_{.05}Cr_{.68}Al_{.32}O_3$	1300	600	
	$La_{.95}Mg_{.05}Cr_{.85}Al_{.32}O_3$	400	~200	2) Hot pressed - W from A-T powders
	Attachment not defined	~200	<100	
	$MgAl_2O_4$	1600	<100	Transtech
8 EP(HP) or W(HIP)	85 ZrO_2-12 CeO_2-3 Y_2O_3	1700	A	1) Cerac 2) A-T Research
	$LaCrO_3$	A	~200	1) Gen. Refr. 2) A-T Research
	Attachment not defined	~200	<100	
	MgO	1600	<100	1) Transtech 2) Norton
9 (A-T/W)	$LaCrO_3$-$SrZrO_3$ graded composite	1700	B	A-T Research
	or			
	$LaCrO_3$-ZrO_2(Y_2O_3) composite	1700	C	Hot pressed at Westinghouse
	Attachment not defined			
	$SrZrO_3$	1600	<100	1) A-T Research or 2) Hot pressed at Westinghouse

performances will be determined by simulating the channel test conditions by use of an oxygen-propane torch and/or a plasma torch. These will be preliminary tests prior to the proof tests to be run at the Westinghouse MTF facility.

4.1.4.1 X-Ray Analysis

Pre-test x-ray analysis of the starting powders and sintered/hot-pressed/plasma sprayed channel materials were determined by x-ray diffraction at NBS. Table 12 lists the results of candidate materials which have been analyzed to date.

The x-ray diffraction results show that a number of the plasma-sprayed powders had additions of secondary phases present, which were not detected in the pre-plasma sprayed powders. This is obviously attributed to the actual plasma-spraying operation, where the powder is heated to high temperatures and is rapidly cooled. Care must be taken that all plasma-sprayed materials be analyzed for these possible second phase formations.

4.1.4.2 Spectrographic Analysis

A number of the candidate channel materials obtained from different suppliers were sent out to Spectrochemical Laboratories Inc.* for qualitative spectrographic analysis. The samples were all random selections from as received starting powders. The results are shown in Table 13.

The impurity levels were all within reason except for the high amount of SiO_2 detected in the $MgAl_2O_4$ supplied by Glasrock. Also the SiO_2 content reported for $SrZrO_3$ from Cerac appears higher than the expected value but still within the experimental error of the spectrograph.

4.1.4.3 Thermal Diffusivity/Conductivity

Thermal diffusivity measurements were made on a number of the candidate channel materials at Batelle Northwest**, using a laser pulse technique. These measurements

---

*Pittsburgh, Pa. 15221.
**L. Bates, Richland, Wash. 99352.

TABLE 12

X-RAY ANALYSIS* OF CANDIDATE MHD CHANNEL MATERIALS

I. Electrodes

Material	From	Supplier	Material Description	X-Ray Diffraction Results
$La_{.95}Mg_{.05}CrO_3$	NBS 6500 A-1A	Cerac	Crushed APS powder -200 μ + 25 mesh, 1% excess Cr_2O_3 added	single phase crystallinity fair to good
$La_{.95}Mg_{.05}CrO_3$	Westinghouse LC-GR02	General Refractories	APS powder crushed	single phase med.-good crystallization no parameter shifts
$La_{.95}Mg_{.05}CrO_3$	Westinghouse LC-CE01	Cerac	APS powder crushed	single phase med. crystallization no parameter shifts
$La_{.95}Mg_{.05}CrO_3$	Westinghouse LC-CE02	Cerac	Fines from 6500 A-1A	single phase good crystallinity
$La_{.95}Mg_{.05}CrO_3$	Westinghouse LC-GR05	General Refractories	Sinterable powder	single phase good crystallization no parameter shifts
$La_{.95}Mg_{.05}CrO_3$	Westinghouse	Cerac	Plasma sprayed-from LC-CE02	$LaCrO_3$ + unknown + La_2O_3 unknown phase 10% La_2O_3 5% poor crystallinity
3 $MgAl_2O_4$- Fe_3O_4	NBS	Trans-Tech	APS powder, spray dried	single phase good crystallinity

*Analysis conducted at NBS, Gaithersburg, Maryland.

TABLE 12 (Continued)

I. Electrodes (Cont)

Material	From	Supplier	Material Description	X-Ray Diffraction Results
CeO_2	NBS	Cerac	APS powder crushed -150+325	single phase good crystallinity
Y_2O_3	NBS	Cerac	APS powder crushed -150+325	single phase fair crystallinity
95 HfO_2-5 Y_2O_3	NBS	Cerac	APS powder crushed -150+325 mesh	Cubic HfO_2 + 5-10% monoclinic very poor crystallinity
12 m/oY_2O_2-3 m/o CeO_2-85 m/o ZrO_2	Westinghouse CZ-CE01	Cerac	APS powder	broad peaks, mostly cubic - small amount tetragonal poor crystallinity
12 m/o Y_2O_3-3 m/o CeO_2-85 m/o ZrO_2 or $La_{.95}Mg_{.05}CrO_3$	Westinghouse CZ-CE01 LC-CE02	Cerac	Both plasma-spray sprayed pieces	CeO_2-Y_2O_3-ZrO_2 - broad peaks single phase cubic + some tetragonal ZrO_2 $LaCrO_3$ - poor crystallinity 2-5% unknown phase

II. Insulators

$MgAl_2O_4$	NBS S-71	Trans-Tech	APS spray dried	single phase good crystallinity
$MgAl_2O_4$	Westinghouse MA-CE02	Cerac	APS powder crushed -150+325 mesh	single phase good crystallinity

TABLE 12 (Continued)

II. Insulators (Cont)

Material	From	Supplier	Material Description	X-Ray Diffraction Results
$MgAl_2O_4$	Westinghouse MA-Ce0301	Cerac	Plasma-sprayed -325+10 μ mesh	single phase med. to good crystallinity
$SrZrO_3$	NBS No. 4283	Cerac	APS powder crushed -150+325 mesh	cubic perovskite single phase
$SrZrO_3$	NBS No. 3451B	Cerac	APS powder crushed -325 mesh	cubic perovskite single phase
$SrZrO_3$	Westinghouse SZ-CE02	Cerac	APS powder -150+325	single phase good crystallinity
$SrZrO_3$	Westinghouse SZ-UM02	U. of Missouri	APS powder	single phase poor crystallinity
$SrZrO_3$	Westinghouse SZ-CE0301	Cerac	Plasma-sprayed powder used -325+10 μ	$SrZrO_3$ + 5-10% tegragonal ZrO_2 $SrZrO_3$ crystallinity good ZrO_2 crystallinity poor
$SrZrO_3$	Westinghouse SZ-CE0102	Cerac	Sintered piece @ 1650°C in air	single phase very good crystallinity
$SrZrO_3$	Westinghouse SZ-UM0203	U. of Missouri	Sintered piece @ 1650°C in air	single phase very good crystallinity

TABLE 12 (Continued)

II. Insulators (Cont)

Material	From	Supplier	Material Description	X-Ray Diffraction Results
$CaZrO_3$	NBS No. 3757	Cerac	APS crushed -150+325	orthorhombic perovskite + 2nd phase of 10-20% cubic Ca stabilized ZrO_2
$CaZrO_3$	NBS No. 375	Cerac	APS crushed powder -325 mesh	orthorhombic pervoskite + 5-10% stabilized ZrO_2

TABLE 13

QUALITATIVE SPECTROGRAPHIC ANALYSIS OF MHD MATERIALS (Starting Powders) IN WT %

Material (Powder) (Powder Source)	MgO (Norton)	85 m/o ZrO_2-12 CeO_2-3 Y_2O_3 (Cerac)	$SrZrO_3$ (U. of Missouri)	$SrZrO_3$ (Cerac)	$MgAl_2O_4$ (Cerac)	$MgAl_2O_4$ (Glasrock)	$La_{.95}Mg_{.05}Cr_{.75}Al_{.25}O_3$ (U. of Missouri)
Analysis (wt. %)							
La_2O_3	-	-	-	-	-	-	Major
SrO	0.001	0.001	Major	Major	0.002	0.02	0.01
ZrO_2	*0.002	Major	Major	Major	*0.002	0.003	0.01
MgO	Major	0.005	0.002	0.002	30.0	30.0	0.05
Al_2O_3	0.001	0.005	0.001	0.01	Major	Major	0.25
Y_2O_3	*0.01	3.0	*0.01	*0.01	*0.01	*0.01	*0.01
CeO_2	*0.01	10.0	*0.01	*0.01	*0.01	*0.01	*0.01
CaO	2.0	0.005	2.0	3.5	1.0	2.0	1.5
NiO	*0.001	0.03	0.01	0.02	0.002	0.01	*0.001
SiO_2	0.005	0.005	0.005	2.0	2.0	10.0	0.005
Na_2O	*0.10	*0.10	*0.10	*0.10	0.10	0.1	*0.10
MnO	0.002	*0.001	0.001	*0.001	0.01	*0.01	*0.01
ZnO	*0.001	0.03	0.01	0.01	*0.001	*0.001	*0.001
Fe_2O_3	0.001	0.001	*0.001	*0.001	0.005	0.02	0.001
TiO_2	*0.001	0.005	0.003	0.002	*0.001	0.002	0.003
CuO	0.001	0.002	*0.0005	*0.0005	0.003	0.005	0.01
MoO_3	*0.001	0.001	*0.001	*0.001	*0.001	*0.001	*0.001
B_2O_3	*0.003	*0.003	*0.003	*0.003	0.003	0.005	*0.003
Cr_2O_3	0.001	*0.001	0.005	0.10	0.002	0.25	1.0
BaO	-	-	-	2.0	-	0.001	0.01

*Not detected. The number indicates the minimum limit of detection.

NOT DETECTED: Cd, As, Te, Sb, Pb, W, Ge, Bi, Be, Sn, V, Ag, Co, Ba.

are on materials which either had not been fully investigated in Phase I or II or have not been examined previously.

Lanthanum Ferrite

$La_{.9}Sr_{.1}FeO_3$ was processed at MIT (LSF-HO-1) by hot-pressing at 1433K for 80 minutes at 1.93×10^7 pascals. The material was heat-treated at 1470K for 27 hours to give a final density of 6.1 g/cc (9.38% TD). There was no apparent change in sample thickness after the thermal diffusivity measurements. A slight reaction did take place with the tungsten wire used to hold the sample. See Figure 35.

$La_{0.95}Mg_{0.05}CrO_3$

$La_{0.95}Mg_{.05}CrO_3$ was fabricated by APS* (APS L-1) by arc plasma spraying the material into a layer with a final density of 5.57 g/cc. The structure was found to be a multiphase body including a metallic phase. During the measurements the sample warped slightly (~0.008 cm). See Figure 36.

$La_{0.95}Mg_{.05}Cr_{0.5}Al_{0.5}O_3$

$La_{.95}Mg_{.05}Cr_{0.5}Al_{0.5}O_3$ was processed by U. of Missouri - Rolla** by sintering in a controlled atmosphere. A final density of 6.12 g/cc was achieved. The thermal diffusivity/conductivity measurements are shown in Figure 37.

$0.75\ MgAl_2O_4 \cdot 0.25\ Fe_3O_4$

$0.75\ MgAl_2O_4 \cdot 0.25\ Fe_3O_4$ was fabricated by APS* (APS-M-1) by arc plasma spraying into a layer with a final density of 3.61 g/cc. Some warpage was observed (~0.06 cm) during the thermal diffusivity measurement. The results are shown in Figure 38.

---

*D. Harris, Dayton, Ohio 45401.
**H. U. Anderson, Rolla, Missouri

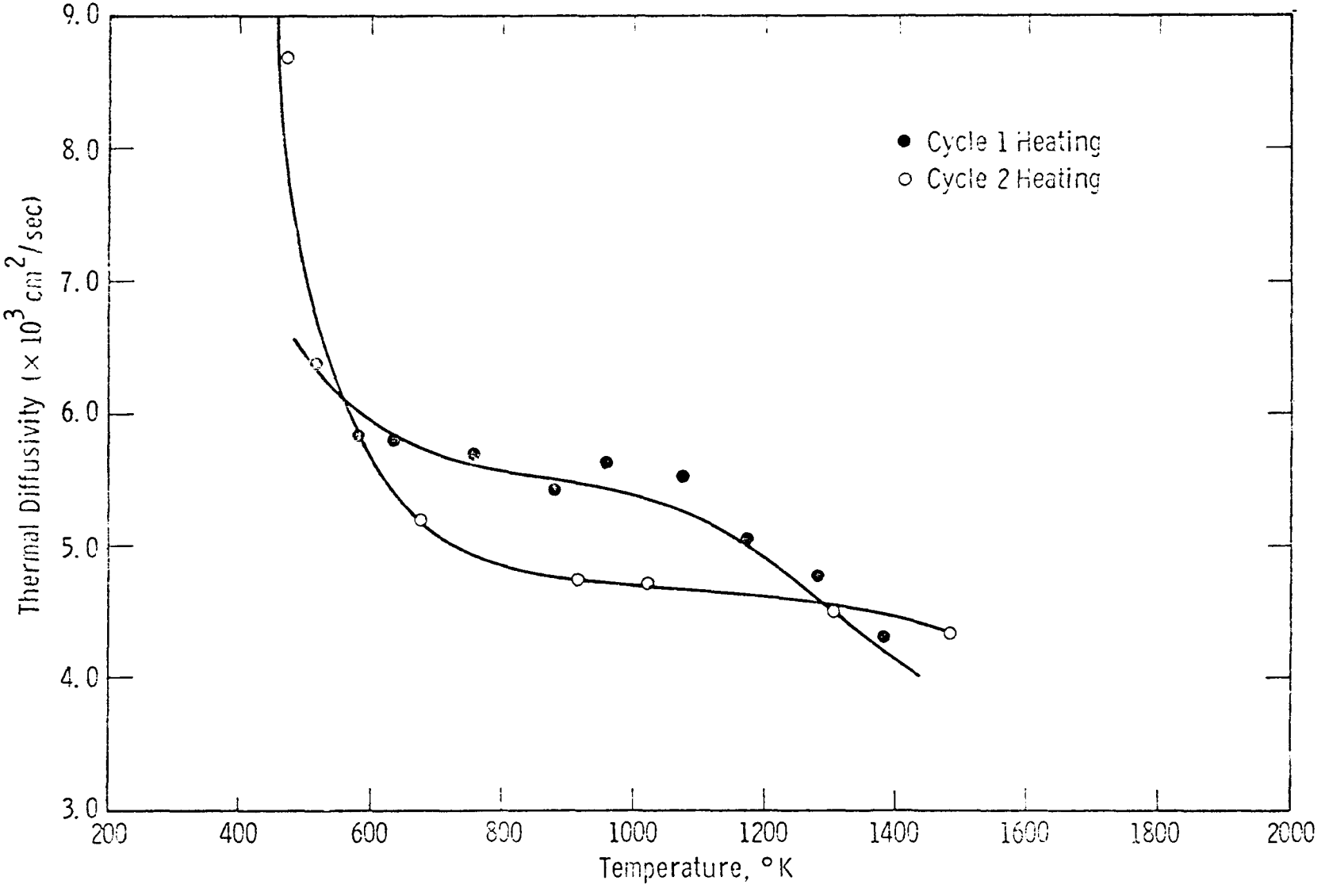

Figure 35. Thermal Diffusivity of $La_{0.9}S_{R_{0.1}}FeO_3$ (MIT)
(Measured by BNW)

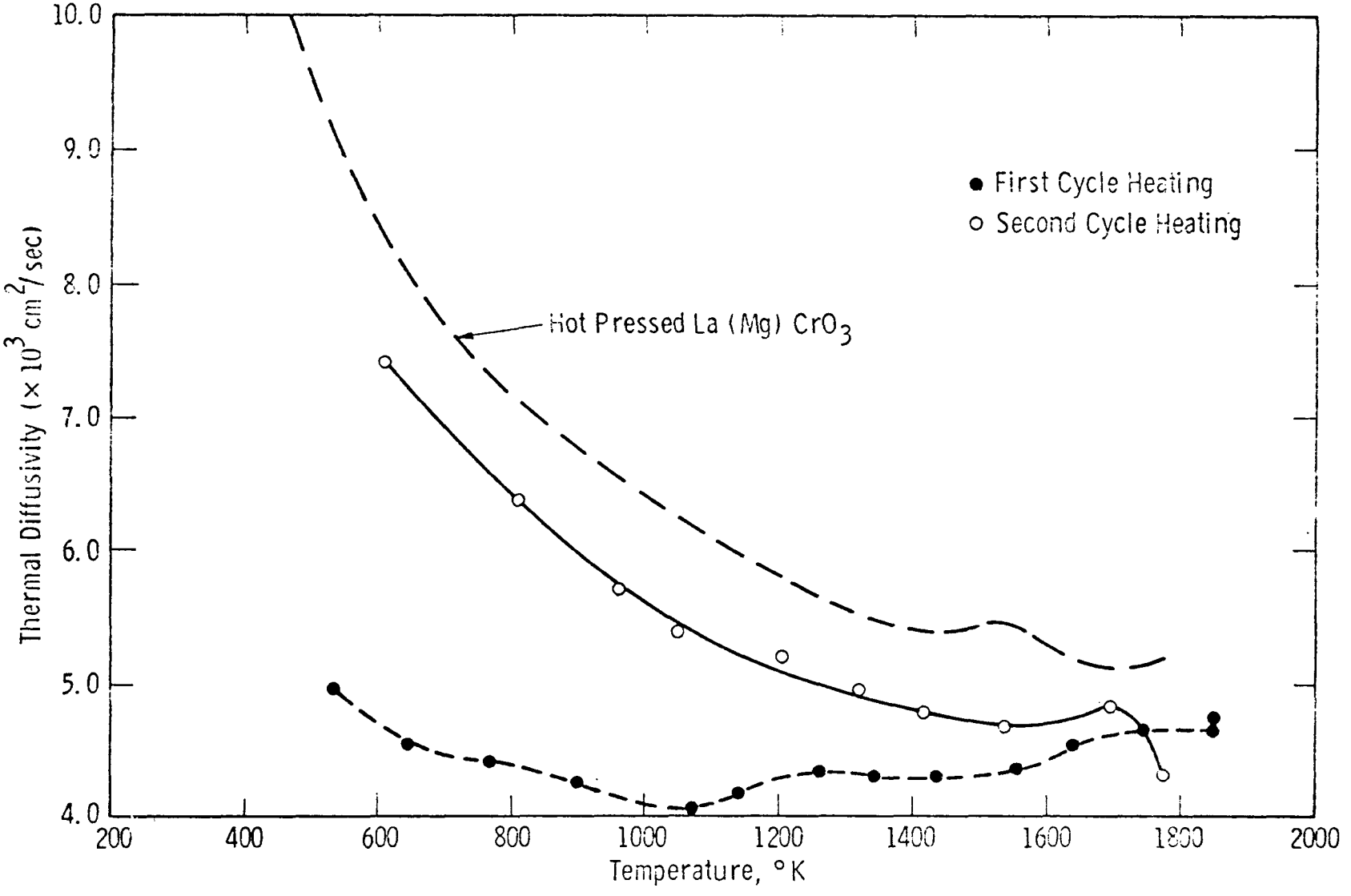

Figure 36. Thermal Diffusivity of Plasma-Sprayed $La_{0.95}Mg_{0.05}CrO_3$ (APS)
(Measured by BNW)

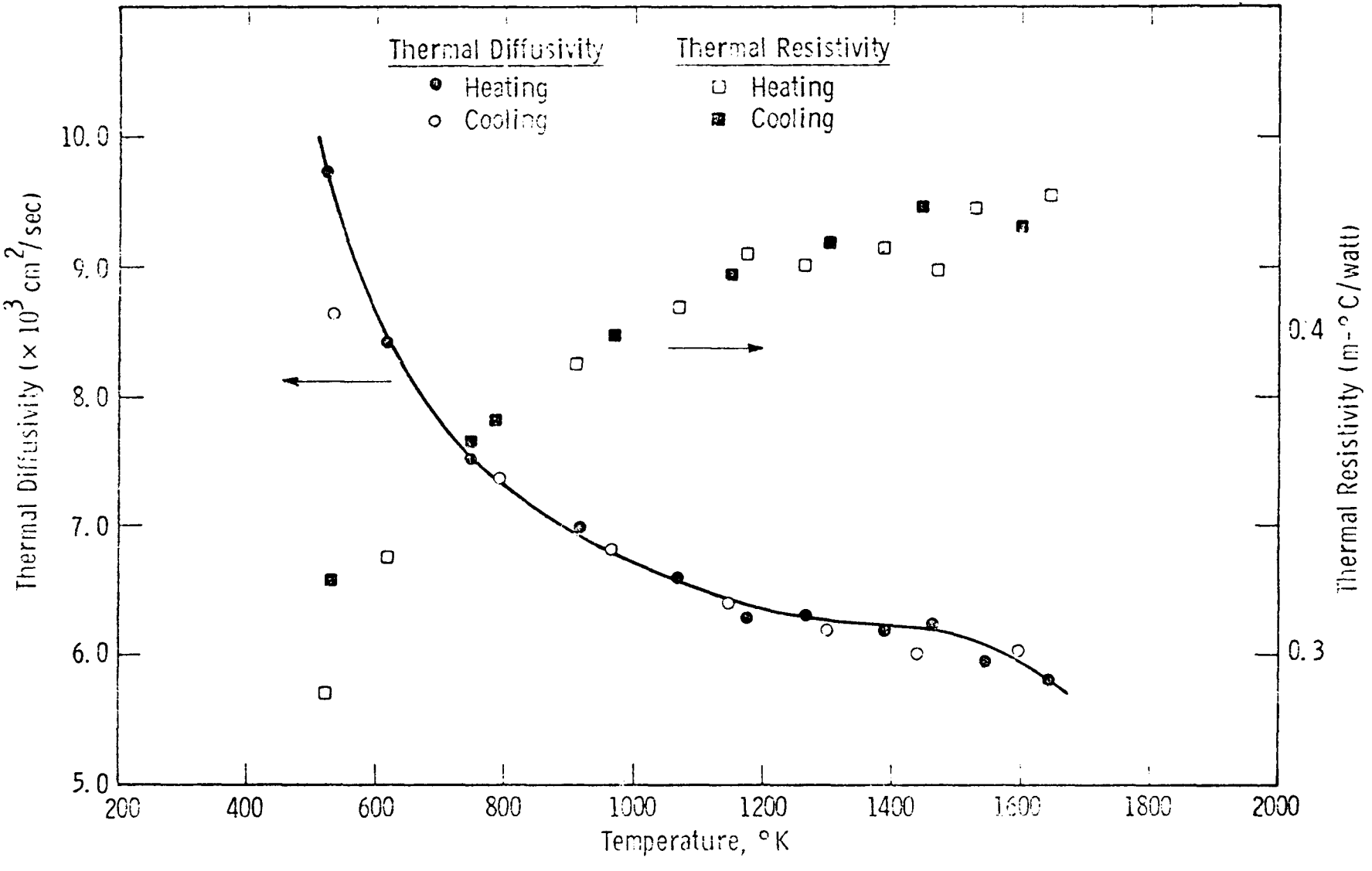

Figure 37. Thermal Diffusivity - Resistivity of $La_{0.95}Mg_{0.05}Al_{0.5}O_3$
(Measured by BNW)

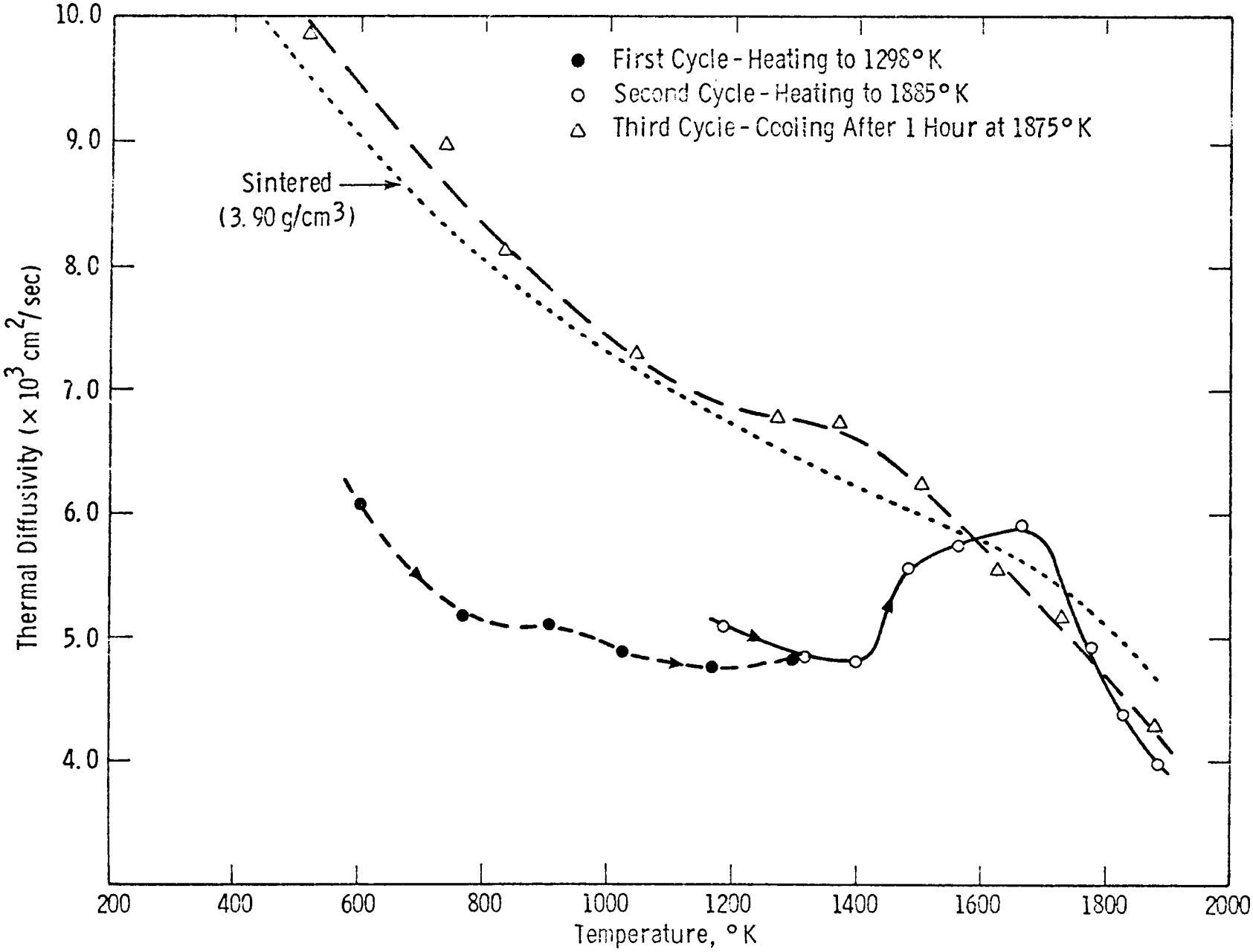

Figure 38. Thermal Diffusivity of 0.75 Mg Al_2O_4 · 0.25 Fe_3O_4
(Measured by BNW)

4.1.4.4 Mechanical Properties of Electrode/Insulator Materials

The three most promising materials for use as insulators in an MHD channel are magnesia (MgO), spinel ($MgAl_2O_4$), and strontium zirconate ($SrZrO_3$). To obtain reliable thermal stress analyses for them for several different designs and channel conditions, accurate elastic modulus data is required. Therefore, experimental values were obtained for all three from room temperature to 1400°C. The fused-grain MgO tested was obtained from Norton* and was high purity with a density of 85% of theoretical. The $MgAl_2O_4$ was obtained from Transtech,** where it was sintered to ~96% of theoretical density. The $SrZrO_3$ was obtained in powder form from Cera, Inc.*** and then sintered to 90% density at Westinghouse. All three samples were machined to approximately 2.0" x 0.25" x 0.175" and the elastic modulus was arrived at by using a four point flexure fixture and measuring the radial deflection using a three rod deflectometer. Each specimen was loaded at a strain rate of 0.005 to approximately 75% of its fracture strength at each of the temperatures listed below.

		Elastic Modulus x 10^6	
Temperature	MgO	$MgAl_2O_4$	$SrZrO_3$
RT	28.0	36.9	20.1
800°C	21.1	32.1	9.7
1000°C	10.3	28.5	8.4
1200°C	Specimen Failed @	14.2	3.7
1400°C	1000°C & 3600 psi	Specimen Failed @ 1200°C & 3350 psi	Specimen Failed @ 1200°C & 1900 psi

The magnesia exhibited minimal plastic deformation up to 1000°C but retained little strength at the higher temperatures. The spinel and $SrZrO_3$ both exhibited initial plastic deformation at 1000°C and extensive deformation at 1200°C.

4.1.4.5 Micro-Structural and -Chemical Characteristization of Vendor Materials

Characterization of ZrO_2 capped $LaCrO_3$ based electrodes, prepared by Eagle Picher Industries for possible inclusion in the upcoming UO_2 Phase III tests, is

*Worchester, Mass.
**Gaithersburg, Md.
***Milwaukee, Wis. 53201

proceeding. These materials are prepared by hot pressing, at temperatures above 1500°C in graphite dies, powders of 85 m/o ZrO_2-12 m/o CeO_2-3 m/o Y_2O_3 which are layered onto $LaCrO_3$ powders. In most instances graded intermediate composition layers are used to minimize chemical and thermal expansion compatibility problems between the $LaCrO_3$ and ZrO_2 end compositions. Though variations in starting powder properties and in pressing temperatures and pressures samples, have been produced which have a wide range of densities. However studies indicate that there are many characteristics common to all samples prepared to date; these are discussed below.

In general, the samples exhibited some degree of cracking, most often confined to the ZrO_2 and graded layers. The cracks were usually perpendicular to the layers (due to stresses resulting from thermal expansion or sintering shrinkage differences between layers) although lamination failures were not uncommon. Samples having both large numbers of intermediate layers and low processing temperatures tended to contain fewer cracks.

Chemical compatibility problems were also encountered in all samples examined. The predominant chemical reaction involves the reduction of the $LaCrO_3$ in the presence of carbon and/or carbon and ZrO_2. Thus, wherever $LaCrO_3$ contacted the graphite wall, walls or plungers of the die, free chromium metal and La_2O_3 were formed (i.e., $LaCrO_3 + C \rightarrow La_2O_3 + Cr + Co$). See Figure 39(a). More significantly, wherever $LaCrO_3$ contacted ZrO_2 in reasonably close proximity to the graphite components of the die, a solid solution of La in ZrO_2 and free Cr metal were formed* as shown in Figure 39(b) (i.e., $LaCrO_3 + C + ZrO_2 \ (La_2O_3)_{ss} + CO$).

The presence of ZrO_2 tends to accelerate and promote the reduction reaction. For example, Cr metal was observed in the graded layers at depths into the sample greater than ten times that found where only pure $LaCrO_3$ contacted the graphite. The extent and severity of Cr metal formation exhibits a strong temperature dependence and is probably controlled by diffusion of oxygen ions from the sample

*Free La_2O_3 may be present but has not yet been confirmed by X-ray diffraction.

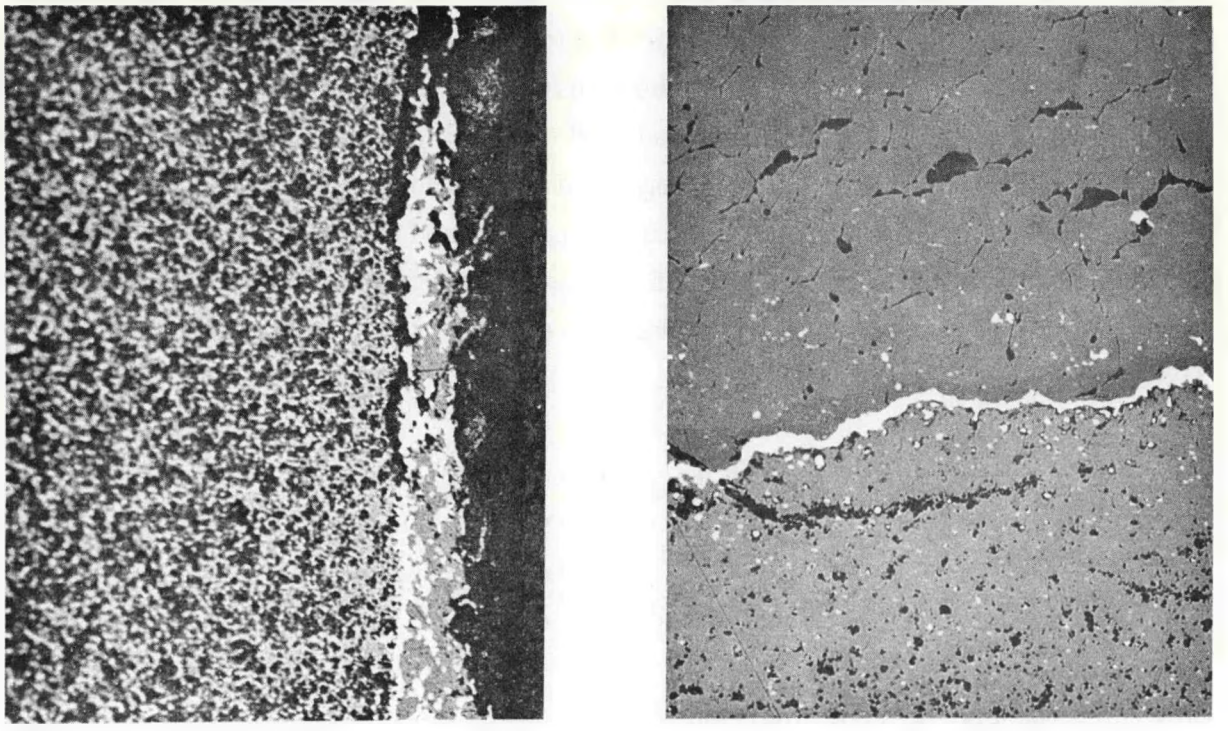

(a) (b)

Figure 39. (a) Interface between $LaCrO_3$ (Left) and Graphite Wall Liner Material (Right) Showing Formation of Free Cr Metal (White). Hot Pressed at 1700°C, 23 Minutes. 200X

(b) Cr Metal Reaction Layer Formed at Interface Between ZrO_2 (Top) and $LaCrO_3$ (Bottom) Layers. Hot Pressed 1720°C, 20 Minutes. 200X

interior to the graphite walls. Because O^{-2} diffuses extremely rapidly through ZrO_2, this material should act as a conduit (pipe) for the reduction reaction. This is consistent with our observations that $LaCrO_3$ reduction is most extensive in those layers where ZrO_2 forms the continuous matrix phase. See Figure 40.

The reduction reaction can be a serious impediment to the use of capped $LaCrO_3$ electrodes in the U-02 channel in at least two ways:

1) The Cr metal can be reoxidized or nitrided when the electrode is operated at high temperatures. The volume expansions associated with these phase changes would create a highly porous, cracked matrix which would in turn be subject to spalling and direct infiltration and reaction with seed and combustion products. Figure 38 illustrates the type of matrix deterioration which occurs when an as-received reduced sample is heat-treated in air at 1200°C for 2 hours.

2) If free La_2O_3 is formed internally (assuming it doesn't go into complete solid solution with the ZrO_2), it can hydrate in air, at room temperature, expand, and effectively destroy the structural integrity of the matrix.

To minimize the chances that the above conditions can exist, suggestions have been made to Eagle Picher to reduce hot pressing temperatures to below 1350°C* (i.e., where Cr metal formation is thermodynamically unfavorable) and to use diffusion barriers in the dies to slow O^{-2} transfer. Eagle Picher has reported some success with this approach and new samples will soon be provided for our further characterization.

---

*Highly surface active powders must now be used to produce high density material.

Figure 40. Corroded Layer of $LaCrO_3$ (Dark Grey) in ZrO_2 (Light Grey) 4 mm Below ZrO_2 Surface Layer of Sample, Hot Pressed with Graphite Plunger. Note: Cr Particles have Precipitated at the Interfaces Between $LaCrO_3$ Grains and ZrO_2 Hot Pressed 1720°C, 20 Minutes. 200X

5.0 REFERENCES

1. Development, Testing and Evaluation of MHD Materials and Component Designs, Quarterly Report, January to March, 1977, on ERDA Contract #Ex-76-C-01-2248, Westinghouse Electric Corp., April 1977

2. Tedmon, C.S.; Spacil, H.S.; Mitoff, S.P.; J. Electrochemical Society 116, (1969), 1170-5

V. CONCLUSIONS

TASK 3 - TESTING AND EVALUATION OF PROTOTYPE ELECTRODE SYSTEMS

Substantial progress has been made in several activities under this task. First, the Materials Test Facility became operational with only minor problems. Fourty hours of operation in this quarter has demonstrated that this facility can provide both the test conditions and durability needed to serve as a test bed for materials and designs.

Secondly, laboratory screening tests, particularly the electro-chemical corrosion tests, provided data under a wide range of test conditions and on additional candidate materials. Confidence in these tests as realistic screening tests has also increased. Two additional materials, $MgCr_2O_4$ and Mo_2Si, demonstrated the lowest recession rates of any materials tested to date.

TASK 4 - TECHNICAL SUPPORT FOR THE COOPERATIVE US-USSR PROGRAM ON MHD

Work has begun on the U-02 Phase III Module test program. This is scheduled for testing in the U-02 Feasibility in February 1978. Nine candidate electrode systems will be tested in in three proof tests in the MTF in August-September 1977. Based on these tests electrodes for the U-02 test will be selected. Design of the module wall, including electrode systems, has been initiated. Material properties are being determined for these materials by BNW and NBS and will be used in elastic analyses of these systems.

A V-02 Phase III Module Status Review Meeting has been scheduled for mid-July.

☆U.S. GOVERNMENT PRINTING OFFICE: 1978-740-094/1281